EXPERIMENTAL INVESTIGATIONS ON ALKALI ACTIVATED CONCRETE DEVELOPED BY INCORPORATING MARGINAL MATERIALS FOR RIGID PAVEMENT

Thesis

Submitted in partial fulfilment of the requirements of the degree of

DOCTOR OF PHILOSOPHY

By

PANDITHARADHYA B J

(Register No. 165055CV16F14)

DEPARTMENT OF CIVIL ENGINEERING

NATIONAL INSTITUTE OF TECHNOLOGY KARNATAKA

SURATHKAL, MANGALORE – 575 025

APRIL, 2022

EXPERIMENTAL INVESTIGATIONS ON ALKALI ACTIVATED CONCRETE DEVELOPED BY INCORPORATING MARGINAL MATERIALS FOR RIGID PAVEMENT

Thesis

Submitted in partial fulfilment of the requirements of the degree

of

DOCTOR OF PHILOSOPHY

By

PANDITHARADHYA B J

(Register No. 165055CV16F14)

Under the guidance of

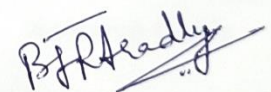**Dr. RAVIRAJ H MULANGI   Dr. A U RAVI SHANKAR**

DEPARTMENT OF CIVIL ENGINEERING

NATIONAL INSTITUTE OF TECHNOLOGY KARNATAKA

SURATHKAL, MANGALORE – 575 025

APRIL, 2022

DECLARATION

I hereby *declare* that the Research Thesis entitled **"Experimental Investigations on Alkali Activated Concrete developed by incorporating Marginal Materials for Rigid Pavement"** which is being submitted to the National Institute of Technology Karnataka, Surathkal in partial fulfillment of the requirements for the award of the Degree of Doctor of Philosophy in **Civil Engineering** is a *bonafide report of the research work carried out by me*. The material contained in this Research Thesis has not been submitted to any University or Institution for the award of any degree.

Panditharadhya B J

Register Number: 165055CV16F14

Department of Civil Engineering

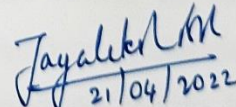Place: NITK, Surathkal

Date: 19/04/2022

CERTIFICATE

This is to certify that the Research Thesis entitled "**Experimental Investigations on Alkali Activated Concrete developed by incorporating Marginal Materials for Rigid Pavement**" submitted by **Panditharadhya B J (Register Number: 165055CV16F14)** as the record of the research work carried out by him, is accepted as the *Research Thesis submission* in partial fulfillment of the requirements for the award of degree of Doctor of Philosophy.

Dr. Raviraj H Mulangi
Research Guide

Dr. A U Ravi Shankar
Research Guide

Jayalekr M
21/04/2022
Chairman - DRPC

Chairman (DRPC)
Department of Civil Engineering
National Institute of Technology Karnataka, Surathkal
Mangalore - 575 025, Karnataka, INDIA

DEPT. OF
CIVIL ENGG.
NATIONAL INSTITUTE OF TECHNOLOGY KARNATAKA, SURATHKAL

ACKNOWLEDGEMENT

ABSTRACT

Road infrastructure projects are very much important in the progress of any country and involves large budget. Concrete roads are being considered over bituminous pavements due to its longer design life and lesser maintenance costs. The higher demand for concrete roads and other infrastructure developments has resulted in the increased production of Ordinary Portland Cement (OPC), which is one of the basic constituents required for concrete production. However, the production of OPC is associated with emissions of large amounts of CO_2, with the cement industry accounting for about 5 to 8 % of worldwide CO_2 emissions. In addition to CO_2 emissions, the production of OPC requires considerable amounts of natural raw materials and energy. The present research community is focused on the development of alternative binders, with the aim of minimization of production of OPC. Alkali Activated Binders (AAB) such as Alkali Activated Slag (AAS), Alkali Activated Slag Fly Ash (AASF), Geopolymers, etc. can be considered as potential alternatives to OPC. Also, there is a huge scarcity of natural aggregates to be used in road projects. Industrial marginal materials can be taken as fine aggregates in pavement quality concrete for sustainable growth. In the present study, Processed Iron Slag (PIS), an industrial by-product obtained from iron and steel industry is identified as an alternative to natural aggregates for concrete production, since there is an acute shortage of natural aggregates for concrete production.

The present study is mainly focussed on evaluating the performance of PIS as fine aggregate in Alkali Activated Slag Concrete (AASC) and Alkali Activated Slag Fly Ash Concrete (AASFC) by replacing river sand. AASC and AASFC mixes are designed to attain a minimum strength of M40 grade and compared with conventional Ordinary Portland Cement Concrete (OPCC) mix of similar grade. AASC mixes were prepared with 100% Ground Granulated Blast furnace Slag (GGBS) as sole binder, while AASFC mixes were prepared by mixing GGBS and Fly Ash (FA) in different proportions, i.e., 75:25, 50:50 and 25:75. Along with slag and fly ash, Aluminium dross – a by-product from aluminium refinery industry was considered as a partial replacement for binder in this study. However, it could not be a suitable binder in AAS and AASF based concrete because of the swelling observed at 5 % replacement itself. It was not considered in further stages of development of AASC and AASFC.

i

Preliminary tests were carried out to identify the optimal activator modulus and dosage of alkaline activators for each of the AASC and AASFC mixes. PIS as fine aggregates were incorporated in the AASC and AASFC mixes by replacing the river sand by weight replacement method at different levels of replacement, i.e., 0, 25, 50, 75 and 100%. The fresh and hardened properties such as workability, compressive strength, split tensile strength, flexural strength, and modulus of elasticity of concrete mixes were evaluated as per the standard test procedures. The durability of concrete mixes in terms of resistance to sulphuric acid attack, magnesium sulphate attack, water absorption and Volume of Permeable Voids (VPV) were investigated. Flexural fatigue behaviour of various concrete mixes was determined by carrying out repeated load tests on beam specimens. The fatigue life data obtained were analyzed using S-N curves to establish fatigue equations. Probabilistic analysis of fatigue data was carried out using two parameter Weibull distribution method. Further, goodness-of-fit test was done to ascertain the statistical relevance of the fatigue data using Weibull distribution model. Survival probability analysis to predict the fatigue lives of concrete mixes with required probability of failure was carried out. The economic benefits of AASC and AASFC mixes in comparison with conventional OPC concrete were analyzed.

The results indicated that incorporation of PIS in AASC and AASFC mixes resulted in slight reduction in mechanical strength. The inclusion of PIS aggregates slightly reduced the durability performance of AASC and AAFC mixes. Water absorption and subsequent VPV were increased with inclusion of PIS in both AASC and AASFC mixes which may be attributed to higher water absorption of PIS as compared to normal aggregates. Alkali Activated Concrete (AAC) mixes with natural aggregates exhibited better resistance to sulphuric acid and magnesium sulphate environments as compared to OPCC, which may be attributed to properties/structure of binders. The acid and sulphate resistance of AAC mixes slightly decreased with replacement of natural aggregates with PIS aggregates. Reduction in number of cycles for fatigue failure was observed in AASC and AASFC mixes containing PIS as compared to river sand. Two parameter Weibull distribution was used for statistical analysis of fatigue data and it was observed that the fatigue data of concrete mixes can be approximately modelled using Weibull distribution.

Cost comparison was done to compare the costs of all the materials per cubic meter of concrete with respect to OPCC, AASC and AASFC mixes. AASC and AASFC mixes showed a slight reduction in cost when compared to conventional OPCC. Incorporation of PIS aggregates in AAC mixes led to further reduction in cost as compared to OPCC. Overall, PIS aggregates reported acceptable performance in AASC and AASFC mixes for its use in pavement quality concrete. AASC and AASFC mixes satisfying the requirements of M30 and M40 grades of concrete are recommended for low and high-volume concrete pavement construction.

Keywords: Alkali activated concrete mixes; Aluminium dross; Cost comparison; Durability; Fatigue behaviour; Marginal materials; Mechanical properties; Processed iron slag aggregates.

CONTENTS

LIST OF FIGURES

x

LIST OF TABLES

LIST OF ABBREVIATIONS

AAB: Alkali Activated Binders

AAC: Alkali Activated Concrete

AAFA: Alkali Activated Fly Ash

AAS: Alkali Activated Slag

AASC: Alkali Activated Slag Concrete

AASF: Alkali Activated Slag Fly Ash

AASFC: Alkali Activated Slag Fly Ash Concrete

Al Dross: Aluminium Dross

ASTM: American Society for Testing Materials

FA: Fly Ash

FL: Flexural Load

GBFS: Granulated Blast Furnace Slag

GP: Geopolymer

GPC: Geopolymer Concrete

GGBS: Ground Granulated Blast furnace Slag

IRC: Indian Road Congress

IS: Indian Standards Specification

MOE: Modulus of Elasticity

MoRTH: Ministry of Road Transport and Highways and Materials Standards

OPC: Ordinary Portland Cement

OPCC: Ordinary Portland Cement Concrete

PIS: Processed Iron Slag

PPC: Portland Pozzolana Cement

PSC: Portland Slag Cement

SR: Stress Ratio

CHAPTER 1

INTRODUCTION

1.1   GENERAL

India being one of the fastest developing nations has concentrated its focus on the development of large-scale road networks. With around 3.315 million kms of road network, India has the second largest road network in the world which comprises of 0.132 million kms of national highways and rest state highways, district roads and rural roads. Roads in India account for about 87% of the passenger traffic and 60% of the freight traffic (https://www.morth.nic.in/road-transport).

Road projects need to be economically and ecologically sustainable apart from being safe in order to benefit from the huge investments made on the road infrastructure projects. Roads in India are under subjected to tremendous overloading due to rapid growth of passenger vehicular traffic and also due to considerable increase in heavy laden freight traffic. This has led to the premature performance failure of highway pavements (Sharma et al. 1995). Moreover, the maintenance of roads is not carried out periodically thus causing inconvenience to the travellers along with higher maintenance cost. The demand for increased highways and reconstruction and maintenance of prematurely failed pavements have also resulted in fast depletion of naturally available road materials. To overcome this, there is need to construct eco-friendly, sustainable and cost-effective highways. Compared to conventional bituminous pavements, construction of concrete pavements is generally preferred nowadays due to lower maintenance, longer design life although the initial investment cost is high. These days concrete pavements have been used extensively for highways, airports as well as business and residential streets.

1.2   CONCRETE PAVEMENTS

Concrete pavements well known as rigid pavements are widely constructed type of pavements across the world. Concrete roads are considered very suitable for

construction of expressways, bypasses, urban roads etc. Concrete roads are generally most preferred in coastal places, places with heavy rainfall etc. (Bhattacharya 2005). Concrete pavements exhibit several advantages over conventional bituminous pavements like long service life, withstand heavy axle roads, provide smoother riding quality and provide better durability even under extreme weather conditions such as heavy rainfall, water logging, high temperatures regions and chemical environments. Concrete roads also have the adaptability to use locally available road materials and industrial waste materials thus saving scarce natural resources (Naik 2008). The adoption of rigid pavements over bituminous pavements is also encouraged due to the cement production scenario, as the raw materials for cement production are available in plenty. As per the guidelines of Indian Roads Congress (IRC), rigid pavement is an alternative for flexible pavements for rural roads where the soil strength is weak, aggregates are costly and at places having poor drainage conditions (IRC: SP: 62 - 2004).

Concrete pavements are generally constructed using conventional Ordinary Portland Cement (OPC) concrete along with aggregates, water and additives. However, various other types of concrete such as Fiber reinforced concrete (FRC), Pervious Concrete, Blended Cement Concrete, High Performance Concrete (HPC), Alakli Activated Concrete (AAC), etc. can also be used to the construction of rigid pavements. In India, until the year 2000, Ministry of Road Transport and Highways (MoRTH), specified the use of conventional OPC concrete with a minimum grade of M40 or higher for construction of rigid pavements. However, in the year 2008, the IRC revised the specifications through Amendment No.3 to IRC: 21 - 2000 which allows the use of blended cements such as Portland Slag Cement (PSC) and Portland Pozzolona Cement (PPC) to be used for construction of rigid pavements.

1.3 CONCRETE PAVEMENTS IN INDIAN SCENARIO

India is hoping to see a revival of its economy through proper road and transport connectivity. The government has launched major initiatives to upgrade and strengthen the highways and expressways in the country. The government of India has formulated several programs such as Special Accelerated Road Development Program for the

North-East region (SARDP-NE) including Arunachal Pradesh, National Highways Interconnectivity Improvement Project (NHIIP), Bharatmala Pariyojana Phase I, Char Dham Pariyojana, Setu Bharatam which are designed to promote nationwide highways and rural connectivity linking all the unconnected villages with fair weather roads. In order to boost the highway sector, the government of India has targeted to construct highways at the rate 40 kms/day which amounts for about 14,500 kms of highways every year. The government of India has set a target to complete 0.2 million kms of highways by the end of 2022 from existing 0.132 million kms in 2020-21. The National Highway Authority of India (NHAI) and the Ministry of Road Transport and Highways (MoRTH) are expected to award projects worth Rs. 2.25 lakh crores in the financial year 2022 (https://www.ibef.org/industry/roads-india.aspx). As a result of the steps taken by the Government, road networks were developed rapidly in the past five years and there is a huge scope for construction of highways, expressways and other roads in India in the upcoming years. Due to this increased demand for materials for road construction has depleted the aggregate sources at a tremendous rate and sand mafia has become a major issue of concern in procurement and usage of river sand.

1.4   CONCRETE

Concrete is one of the most basic and critical components for any type of construction and plays an important role in building the nation's infrastructure. Concrete is a composite material which is composed coarse and fine aggregates embedded in matrix and bound together by a binder which fills the space or voids between the aggregates and bonds those together (Mindess et al. 2003). Basically, concrete is a mixture of binder, water, aggregates and additives. The binder generally used for concrete production is OPC, which is mainly responsible for the mechanical strength. Therefore, the demand for OPC is huge in road infrastructure projects as well as other construction sectors in India. Also, India is the second largest producer of cement in the world which accounts for more than 7% of the global installed capacity. Cement production reached 294.4 million tonnes (MT) in the year 2020-21 and is projected to reach 381 MT by the end of the year 2022-23. However, the consumption stood at 327 MT in 2020-21 and will reach 379 MT by the end of 2022-23. The cement production capacity is estimated to touch 550 MT by 2025. As India has a high quantity and quality of limestone deposits

through-out the country, the cement industry promises huge potential for growth (https://www.ibef.org/industry/cement-india.aspx).

It is well known that the production of OPC is associated with release of greenhouse gases in huge quantities and also is high energy intensive process. The production of one ton of cement leads to carbon dioxide (CO_2) emission in the range 0.8-1.3 ton along with high energy consumption in the range 100-150 kWt (Satish 1996). The production of OPC also consumes huge quantities of virgin raw materials. The cement industry is making significant research through improvements and advancements in the cement production technology and process efficiency in order to reduce the CO_2 emissions, however further improvements may be limited as CO_2 generation is inherent and inevitable during the basic process of calcinations of limestone. Moreover, the mining of limestone which is one of the main raw materials for cement production has impact on the land use patterns, local water bodies and ambient air quality. The cement industry other than consumption of raw materials is one of the major consumers of coal for production of cement. Dust emissions from the cement industry also have affected the ambient air quality.

Considering the crucial importance of infrastructure development for India and other emerging countries, the demand for cement production has increased rapidly, which have led to increased concerns on the environmental aspects involved in the use and production of concrete. The eco-friendly and sustainable development is the need of day which demand new concrete technologies which consume lower natural resources, lower energy and generate less CO_2 without compromising on the strength and durability performance. Eco-friendly technologies and effective management of natural raw materials is necessary to counter to ill-effects occurring from concrete production.

In the context of increased awareness to reduce the production of OPC, the research community is mainly focused on the use of industrial waste materials such as Fly Ash (FA), Ground Granulated Blast furnace Slag (GGBS), Silica Fume, etc. in concrete production. Attempts to replace OPC partially with FA, GGBS have proved to be successful. The use of GGBS, FA as partial replacement to OPC have displayed improved workability, reduced segregation, bleeding, heat evolution, permeability and

improved the durability properties of conventional OPC concrete. Apart from improving the properties of OPC concrete, the use of such wastes has ecological and economic benefits and hence may be used as partial replacement to cement in concrete production (Tripathy and Mukherjee 1997; Chandrashekhar et al. 2010). Apart from techniques which involve partial replacement of OPC binder with industrial waste materials in conventional OPC concrete, there are techniques which involve the complete replacement of OPC binders with industrial waste materials such as Alkali Activated Slag (AAS), Alkali Activated Slag Fly Ash (AASF) which are the examples of Alkali Activated Binders (AAB). AABs can be looked upon as alternative to conventional OPC binders, which have the capabilities to be used in construction industry, causing significant reduction in the production of OPC (Rashad et al. 2012). Along with reduced emission of CO_2 and consumption of energy in the manufacture, the alkali activated binders also exhibit superior mechanical and durability performance than OPC binders (Morsy et al. 2008 and Rashad 2013a).

1.5 ALKALI ACTIVATED BINDERS

Alkali activated binders are new generation binders which include a clinker-free binder matrix such as Alkali Activated Slag (AAS), Alkali Activated Fly Ash (AAFA or Geopolymers), Alkali activated Slag/Fly Ash (AASF), etc. The alkali activated binders are produced by alkali activation of finely divided materials (generally industrial waste materials) such as FA, GGBS, Rice Husk Ash (RHA), Metakaolin, etc. using strong alkaline activators such as sodium silicate, sodium hydroxide, potassium silicate, potassium hydroxide, sodium bicarbonate, etc. or combination of these. The idea of the usage of slag and alkali combination was given by Purdon in 1939 (Purdon 1940). Later in 1959, Glukhovsky demonstrated in his book named 'Gruntosilikaty', the possibility of preparing new materials by means of the reaction of alumino-silicate raw materials (slags, fly ashes, clay materials) with alkaline compounds (carbonates, hydroxides, silicate) (Glukhovsky 1959). Krivenko (1994) proposed the classification of alkali activated cementitious materials based on the composition of hydration products. The system where the formation process is a poly-condensation rather than hydration was named "Geopolymer" (Davidovits 1994). The hydration products are low basic calcium

silicate hydrates (C-S-H gel with low Ca/Si ratio). These include the alkali activated slag and alkaline Portland cement.

Over the past few decades, extensive studies on AAS and AAFA have been carried out. In case of AAS, GGBS is used as the sole binder material, while in AAFA; FA is used as the sole binder. Although the activation techniques for AAS and AAFA are quite similar, they differ in their chemical reactions and also in their mechanical and durability properties. The AAS based concretes are characterized with high strength even at room temperatures, rapid setting, improved fire resistance etc. (Shi et al. 2006). On the other hand, AAFA based concrete exhibit better resistance to acid environments, high heat resistance etc. (Lee and Van Deventer 2002). However, AAFA based concrete do not achieve sufficient strength at room temperature and hence require heat curing to gain sufficient strengths (Fernandez et al.1999). It has been also studied that joint activation of GGBS and FA as a combined binder has reported sufficient strength even at room temperatures. Such a type of binder is termed as Alkali Activated Slag Fly Ash (AASF), may be considered as separate type of binder whose properties vary with the ratio of GGBS and FA.

The primary difference between AAS and AASF is that AAS contains only GGBS as the binder while AASFC contains GGBS along with FA mixed in different proportions. The main reaction product in AAS is Calcium Silicate Hydrate (C-S-H) with low Ca/Si ratio; whereas Alumino Silicate Hydrate (A-S-H) is mainly formed reaction product in AAFA (Chen and Brouwers 2007; Fernández and Palomo 2005). Studies carried out by researchers (Puertas et al. 2000) claim that the main product formed in AASF to be C-S-H with no existence of A-S-H; while others (Chi and Huang 2013) have reported the existence of both. Idawati et al. (2014) found C- A- S- H phase and hybrid C-(N)-A-S-H phases also in smaller quantities. The addition of higher amounts FA in AASF concrete has resulted in the reduction of strength, however the workability was found to increase (Rashad 2013b). The AASF containing up to 50% FA (% by weight of binder) develop sufficient strengths even at room temperature, however the strength development reduces with higher contents of FA greater than 50% (% by weight of binder) (Rajamane 2013). The strength and durability of AAB are strongly affected by various parameters such as curing regime, type of curing, type of

6

alkaline activators, dosage and activator modulus of alkaline activator, type of source materials, water to binder ratio, total water content, chemical composition of binder and alkaline activators, etc. (Rashad 2013a). Several studies carried out by researchers have claimed that the AABs develop better mechanical and durability properties as compared to conventional OPC and hence can be considered as a potential alternative to OPC.

1.6   BINDERS FOR ALKALI ACTIVATED SYSTEM

In view of global sustainable development, it is essential to discover new supplementary cementitious or fine filler materials from hazardous wastes to replace larger proportions of cement and sand while mass concreting. The use of wastes such as FA, GGBS, silica fume, RHA and others in producing concrete and other building materials are gaining importance day by day because of ecological considerations. Various researches have experimented with FA, GGBS, RHA, metakaolin, silica fume as partial replacement materials for cement in plain and structural concrete. These marginal materials act as supplementary cementitious elements.

1.6.1   Fly Ash

Fly Ash is a by-product generated from the combustion of coal in thermal power plants which are transported by flue gases and captured by electrostatic precipitators before the gases reach chimneys. FA has fine particles with sizes ranging from 1 to 100 µm. FA is usually divided into two types based on the amount of calcium content (CaO) present in it, i.e., Class-C and Class-F FA. Class-C FA is generally obtained from the combustion of lignite and bituminous coals and contain 15 to 35 percent of CaO content. Class-F FA is obtained from the combustion of anthracite coals and contain CaO content less than 5 %. FA is used as supplementary cementitious material and has been used extensively to partially replace OPC in concrete. Unused FA is dumped into landfills and hence contributes to air, water and soil pollution (Palomo et al. 1999; Duxson et al. 2007).

FA is considered as a pozzolanic material due to the presence of high contents of silica and alumina, which react with the calcium hydroxide formed during hydration of cement to provide cementitious properties. Due to the high availability of reactive

7

silica and alumina, Class-F FA is preferred for synthesis of geopolymer concrete. Class - F FA is also preferred as a source material due to the presence of low amount of calcium, since presence of high content of calcium may hinder the geopolymerization process and alter the microstructure (Gourley 2003).

1.6.2 Ground Granulated Blast furnace Slag

Granulated Blast-furnace Slag (GBFS), a by-product from iron and steel industry, is a granular material which is generated when the molten blast furnace slag is rapidly quenched with water. When this granular GBFS is ground to the fineness of cement, it is called Ground Granulated Blast-furnace Slag (GGBS). The GGBS is majorly constituted of oxides of calcium (CaO), silica (SiO_2), alumina (Al_2O_3), magnesia (MgO), with some other oxides SO_3, FeO or Fe_2O_3, TiO_2, K_2O, Na_2O, etc.) in small quantities. GGBS is one of the most widely investigated, used and probably the most effective cement replacement material used for concrete manufacturing.

1.7 ALUMINIUM DROSS

Aluminium dross is a by-product obtained from the aluminium smelting process. Currently, this dross is processed in rotary kilns to recover the residual aluminium, and the resultant salt cake is sent to landfills. Aluminium dross is a by-product obtained from the aluminium smelting process. Currently, this dross is processed in rotary kilns to recover the residual Al, and the resultant salt cake is sent to landfills. The wastes are irregular in shape, black in colour and contain lumps and small particles of aluminium produced by burning aluminium scraps (raw material) in a furnace at about 1900°C. The composition of recycled aluminium dross is typically variable and unique to the plant generating the waste. The recycled aluminium dross contains some volume fraction of toxic materials and land filling of these toxic substances is not ecologically fair.

The aluminium dross admixture is utilized as a retarder in order to manufacture concrete suitable for hot weather concreting. The particle sizes in Aluminium dross vary from less than 45 μm up to 150 μm with the typical particle size measuring under 90 μm. Only about 30% of the particles by mass are larger than 90 μm. The specific

8

surface area is about 375 m^2/kg. The specific surface area of Aluminium dross is comparatively higher than that of cement and has a direct influence on the pozzolanic reaction. The Aluminium dross functions as a filler material to seal the voids present in the mix and also aids in the strength development of concrete.

IS: 9103-1999 specifies that whenever any retarding admixture is used, the minimum compressive and flexural strength should be 90 percent of the control sample at 28 days. The aluminium dross causes a delay in the setting time of concrete by one or more mechanisms. It adsorbs over the surface of cement particles and acts as a diffusion barrier, thereby developing a shielding covering which decelerates the hydration process. It also adsorbs over the nuclei of calcium hydroxide $Ca(OH)_2$, thereby reducing its intensification, which is mandatory for continued hydration of cement. The inorganic salts present in the aluminium dross (for e.g., the metal oxides) form insoluble hydroxides in alkaline solution and suppress the cement hydration by forming a protective coating over the cement grains (Gireesh et al. 2016).

1.8   PROCESSED IRON SLAG

The indiscriminate mining of river sand has destroyed the ecology of many river channels and floodplains. The scientific community has been attempting to discover alternatives to river sand for construction. Some of the options being considered include crushing rock to fines (manufactured sand), recycled fine aggregate, mining for sand in submerged areas and producing sand from molten iron slag which is a by-product of iron and steel industry. About 30% of the ore on iron and steel production turns to slag, and this can be utilized to meet the present-day sand deficiency.

Slag from iron and steel industry is durable, has consistent shape and volume and is safe for use in construction (Tripathi et al. 2012). The slag after processing, is superior to river sand because the latter contains fossils and other irregular particles like clay and silt that affects the quality and durability of concrete. Some studies have substantiated that with high volumes of substitution (about 40%) of this slag as fine aggregate, high-quality concrete having a dense internal structure can be produced (Singh and Siddique 2016). At this slag content of more than 60% in concrete, researchers have witnessed a considerable reduction in the rate of heat evolution

(Siddique 2008), a significant resistance to chemical attack (Yuksel 2017) and high-energy radiation shielding applications (Ouda and Abdel-Gawwad 2015).

1.9 NEED FOR THE STUDY

The development of eco-friendly and sustainable construction materials has gained major attention by the construction industry. With the augmented emissions of greenhouse gases, high energy consumption and environmental hazards occurring from the increased OPC production; the researchers are focusing on development of possible alternatives to OPC. The primary approach is aimed at the minimisation of OPC with the use of industrial waste materials such as FA, GGBS, silica fume, etc., as supplementary cementing materials as partial replacement for OPC in concrete. Alkali activated binders can be looked upon as alternative to conventional OPC binder, which have the capabilities to be used in construction industry, causing significant reduction in the production of OPC (Rashad et al. 2012). Alkali activated binders include clinker-free binders such as AAS, AASF, Geopolymers, etc., which include the use of a strong alkaline activator along with calcium or silicate rich precursor material such as GGBS, FA, etc.to form a final product, having properties equivalent or better than OPC. The energy required for the production of alkali activated binders is less than that required for OPC concrete and are further associated with low CO_2 emissions.

Over the years, the natural sand has been used as the filler material in concrete. However, the faster depletion of river sand has created concern to the construction industry for future works. The present-day research has been concentrated on seeking alternative low-cost materials as replacements for natural sand in concrete.

The present experimental study focuses on the possibility of utilization of industrial waste materials such as GGBS, FA, Aluminium dross and PIS in the production of a sustainable concrete for construction industry. The aim of the study is not just to protect the natural raw materials but to recycle the disposal wastes from the industries. Since the kind of curing adopted here is air curing, this type of concrete will be of great advantage in arid and desert regions where there is acute scarcity of water. Presently in India, there is no practical field application of AAB based concrete in pavements or any other applications, which is mainly due to limited research, non-

acceptability of new materials, lack of expertise and confidence, etc. The scenario can be changed by conducting the proper research and communicating the performance of AAB concrete for different applications.

1.10 SCOPE OF THE WORK

The current research focuses on strength and durability properties of air cured alkali activated - GGBS and FA based concrete mixes made with PIS as fine aggregate and Aluminium dross as partial replacement for binder to use in rigid pavement. This type of concrete caters the need for conservation of natural resources and also helps in reducing stockpiles of the waste materials. Due to limited literature available on incorporation of PIS as fine aggregate with Aluminium dross as binder to produce AASC and AASFC mixes, the present study was focused to carry out detailed experimental investigations to address the suitability and performance of air cured AASC and AASFC mixes for rigid pavement construction.

1.11 RESEARCH OBJECTIVES

Based on the literature review and the gaps observed, the specific objectives of the study were framed and are as follows,

1. To design OPC based control concrete mix to arrive at the optimum percentage replacement of Aluminium dross.
2. To evaluate the mechanical properties of AASC and AASFC mixes incorporating PIS as fine aggregate.
3. To study the durability properties of AASC and AASFC containing PIS as fine aggregate.
4. To study the flexural fatigue behaviour of developed concrete mixes.
5. To recommend the mixes for high and low volume roads quoting the comparison of costs with respect to OPC based control concrete mix.

1.12 ORGANIZATION OF THESIS

This thesis is organized into eight chapters followed by the appendices and list of references.

CHAPTER 1:

The background on road network and the need for use of concrete roads in India; brief note on alkali activated binders and PIS; need and significance, objectives and scope of the research are presented in this chapter.

CHAPTER 2:

A comprehensive literature review has been carried out to collect adequate information about alkali activated binders, aluminium dross, PIS and other materials. Information gathered about the research works carried out so far on mechanical, durability properties and flexural fatigue studies of alkali activated binders, PIS, are also presented.

CHAPTER 3:

The details of various materials used during laboratory investigation of basic properties of concrete ingredients and the design mix for M_{40} concrete are presented in this chapter. Further, the preliminary laboratory tests carried out for obtaining the optimal design mix for AASC and AASFC are also presented. The test methodology adopted for determining the mechanical, durability and flexural fatigue performance of concrete mixes are discussed in detail.

CHAPTER 4:

This chapter presents the laboratory tests and outcomes of concrete properties such as compressive strength, split tensile strength, flexural strength and modulus of elasticity which are significantly affecting the performance of concrete pavements. The results are discussed in detail in this chapter.

CHAPTER 5:

The results of durability tests carried out on AASC and AASFC mixes are discussed in detail in this chapter.

CHAPTER 6:

This chapter deals with the flexural fatigue test details, results discussion of the fatigue strength studies of AASC and AASFC mixes with/without PIS carried out on beam

specimens at various stress ratios. A probabilistic analysis is carried out on the test data to describe suitable life prediction models.

CHAPTER 7:

This chapter deals with the recommendation of AASC and AASFC mixes for high and low volume road construction based on the outcomes of the present work. Cost comparison is done in this chapter to arrive at cost of materials per cubic meter of developed concrete mixes.

CHAPTER 8:

Observations and conclusions drawn based on the investigations; recommendations and scope for further study are presented in this chapter.

CHAPTER 2

LITERATURE REVIEW

2.1   GENERAL

The term 'Geopolymer' was first introduced by Davidovits in 1978 (Davidovits 1979) to describe a family of mineral binders with a chemical composition similar to zeolites but with an amorphous microstructure. Unlike ordinary Portland/pozzolanic cements, Geopolymers do not form calcium-silicate-hydrates (C-S-Hs) for matrix formation and strength, but utilize the polycondensation of silica and alumina precursors to attain structural strength. Two main constituents of Geopolymers are: source materials and alkaline liquids. The source materials should be alumino-silicate based and rich in both silicon (Si) and aluminium (Al). They could be by-product materials such as FA, silica fume, slag, rice-husk ash, red mud, etc. Geopolymers are also unique in comparison to other aluminosilicate materials (e.g., aluminosilicate gels, glasses, and zeolites). The concentration of solids in Geopolymerization is higher than in aluminosilicate gel or zeolite synthesis.

2.1.1   Composition of Geopolymer Cement Concrete Mixes

The materials used in GPCC system are binders (usually FA and GGBS), water, fine and coarse aggregates, and liquid activator solution. Activator solution or Catalytic Liquid System (CLS) is an Alkaline Activator Solution (AAS) for GPCC. It is a combination of solutions of alkali silicates and hydroxides, besides distilled water. The role of AAS is to activate the Geopolymeric source materials (containing Si and Al) such as FA and GGBS. Unlike conventional cement concrete, GPCCs are a new class of materials and hence, conventional mix design approaches are not generally applicable. The formulation of the GPCC mixtures requires systematic numerous investigations on the materials available.

2.2 GEOPOLYMERIZATION

The Geopolymer (GP) initiated by Davidovits (1979) has great potential for adoption of concrete construction industry as an alternative binder to the Portland cement (Duxson et al. 2007). GP could significantly reduce the CO_2 emission to the atmosphere caused by the cement industries. The alkaline liquid was proposed by Davidovits (1994) for reacting with the silicon (Si) and the Aluminium (Al) present in an alumino-silicate source material which may be either of geological origin or by-product materials such as FA and rice husk ash. Since, the chemical reaction involved is an inorganic polymerization process (but under alkaline condition), the word polymer in 'Geopolymer' to represent the new binders seems to be logical. The chemical composition of Geopolymer material is similar to zeolitic materials, but the microstructure is amorphous. The fast chemical reaction under alkaline condition of Si-Al minerals result in a three-dimensional polymeric chain and ring structure consisting of Si-O-Al- O bonds (Davidovits 1994). The formation of Geopolymer material can be described by following two Equations (2.1) and (2.2) (Davidovits 1994).

$$(Si_2O_5, Al_2O_2)n + nSiO_2 + nH_2O \xrightarrow{NaOH, KOH} n(OH)_3 \text{-Si-O-}\overset{(-)}{\underset{|}{Al}}\text{-O-Si-}(OH)_3$$
$$(OH)_2$$

$$(2.1)$$

$$n(OH)_3 \text{-Si-O-}\overset{(-)}{\underset{|}{Al}}\text{-O-Si-}(OH)_3 \xrightarrow{NaOH, KOH} (Na,K)^{(+)} -(\text{-Si-O-}\overset{(-)}{Al}\text{-O-Si-O-}) + nH_2O$$
$$(OH)_2 \qquad\qquad\qquad O \quad O \quad O$$

$$(2.2)$$

The Equation 2.2 indicates that water is released during the formation of Geopolymers and forms discontinuous nano pores in the matrix. The atomic ratio Si:Al in the polysialate of Geopolymer is selected based on the particular application and low Si:Al ratios are suitable for most of the civil engineering applications. Low-calcium (ASTM Class F) FA is more common and can be adopted to manufacture Geopolymer concrete (GPC). Usually, 80% of the FA particles have been smaller than 50 μm.

16

(Gourley 2003; Rangan and Hardijto 2005; Wallah and Rangan 2006). The reactivity of low-calcium FA in Geopolymer matrix is found to be adequate (Fernandez et al. 2005). Coarse and fine aggregates of the conventional concretes are suitable to produce GPCs and grading curves are usually applicable to GPC mixes also (Rangan and Hardijto 2005; Wallah and Rangan, 2006; Gourley, 2003). It is recommended that the Alakali Activtor Solution (AAS) is prepared at least 24 hours prior mixing of GPC. Alkali silicate solutions are commercially available with different solid contents and Molar Ratio (MR). The ratio of $[SiO_2]/[M_2O]$ is defined as MR where $[SiO_2]$ and $[M_2O]$ are the contents of SiO_2 (silica) and M_2O (alkali oxide) in the alkali silicate. Sodium hydroxide is commercially available in the form of in flake or pellet. The primary difference between Geopolymer concrete and Portland cement concrete is the binder. The silicon and aluminum oxides in the low-calcium FA reacts with the alkaline liquid to form the Geopolymer paste that binds the loose coarse aggregates, fine aggregates, and other un-reacted materials together to form the Geopolymer concrete. The compressive strength and the workability of Geopolymer concrete are influenced by the proportions and properties of the constituent materials that make the Geopolymer paste.

Experimental works of (Rangan and Hardijto 2005) indicate the facts that, higher concentration of sodium hydroxide results in higher strength of GPC; higher the ratio of sodium silicate solution-to-sodium hydroxide solution ratio by mass, the higher is the compressive strength of Geopolymer concrete; addition of naphthalene sulphonate-based super plasticizer can improve the workability of the fresh Geopolymer concrete, however, there is a degradation in the compressive strength of hardened concrete; slump value of the fresh Geopolymer concrete increases when the water content of the mixture increases.

Geopolymer concrete can be manufactured by adopting the conventional techniques used in the manufacture of Portland cement concrete. Binder material and the aggregates are mixed in a mixer. The AAS, the liquid component of GPC mixture, is then added and the mixing continued. The fresh GPC is cohesive and can be handled up to about 2 hours (depending upon the formulation) without any sign of setting and without much effect on the compressive strength. Moulding of specimens, compaction,

17

including workability measurement is similar to Portland cement concrete (Rangan and Hardijto 2005; Wallah and Rangan, 2006).

Rangan and Hardijto (2005) at Curtin University had steam-cured the FA-based GPC test specimens at 60ºC for 24 hours and then storing in ambient conditions till testing. Heat-curing substantially assists the chemical reaction that occurs in the Geopolymer paste. Both curing time and curing temperature influence the compressive strength of Geopolymer concrete and can be manipulated to fit the needs of practical applications. A two-stage steam-curing regime was adopted by Siddiqui (2007) in the manufacture of prototype reinforced Geopolymer concrete box culverts. It was found that heat curing at 80°C for a period of 4 hours provided enough strength for de-moulding of the culverts; this was then followed by heat curing further for another 20 hours at 80°C to attain the required design compressive strength. Also, the start of heat-curing of Geopolymer concrete can be delayed for several days (say up to 5 days) without any degradation in the compressive strength. A delay in the start of heat-curing substantially increases the compressive strength of Geopolymer concrete (Rangan and Hardijto 2005). The role and the influence of aggregates in GPC are considered to be the same as in the case of Portland cement concrete. Rangan and Hardjito (2005) suggests that the ratio of sodium silicate solution to sodium hydroxide solution by mass may be taken approximately as 2.5. Test data shows that the strain at peak stress for FA-based GPC is in the range of 0.0024 to 0.0026 (Rangan and Hardjito 2005).

Collins et al (1993) has proposed that the stress-strain relation of Portland cement concrete in compressive can be predicted using the parameters: peak stress and strain at peak stress. The splitting tensile strength of Geopolymer concrete is only a fraction of the compressive strength, as in the case of Portland cement concrete, but larger than the values recommended by IS: 456-2000 and Neville (2000) for Portland cement concrete (Sofi et al. 2007a; Rangan and Hardjito 2005). The unit-weight of concrete, primarily depends on the unit mass of aggregates used in the mixture. Tests show that the unit-weight of the low-calcium FA-based Geopolymer concrete is similar to that of Portland cement concrete (Rangan and Hardjito 2005). The drying shrinkage of heat cured FA-based GPCs over a period of one year is significantly smaller than that experienced by Portland cement concrete (Wallah and Rangan, 2006).

The studies carried out by Sarker et al. (2007a, 2007b) and Sofi et al. (2007b) demonstrate the application of FA-based Geopolymer concrete. They carried out experiments on Geopolymers using two types of FA. They found that the compressive strength after 14 days was in the range of 5 to 51 MPa. The factors affecting the compressive strength were the mixing process and the chemical composition of the FA. A higher CaO content decreased the microstructure porosity and, in turn, increased the compressive strength. Besides, the water to FA ratio also influenced the strength. It was found that as the water to FA ratio decreased the compressive strength of the binder increased. Geopolymer has also been used to replace organic polymer as an adhesive in strengthening structural members. Geopolymers were found to be fire resistant and durable under UV light (Balaguru et al. 1997). Palomo et al. (1999) studied the influence of curing temperature, curing time and alkaline solution to FA ratio on the compressive strength. It was reported that both the curing temperature and the curing time influenced the compressive strength.

The utilization of sodium hydroxide (NaOH) combined with sodium silicate (Na_2SiO_3) solution produced the highest strength. Compressive strength up to 60 MPa was obtained when cured at 85°C for 5 hours. Xu and Deventer (2000) investigated the Geopolymerization of 15 natural Al-Si minerals. It was found that the minerals with a higher extent of dissolution demonstrated better compressive strength after polymerization. The percentage of calcium oxide (CaO), potassium oxide (K_2O), the molar ratio of Si-Al in the source material, the type of alkali and the molar ratio of Si/Al in the solution during dissolution had significant effect on the compressive strength. Swanepoel and Strydom (2002) conducted a study on Geopolymers produced by mixing FA, kaolinite, sodium silica solution, NaOH and water. Both the curing time and the curing temperature affected the compressive strength, and the optimum strength occurred when specimens were cured at 60°C for a period of 48 hours.

Jaarsveld et al. (2002) studied the inter-relationship of certain parameters that affected the properties of FA-based Geopolymer. They reported that the properties of Geopolymer were influenced by the incomplete dissolution of the materials involved in Geopolymerization. The water content, curing time and curing temperature affected the properties of Geopolymer; specifically, the curing condition and temperature influenced the compressive strength. When the samples were cured at 70°C for 24 hours a substantial increase in the compressive strength was observed. Curing for a longer period of time reduced the compressive strength. Davidovits (1991) described his new breed of aluminosilicate binders (synthesized by activating calcined kaolinitic clay with sodium silicate solution at low temperature) as 'Geopolymer' for the first time, the real impetus to the field of GP technology started. The 'Geopolymer' was an aluminosilicate gel, where the silicon and aluminium are tetrahedrally-bonded through sharing oxygen atoms forming the basic monomer unit is a sialate (O-Si-O–Al-O) carrying excess negative charge which occurs when the Al^{3+} (of the source material such as clay) is substituted by Si^{4+}.The polysialate structure is charge-balanced by alkali metal cations (K+ or Na+). The typical polysialate structure of geopolymerization is as shown below in Figure 2.1.
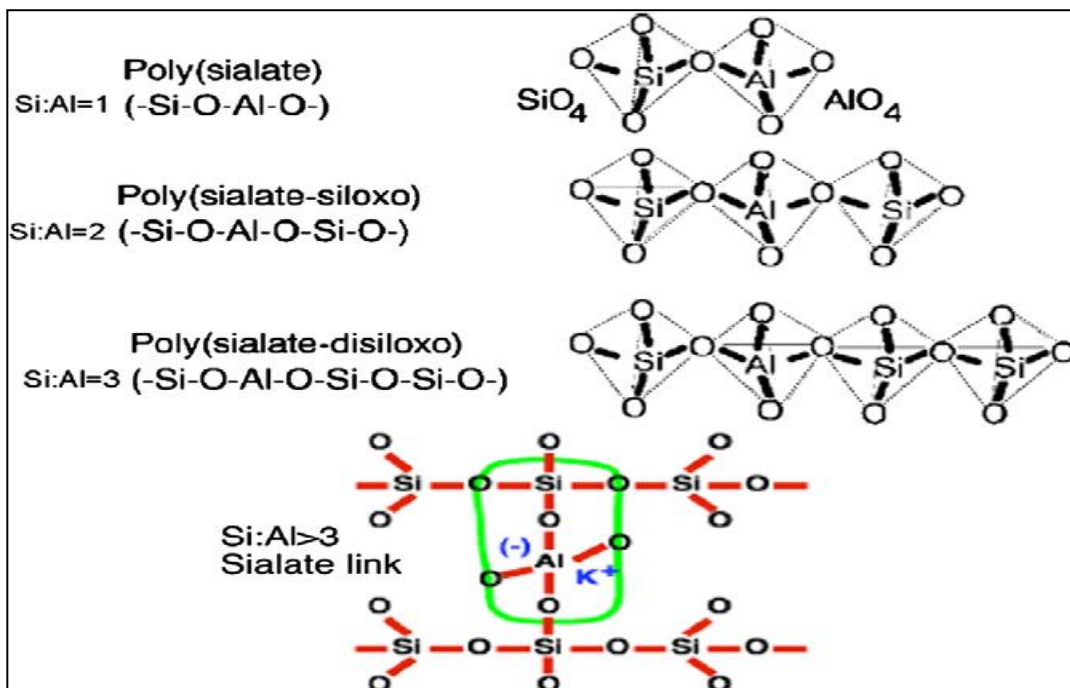
Figure 2.1 Polysialates structures according to Davidovits (2005)

2.3 SOURCE MATERIALS AND ALKALINE ACTIVATORS

Various source materials can be considered as binders provided that the molecules of the materials should facilitate Alumino-silicate bond formation. This will be ensured by activating the binder molecules with an alkaline silicate solution. FA and GGBS are the widely used admixtures for GPC because of their easy availability and provision of better strength along with required workability.

2.3.1 Fly Ash

Fly Ash (FA) is a by-product generated from the combustion of coal in thermal power plants which are transported by flue gases and captured by electrostatic precipitators before the gases reach chimneys. FA has fine particles with sizes ranging from 1 to 100 µm. FA is usually divided into two types based on the amount of calcium content (CaO) present in it, i.e., Class-C and Class-F FA. Class-C FA is generally obtained from the combustion of lignite and bituminous coals and contain 15 to 35 per-cent of CaO content. Class-F FA is obtained from the combustion of anthracite coals and contain CaO content less than 5 percent. Unused FA is dumped into landfills and hence contributes to air, water and soil pollution (Palomo et al. 1999; Duxson et al. 2007; Fernando et al. 2022). As per the latest data available, power plants in India generated 232.56 million tonnes (MT) of fly ash in the year 2020-21 and utilized 214.91 MT which accounts for 92.41 % utilization. Government of India is aimed at achieving 100 % utilization of fly ash generated for various construction activities (https://cea.nic.in/wp-content/uploads/tcd/2021/09/Report_Ash_Yearly_2020_21.pdf)

FA is considered as a pozzolanic material due to the presence of high contents of silica and alumina, which react with the calcium hydroxide formed during hydration of cement to provide cementitious properties. Due to the high availability of reactive silica and alumina, Class-F FA is preferred for synthesis of geopolymer concrete. Class-F FA is also preferred as a source material due to the presence of low amount of calcium, since presence of high content of calcium may hinder the geopolymerisation process and alter the microstructure (Gourley 2003). The fineness of FA plays a significant role in the development of mechanical strength (Fernandez and Palomo 2003; Hansen and Sadeghian 2020). The breakdown of glassy surface of FA requires

high activation energy, which can be overcome by providing higher temperature and higher alkaline environment (Rajamane 2013). Table 2.1 presents the physical properties and chemical composition of Class F FA.

Table 2.1. Chemical and Physical properties of Fly Ash (Suman et al. 2017)

Particulars	Values
CaO	0.79 %
Al_2O_3	32.17 %
Fe_2O_3	2.93 %
SiO_2	58.87 %
MgO	0.92 %
Na_2O	0.37 %
K_2O	1.14 %
Insoluble Residue	2.31%
Loss on Ignition	0.03 %
Blaine's Fineness (m^2/kg)	425
Specific gravity	2.20

2.3.2   Ground Granulated Blast furnace Slag

Granulated Blast-furnace Slag (GBFS), a by-product from iron and steel industry, is a granular material generated when the molten blast furnace slag is rapidly quenched with water. When this granular GBFS is ground to the fineness of cement, it is called Ground Granulated Blast furnace Slag (GGBS). The GGBS is majorly constituted of oxides of calcium (CaO), silica (SiO_2), alumina (Al_2O_3), magnesia (MgO), with some other oxides SO_3, FeO or Fe_2O_3, TiO_2, K_2O, Na_2O, etc.) in small quantities. GGBS is one of the most widely investigated, used and probably the most effective cement replacement material used for concrete manufacturing. The Steel industry in India is producing about 24 million tonnes (MT) of blast furnace slag and is expected that the blast furnace slag generation may reach around 45-50 MT per year by 2030 (https://www.niti.gov.in/writereaddata/files/RE_Steel_Scrap_Slag-FinalR4_28092018.pdf). This can meet large requirement of cement industry as well as road infrastructure

projects. Table 2.2 presents the physical properties and chemical composition of the GGBS.

Table 2.2. Chemical and Physical properties of GGBS (Suman et al. 2017)

Particulars	Values
CaO	34.77 %
Al_2O_3	16.70 %
Fe_2O_3	1.20 %
SiO_2	32.52 %
MgO	9.65 %
Na_2O	0.16 %
K_2O	0.07 %
Insoluble Residue	4.03 %
Loss on Ignition	0.04 %
Blaine's Fineness (m^2/kg)	370
Specific gravity	2.90

2.3.3   Alkali Activators

The source materials for alkali activated binders need to be activated using strong alkalis in order to form the resulting binding material. Caustic alkalis or alkaline salts are the most widely used alkaline activators. The alkaline activators are classified into six groups based on their chemical composition and are tabulated in Table 2.3.

Table 2.3. Classification of Alkali Activators (Glukhovsky et al. 1994)

Alkali Activator	Chemical Formula
Hydroxides	*MOH
Non-silicate weak acid salts	M_2CO_3, M_2SO_3, M_3PO_4, MF
Silicates	$M_2O \cdot nSiO_2$
Aluminates	$M_2O \cdot nAl_2O_3$
Aluminosilicates	$M_2O \cdot Al_2O_3 \cdot (2–6)SiO_2$
Non-silicate strong acid salts	M_2SO_4

*M - Metal

23

The alkali activators generally consist of mixtures of alkali silicates and alkali hydroxides. Sodium silicate (Na_2SiO_3), sodium hydroxide (NaOH), sodium carbonate (Na_2CO_3) or a mixture of sodium – potassium hydroxide (NaOH, KOH) with sodium silicate - potassium silicate or any other combinations are the most widely used alkaline activators. A combination of sodium hydroxide with sodium silicate has been agreed to provide the best strength performance for activation of alkali activated binders (Rashad 2013a). The strength of AAB's is governed by the type of alkaline activator, activator modulus and dosage of alkaline activator (Fernandez et al. 1999). The Activator Modulus (Ms) is the ratio of mass ratio of SiO_2 to Na_2O components present in the alkaline activator, while the Dosage (usually referred as %Na_2O) is the total sum of mass of Na_2O present in the alkaline activator (mass of Na_2O present in liquid sodium silicate + mass of Na_2O equivalent in sodium hydroxide if combination of sodium silicate and sodium hydroxide is used as alkaline activator).

Wang et al. (1994) reported that mechanical strength and other properties of AAS mortars were influenced by the nature of the alkaline activators. The dosage and the activator modulus have significant effects on the properties of AABs (Prosek et al. 2019). They provided a range of activator modulus depending upon the GGBS type within which maximum compressive strength may be obtained. Ranges of activator modulus are as given below,

> a) Acid slag 0.75 – 1.25,
> b) Neutral slag 0.90 – 1.3 and
> c) Basic slag 1.0 – 1.5

Figure 2.2 presents the variation of 28-day strength with activator modulus for different type of GGBS. It may be noticed that the strength increases with higher activator modulus Up to an optimal activator modulus, however, with further increase in activator modulus, the strength decreases.
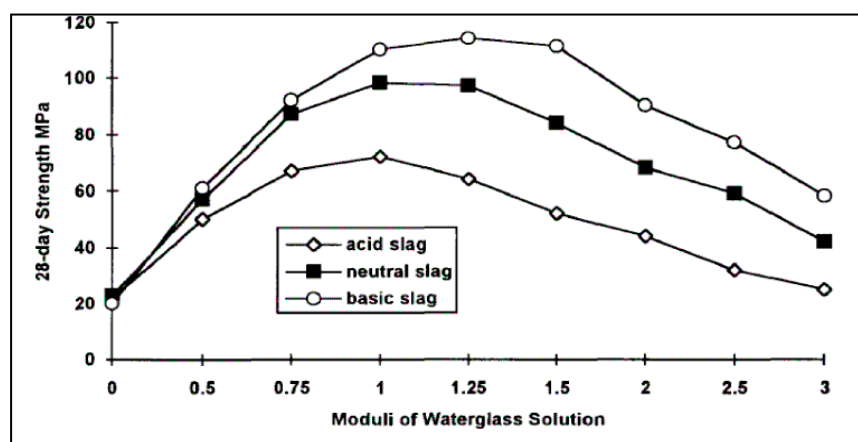
Figure 2.2 Modulii of sodium silicate solution v/s 28-day strength for different types of slags (Wang et al. 1994)

Bakharev et al. (1999) investigated the activation of Australian GGBS using different activators such as sodium silicate, sodium hydroxide, sodium carbonate, sodium phosphate, and combinations of these activators and recommended sodium silicate solution with 5% Na_2O dosage with 0.75 activator modulus for better results. Fernandez et al. (1999) reported that the mechanical strength of AAS mortars is mostly influenced by the type and nature of alkaline activator, dosage of alkaline activator and observed that optimum dosage of alkaline activator varies in the range 3% and 5.5 % of Na_2O by mass of GGBS. Na_2O dosage above this limit may cause efflorescence problems along with inefficient uneconomical mixtures. Ultimate strength higher than OPC can be achieved with GGBS cements activated using sodium silicate with modulus between 0.6 and 1.5 with appropriate Na_2O dosage (Krizan and Zivanovic 2002). Fernandez and Palomo (2005) studied the activation of FA using different types of alkaline activators and by varying the Na_2O dosage between 5% and 15% (mass of binder). The activator modulus along with water/ binder (w/b) ratio, affect the mechanical strength. It was observed that the Na_2O dosage of 5.5% (mass of FA) lead to very low pH, which affected the reaction development negatively; while the increase in Na_2O dosage leads to higher strengths with 14% (mass of FA) Na_2O dosage providing the maximum compressive strength.

Garcia et al. (2006) studied activation of AASFC mixes with different GGBS:FA ratios of 100:0, 75:25, 50:50, 25:75 and 0:100 activated using sodium

silicate solution. The Na_2O dosages 4%, 6% and 8% (mass of binder) were selected and the activator modulus was varied from 0, 0.75, 1, 1.5 and 2. The pastes were subjected to heat curing at 75°C for 24 hour and then at 20°C up to 28 days. The results indicated that the best modulus for all the mixes were in the range of 1 to 1.5. Cengiz et al. (2009) investigated the AAS mortars using different types of activators (sodium hydroxide, sodium carbonate, and sodium silicate, with varying activator modulus and with Na_2O dosages in the range 4-8% (mass of GGBS). It was observed that the compressive and tensile strengths of AAS mortars increased with Na_2O dosage of alkaline activators and also suggested that there exists an optimal alkaline modulus for which the highest compressive and tensile strengths can be obtained. Law et al. (2012) reported that the activator modulus between 1.0 and 1.25 may be considered optimal for AAS mixes.

Chi (2012) reported that the mechanical and durability properties of AAS concrete mixes were significantly dependent on Na_2O dosage of the alkaline activators. Shekhovtsova et al. (2014) studied the effect of Na_2O dosages on the compressive strength of AAFA pastes in the range 3% to 15% (by weight of FA) and reported that increase in the Na_2O dosage greatly affected the compressive strength of AAFA pastes, with highest strength reported at 9% (by weight of FA). Mehrzad (2015) tested nine series of geopolymer pastes differing in Na_2O content (4%, 7% and 10%), silica modulus (0.52, 0.6 and 0.68) and w/b ratios (0.36, 0.40 and 0.44) which were manufactured to activate the ground pumice. The test results indicated that the mix with M_s = 0.68, Na_2O = 0.10 %, w/b = 0.36 gave the higher compressive strength approximately 40 MPa and can be used as a structural material.

Kovtun et al. (2016) considered direct electric curing of FA concrete samples to ensure the effective use of FA in the production of concrete which achieves Up to 33.8 MPa and 48.5 MPa of compressive strength after 2 and 28 days of curing. Young-Keun (2017) revealed that the higher compressive strength can be obtained with higher Na_2O content, higher curing temperatures, and longer pre-curing periods at the relatively low temperature (23°C). On the other hand, an extension of curing period at high temperatures leads to strength reduction due to increasing macro-pores over 50 nm.

Maochieh and Ran (2012) investigated the properties of alkali activated slag mortars with Sodium oxide (Na_2O) concentrations of 3%, 4%, 5% and 6% of slag

weight and liquid sodium silicate with different modulus ratios (mass ratio of SiO_2 to Na_2O) of 0.6, 0.7, 0.8 and 0.9. Properties of the AAS mortars were significantly dependent on dosage and modulus ratio of alkali-activated solution. The Na_2O dosage of 4 % and the modulus ratio of 0.8 % were the lowest levels needed for the activation. Maochieh (2015) investigated the properties of Alkali Activated Fly Ash Mortars (AAFM) with Na_2O dosage of 121 and 150 kg/m^3, modulus ratio of 1.23 and 0.8, liquid to binder ratios of 0.35, 0.50 and 0.65. Test results show that both alkaline modulus ratio and the dosage of Na_2O are two significant factors influencing the characteristics of AAFMs. The higher alkaline modulus ratio and dosage of Na_2O are, the superior properties of AAFMs achieved. SEM and XRD demonstrate that the activation products of AAFMs are mainly amorphous alkaline aluminosilicate gels, which are attributed to the compressive strength. Under the alkaline modulus ratio of 1.23 and liquid / binder ratio of 0.5, AAFMs with Na_2O dosage of 150 kg/m^3 may be considered as the optimum mix design based on the results. This proves that each mix proportions and each binder will have their own influence on fixing the dosage of Na_2O, Modulus ration and liquid to binder ratio.

2.4   MECHANICAL PROPERTIES OF ALKALI ACTIVATED BINDERS

2.4.1   Physical Properties of Alkali Activated Slag

The mechanical properties of AAS mixes are influenced by various parameters such as type and nature of alkaline activators, Na_2O dosage and activator modulus, curing regime, water to binder ratio, chemical admixtures etc. Various studies have reported that the AAS concretes display similar or better mechanical properties as compared to OPC concretes. Collins and Sanjayan (1999) investigated AAS concrete mixes with the emphasis of achieving reasonable workability and equivalent one-day strength as compared to OPC concrete under normal curing temperatures and concluded that AAS concrete displayed similar one-day strength and superior ultimate strengths as compared to OPC concrete. Sakulich et al. (2009) reported AAS concretes achieved compressive strengths Up to 45 MPa and flexural strength up to 4 MPa when cured for 28 days under normal room temperatures activated using NaOH-activated formulae. Bernal et al. (2011) studied the effect of binder content on the strength performance of

27

AAS concretes and reported that regardless of the binder content, AAS concrete developed higher compressive strengths as compared to conventional OPC concrete; however higher binder content led to increase in strength in both AASC and OPCC at 28 days. Bernal et al. (2012) says that at high activator concentration, compressive strengths at early age are enhanced by the inclusion of metakaolin in the binder. A similar effect is observed in the flexural strength of the concretes, as dissolution and reaction of metakaolin is favoured under higher-alkalinity activation conditions.

The use of AAS concrete mixes is associated with certain problems such as high shrinkage and poor workability impede its practical application (Bakharev et al. 2000; Rao and Rao 2018; Subash and Kumar 2021). Investigations on the use of chemical admixtures to overcome problems related to high shrinkage and poor workability have been carried out by researchers. Bakharev et al. (2000) investigated the use of various chemical admixtures which were used for OPC concrete such as superplasticiser based on modified naphthalene formaldehyde polymers, air-entraining agent, water-reducing, shrinkage-reducing admixtures at dosages of 6±10 ml/kg, and gypsum (6% of slag weight) on AAS mixes. It was observed that the use of air-entraining agent, shrinkage-reducing admixtures and gypsum reduced the shrinkage significantly. While the naphthalene-based superplasticizer significantly increased the shrinkage and reduced the strength of AAS concrete, the air-entraining agent improved the workability without any negative effects on the compressive strength and recommended its use in AAS concrete. Similar observations were made by several other researchers (Douglas and Brandstetr 1990; Wang et al. 1994).

2.4.2   Curing Regime

The properties of AAS mixes are affected considerably with the curing condition to which they are subjected. Over the years, the properties of AAS mixes have been studied by subjecting the AAS mixes to different curing conditions such as heat curing, steam curing, normal room temperature curing (air curing), water curing, etc. Altan and Erdogan (2012) studied AAS mortar mixes activated using a combination of sodium silicate and sodium hydroxide at room and elevated temperatures. They observed that the heat cured samples gained strength rapidly, however samples cured at room

temperature also gained comparable strengths with time. It was also reported that the heat evolution of AAS hydration was lesser compared to OPC hydration and lower water to binder ratio provide higher strength at early ages.

Aydın and Baradan (2012) reported that high strength mortars with strengths Up to 70 MPa can be produced with alkaline activators having alkali content as low as low 2% by mass of binder when subjected to autoclave curing. They also observed that AAS mixes provided similar performance as compared to autoclave curing when activated using activator solutions with high activator modulus. In case of heat curing, the curing time and temperature are one of the critical factors in determining the strength of alkali activated mixes (Datta and Ghosh 2014; Shekhovtsova et al. 2014). Bilim et al. (2015) investigated the AAS mixes with Na_2O dosages of 4% and 6% by mass of slag to study the effect of curing conditions on AAS mixes and reported that curing conditions affected the mechanical behaviour of AAS mixes as compared to OPC mixes. The AAS mixes attained high early strength as compared to OPC mixes when subjected to elevated temperatures.

2.4.3 Physical Properties of Alkali Activated Slag - Fly Ash

The performance of AASFC mixes is significantly dependent on the proportion of GGBS and FA used in the mix apart from various other parameters such as type and nature of alkaline activators, Na_2O dosage and activator modulus, curing regime, water to binder ratio, chemical admixtures. The strength properties of AASF are strongly dependent on the amount of GGBS present in the AASFC binder. Puertas et al. (2000) studied the strength behaviour of AASF mixes and reported increase in compressive strength with increase in GGBS content. Similar observations have been made by several other researchers (Zongjin and Sifeng 2007; Rajamane 2013). Increase in the compressive strength with increased Na_2O dosage has been studied by Guerrrieri and Sanjayan (2009) just as in case of AAS mixes.

Higher content of FA in the AASF mixes tends to decrease compressive strength drastically, which is mainly due to the lower reactivity of FA as compared to GGBS. The breakdown of glassy surface of FA requires high activation energy, which can be overcome by providing higher temperature and higher alkaline environment (Rajamane

29

2013; Raheel et al. 2020). However, AASF mixes with proper proportions of GGBS: FA ratios can achieve sufficient strengths even at ambient room temperatures without any need for heat curing (Nath and Sarker 2012). Compressive strengths Up to 50 MPa have been achieved for AASF mixes with equal blending (50:50) of GGBS and FA without heat curing (Narasimhan et al. 2011).

Rajamane (2013) reported that GGBS when replaced beyond 50% by FA in AASF systems resulted in reduction in strength and suggested higher concentration of alkaline activator solution for mixes containing more than 50% FA to achieve sufficient strength level. It was concluded that AASF mixes containing FA content Up to 50% develop considerable amount of strength at ambient temperature and can be easily adopted for practical applications. Idawati et al. (2013) observed that the reduction in the strength of mixes with high contents of FA can be countered by lowering the water to binder ratios and stated that water to binder ratios can be controlled to achieve the desired strength in AASF concrete mixes with high amounts of FA. Suman et al. (2017) enhanced the properties of FA based geopolymer paste by incorporating GGBS at various percentage levels, which showed better setting time and compressive strength of the mix. This makes us to consider the combination of GGBS and FA instead of FA alone or GGBS alone as a binder.

2.4.4 Effect of FA on the Workability Properties of Alkali Activated Slag - Fly Ash

The inclusion of FA in AAC mixes has significant effect with respect to the strength and workability of the mixes. Several studies have reported the use of FA has positive effect on the workability, however the compressive strength reduced with the increase in the FA content. Rashad (2013a) investigated with workability properties of slag-FA-based mixes and reported increase in the workability of the mixes. Yang et al. (2008) investigated the workability properties of AAS and AAFA mortar mixes with constant w/b ratio of 0.5 and sand to binder ratio of 1: 3 and observed that the AAS mortar had lower workability than FA-based alkali-activated mortar. Rashad (2013b) presented a comprehensive overview of the previous works carried out using different additives in AAS system and the influence of different additives on the properties of alkali-activated

slag. It was concluded that the inclusion of FA in AAS matrix increased the workability. The improved workability with higher FA contents is mainly due to the particle size and morphology of this precursor (Wang et al. 2003). Although most of the researchers reported that inclusion of higher content FA resulted in reduction of strength in the AASF mixes, few others believe that optimal content of FA in AASF mixes can provide the highest compressive strength, which is further dependent on other parameters such as activator type, activator concentration, modulus ratio and curing condition.

Apart from improving the workability, the inclusion of FA has a positive effect on the setting time of alkali activated mixes. The setting time of AAS and AASF mixes increased with the inclusion of FA (Rashad 2013b; Nath and Sarker 2012). One of the major drawbacks of AAS mixes related to poor workability can be overcome with the inclusion of proper amount of FA. AASF mixes formulated with proper amount of FA, with optimal contents of Na_2O dosage and activator modulus of alkaline activators and reduction of water binder ratios can achieve sufficient strength with desired workability along with prolonged setting time even at ambient room temperatures (Idawati et al. 2013).

2.5   DURABILITY PROPERTIES OF ALKALI ACTIVATED BINDERS

Durability is one of the most important properties of concrete. Concrete is inherently a durable material. However, concrete is susceptible to attack in a variety of different exposure conditions, unless some precautions are taken. Concrete is well known for its strength, ease of production, water tightness and certain durability properties. However, concrete is most of the times exposed to aggressive environments which may arise naturally such as sea-waters, soils rich in sulphates, etc., or man-made such as chemical effluents from industries, waste water from drainage infrastructure, etc., which affect the long-term performance of concrete. Concrete undergoes degradation under the influence of such aggressive environments due to chemical processes involving exchange of ions, thus causing changes in the microstructure of the binding matrix, leading to reduction in the mechanical strength. The cement paste is affected by the presence of acids, sulphates, chlorides, etc., in the surrounding environments.

31

The durability of concrete subjected to chemical attacks such as acids and sulphates are still the aspects of concern. Due to the presence of high calcium compounds in chemical composition of OPC, the resistance of OPC to acid and sulphate resistance is low. The acids and sulphates usually attack the products of hydration of cement to form products such as gypsum along with changes in the C-S-H structure. The formation of the additional products leads to internal expansive stress, which leads to the deterioration of the concrete. Water absorption, total porosity and sorptivity are related to the ability of water or fluid to move into mortar and concrete and therefore have significant importance in the durability related properties of concrete structures. The water absorbed in the presence of oxygen may initiate the corrosion of steel reinforcement in reinforced concrete structures. Water may enter into the concrete through capillary action of pore systems (Alexander et al. 2013). Increased metakaolin contents and higher activator concentrations also lead in most cases to reduced water sorptivity and lower chloride permeability (Bernal et al. 2012). However, better durability properties of Ordinary Portland Cement Concrete (OPCC) are reported with addition of pozzolanic materials such as FA, GGBS, etc. in the binder (Gambhir 2004).

Efforts to study the durability properties of alkali activated binders have been carried out by several researchers (Bakharev 2005; Pacheco-Torgal et al. 2007; Rajamane 2013; Kapoor et al. 2020; Bajpai et al. 2020). The AAS and AASF are known to have reported better durability properties when exposed to aggressive environments (Duxson et al. 2007; Mithun and Narasimhan 2015). The better durability properties of AAS and AASF mixes are mainly due to the absence of calcium hydroxide (Portlandite) in the reaction products (Bakharev et al. 2003). The durability properties alkali activated binders are affected by various parameters such as type and concentration of the alkaline activator, activator modulus ($M_s = SiO_2/Na_2O$), binder type, fineness, curing conditions, water/binder ratio, use of admixture as well as fibers, etc. (Palacios and Puertas 2005; Rodriguez el al. 2008; Hafa et al. 2011). The mechanism of sulphate attacks on OPC, AAS and AASF is expected to be different due to differences in the binder chemistry, reaction products, large differences in the amount and roles played by calcium in these systems (Bakharev et al. 2003). Bakharev et al. (2002) studied the sulphate resistance of AAS systems and reported that AAS samples did not expand,

however, it showed visible cracks and traces of gypsum. Increase in the strength of AAS and AASF concrete samples have been reported when immersed in sodium sulphate solution due to ongoing binder formation reactions; however, strength decreased when immersed in magnesium sulphate solution (Bakharev et al. 2002).

Rajamane et al. (2013) investigated sulphuric acid resistance of AAS and AASF in comparison with Portland pozzolana cement containing FA and reported that AAS and AASF when immersed in 2% and 10% sulphuric acids displayed reduced weight loss, thickness loss and strength loss as compared to Portland pozzolana cement concrete. Chi (2012) investigated the effect of Na_2O dosages and curing conditions on the sulphate attack resistance of AAS concrete and concluded that durability in terms of sulphate attack improved with increase in dosage of Na_2O and also stated that AAS concrete cured at $60^{\circ}C$ proved the best durability performance followed by air curing and limewater curing.

Law et al. (2012) studied the durability properties of AAS concrete such as water sorptivity, chloride and carbonation resistance and reported lower durability performance as compared to OPC and blended concrete mixes, which was attributed to surface micro cracking in AAS concrete. Chi and Huang (2013) studied the water absorption properties of AAS and AASF activated at 4% and 6% Na_2O dosages with activator modulus of 1 and reported that reduction in the percentage of water absorption with increasing GGBS and decreasing FA content at both concentrations. Datta and Ghosh (2014) studied the effect of incorporation of GGBS on the magnesium sulphate resistance of AAFA mixes and reported that addition of GGBS in AAFA resulted in high residual strength after immersion in 10% magnesium sulphate solution for 15 weeks.

Alkaline activated concretes based on a mixture of FA (FA) and blast furnace slag (GBFS), as well as FA and Portland cement (OPC), both at a ratio of 80:20, were exposed to temperatures between $25^{\circ}C$ and $1100^{\circ}C$. Then, the physicochemical and mechanical changes were evaluated. The results indicate that the activated concretes have better performance than the reference ones (100% OPC). At temperatures of $1100^{\circ}C$, the residual strengths of the FA/GBFS and FA/OPC concretes are 15 and 5.5 MPa, respectively, unlike the OPC concrete that lost 100% of its strength. At

temperatures above 900ºC, the activated matrix densified, and the crystalline phases, such as sodalite, nepheline, albite and akermanite, were identified (William and Ruby 2017).

2.6 FLEXURAL FATIGUE CHARACTERISTICS OF CONCRETE PAVEMENTS

Fatigue failure is one of the major modes of failure in structures like concrete pavements which are subjected to repeated application of loads. The fatigue failure in concrete pavements occur under the influence of repetitive loads or cyclic load, whose peak values are considerably lower than the safe loads estimated through static tests. In fatigue failure, the materials fail by repeated application of load which is not large enough to cause failure due to single application. The fatigue failure in concrete structures causes progressive, localized and permanent damage due to dynamic or moving or cyclic loads. Usually, this change leads to cracking or failure. The failure due to fatigue occurs as a result of development of internal cracks and progressive growth of cracks under the action of cyclic loadings, which leads to failure of the pavements at loads smaller than the modulus of rupture of the concrete (Hui et al. 2007; Lee and Barr 2004).

Although studies on fatigue failure began over many decades, there is still lack of understanding regarding the nature of fracture mechanism in cementitious composite materials due to fatigue. This is due to complex nature of cementitious composite materials and their properties which are influenced greatly by a large number of parameters. The fatigue failure in plain concrete is influenced by several parameters such as composition and quality of the concrete, age of the concrete, moisture conditions, load frequency, minimum stress used in load cycle, stress ratios, rest period, waveform of cyclic load, etc. Fatigue loading can be classified as low cycle and high cycle loading. Low cycle loading is the one which involves application of few load cycles at higher stress ratios; while high cycle loading involves application of large number of load cycles at lower stress ratios. Generally, concrete pavements in highways and airport pavements are classified as high cycle loading. Hence, fatigue strength is one of the important parameters to be considered while designing concrete pavement

for roads and airfields. Most common method of fatigue testing is by using flexural tests.

The development of reliable flexural fatigue life prediction model is one of the toughest challenges in research (Phull and Rao 2007). Over the years, various studies on fatigue behaviour of plain OPC concrete mixes, OPC concrete containing mineral admixtures, fiber reinforced concrete, high performance concrete, etc. have been carried out by researchers. However, there is very meagre research available on the fatigue performance of alkali activated binder concrete mixes. The performance of alkali activated GGBS-FA concrete mixes incorporating steel fibres under fatigue was investigated by Kumar (2012). It was concluded that GGBS-FA concrete mixes with 1% steel fibres displayed better strength as compared 0.5% steel fibres. The addition of steel fibres improved the fatigue life of GGBS-FA concrete mixes. Silva et al (2006) evaluated the performance of AAS concrete in comparison to OPC concrete with emphasis to the fatigue behaviour and reported that the AAS concrete performed better than OPC concrete, which may be mainly due to the strong matrix/aggregate bonding in AAS concrete, probably due to the massive nature of the AAS matrix. The fatigue behaviour of concrete made with two different lightweight aggregate, at stress ratios of 40, 50, 60, 70, and 80 percent of the ultimate static compressive strength was studied by Gray et al. (1961) and it was reported that the fatigue behaviour of light weight concrete as compared to the normal concretes is essentially the same.

Klaiber et al. (1979) investigated the effect of aggregate types, gravel and crushed limestone on the fatigue behaviour of plain concrete in flexure and reported that the flexural fatigue performance of plain OPC concrete was influenced by the type of coarse aggregates used in the concrete. It was observed that the concrete made with gravel displayed better fatigue performance as compared to limestone aggregates. Hui et al. (2007) investigated the flexural fatigue performance of plain concretes containing nano-particles (TiO_2 and SiO_2) and reported improved fatigue life and sensitivity to change in stress. Therefore, addition of fibers or any admixtures may improve the fatigue properties of the concrete.

2.7 ALUMINIUM DROSS

The present study investigates the utilization of recycled aluminium dross from aluminium re-smelting process, in producing pavement quality concrete. There are relatively few successful applications employing recycled aluminium dross and aluminium waste materials in concrete technology.

Aluminium dross is a hazardous waste generated in large quantities during smelting process in aluminium industry. India generates more than 100 thousand tons dross annually (Upendra et al. 2017). The presence of leachable salts like NaCl and KCl in aluminium dross aggravates the environmental crisis, whereas the metallic aluminium entrapped in the matrix of alumina can be used as raw material for metal extraction. Newer applications of aluminium dross include its direct utilization in the production of zeolites, ion exchangers, refractories, composites, cement and concrete products and generation of gases like hydrogen, ammonia, methane. Newer applications of aluminium dross include its direct utilization in the production of zeolites, ion exchangers, refractories, composites, cement and concrete products and generation of gases like hydrogen, ammonia, methane (Arunabh et al. 2018). Aluminium dross has a potential to be converted into other useful material such as catalyst and absorbent by treating it with sodium hydroxide (NaOH) (Ahmad et al. 2016).

Aluminium dross is a mixture of free metal and non-metallic substances (e.g., aluminum oxide and salts). Aluminium nitrides and carbides may also be present, as well as metals oxides derived from the molten alloy. The free-metal content of the dross depends on how carefully skimming from the melt was executed, the composition of the molten alloy, the fluxing, and the dross-cooling process. Drosses with a high metal content (white, or wet, dross that is rich in free metal) typically occur as a compact material in large clotted lumps or blocks. A low metal content typically occurs when scrap is remelted with salts in an open-hearth furnace. This black, or dry, dross is usually granular with a high metal content in the coarse fraction and chiefly oxides and salt in the fines (Manfredi et al. 1997). The percentage of constituents in the respective dross are tabulated in Table 2.4.

Table 2.4. Chemical Composition and Physical Properties of Aluminium Dross
(Gireesh et al. 2016 and Shriraksha et al. 2017)

Particulars	Value
Aluminium Oxide (Al_2O_3)	63.29 – 79.68 %
Silica (SiO_2)	4.14 – 6.36 %
Calcium Oxide (CaO)	4.25 – 20.20 %
Magnesium Oxide (MgO)	0.45 %
Zinc Oxide (ZnO)	0.93 %
Manganese Oxide (MnO)	0.73 %
Ferric Trioxide (Fe_2O_3)	0.32 %
Sodium Oxide (Na_2O)	0.36 %
Ferric Sulphite ($FeSO_3$)	0.68 %
Aluminium Chloride ($AlCl_3$)	0.52 %
Aluminium Nitride (AlN)	0.10 %
Gibbsite ($Al(OH)_3$)	2.18 %
Loss on Ignition	0.05 – 5.30 %
Specific Gravity	3.20 - 3.39
Surface Area, m^2/kg	375 - 380

The aluminium dross was found to retard the hydration reactions in cement mortar during the calorimetric study. The initial and final setting time was found to be extended for more than 2 hours. On the other hand, a decrease in the average size of the pores was seen, which had a progressive influence on the durability characteristics of the final material. Ewais et al. (2009) investigated on calcium aluminate cement mixes. They used both aluminium sludge and aluminium slag in their study.

Few investigations have been done to examine the applicability of using aluminium wastes to manufacture concrete samples. Elinwa and Mbadike (2011) carried out tests on the setting time, flexural and compressive strengths at 5, 10, 20, 30 and 40% cement replacement levels. They conclude that under hot weather concreting, the aluminium wastes serve as a retarder. The optimum substitution level for the better flexural and compressive strengths was found to be at 10% by weight of cement.

Arimanwa et al. (2011) examined the characteristics of concrete produced using aluminium waste (an auxiliary cementitious element) and proposed a prediction model based on Scheffe's theory for the prediction of the compressive strength of aluminium waste-cement concrete. The residue produced from aluminium extrusion plants was employed as a partial substitute for cement in different mix ratios. The initial and final setting times of concrete decreased due to the addition of aluminium waste. The partial replacement of cement with aluminium waste did not modify the density of the resulting concrete significantly. But the aluminium waste absorbed water from the design mix and thereby degraded the workability of the concrete. Mbadike (2014) reports the influence of integration of aluminium waste for producing concrete matrix of diverse water to cementitious ratio and mix proportions. The increase in compressive strength is observed with 5% replacement of aluminium waste.

Petavratzi and Wilson (2007) used aluminium dross as filler in production of non-aerated concrete, concrete bricks and concrete roof tiles. Gireesh et al. (2016) observed that the initial setting time of the recycled aluminium dross concrete extended by about 30 minutes at 20% replacement level. This property of recycled aluminium dross concrete renders it to be suitable for hot weather concreting conditions. Based on the results obtained, the replacement of cement with 20% of Al dross yields superior mechanical and durability characteristics. Studies on mechanical and durability aspects of concrete incorporated with secondary aluminium dross have been done by Satish and Neerja (2016). They observed that up to 15% replacement of cement by secondary aluminium dross, the responses are comparable with the conventional concrete. In this case, water available in the system for maintaining workability decreased due to absorption of water over the high specific surface area of aluminium dross, compared to cement. This makes the mix less workable. Other supplementary cementitious materials such as FA and silica fume were added in various proportions along with secondary aluminium dross and found the improved mechanical and durability properties. They concluded that the concrete incorporated with secondary aluminium dross can be used for making paver blocks, refractory bricks and for normal concrete strength applications.

Shriraksha et al. (2017) used aluminium dross and granular iron slag as partial replacement materials for cement and natural sand, respectively, to develop eco-concrete. Nine mixes were produced with different proportions of cement, aluminium dross, sand and granular iron slag content. The aluminium dross was replaced at 5, 10, 15 and 20% and iron slag at 10, 20, 30 and 40%. The strength and durability properties of the M40 grade concrete employing these two admixture combinations were analysed. It was noticed that the strength and durability properties of the eco-concrete produced by incorporating 5% aluminium dross and 20% iron slag were comparable to that of conventional concrete. The leaching studies on treated and untreated aluminium dross were conducted and found that heavy metals leach within the allowable limits. Therefore, aluminium dross can be used efficiently in construction works without any hazard to the workers and end users (Shriraksha et al. 2017). Also, aluminium dross finds its application in High Performance Concrete which acts as reducing agent for drying shrinkage (Mithun et al. 2021).

2.8   PROCESSED IRON SLAG

The overuse of river sand for construction has various undesirable social and ecological consequences. As a solution for this, various alternatives such as copper slag, iron slag, granite sand, steel slag, quarry dust (or manufactured sand), dune sand, have been considered. This research focuses on using the iron slag as the most viable alternative for fine aggregate in Geopolymer concrete for application in rigid pavements. Anshuman et al. (2016) reviewed the feasibility of a wide variety of industrial by-products such as bottom ash, waste foundry sand, copper slag, plastic waste, recycled rubber waste, crushed glass aggregate etc., as a potential replacement for fine aggregate in the concrete manufacturing process in terms of strength and durability characteristics. A framework for further research has been proposed to attain reliable, robust, eco-friendly and economic concrete as the end product.

Iron slag is less risky to the operators and lower levels of dangerous contaminants, such as asbestos (in olivine) and arsenic (in copper slag). Till now many researches has been carried out in the field of Geopolymer concrete by replacing fine

aggregate using iron slag at 40-50%. The properties of Iron slag are tabulated in Table 2.5.

Table 2.5. Chemical Composition and Physical Properties of Iron Slag (Shriraksha et al. 2017)

Particulars	Value
Aluminium Oxide (Al_2O_3)	3.25 %
Silica (SiO_2)	28.23 %
Ferric Oxide (Fe_2O_3)	62.45 %
Magnesium Oxide (MgO)	1.83 %
Lead Oxide (P_2O_5)	1.45 %
Manganese Oxide (MnO)	1.13 %
Loss on Ignition	0.77 %
Specific Gravity	2.66
Water Absorption	2.95 %
Grading	Zone I

The granular iron slag is a waste/by-product brownish black in colour, which remains after iron ore smelting process. When the furnace is operating at a temperature more than 1500°C, the molten slag is obtained from the bottom of the furnace, which is later cooled by a jet of water and quenched. As the ore materials are heated above 1500°C, at this temperature the slag constituents become inert. So, there will be no reactive silica or alkali in the granular iron slag (Shriraksha et al. 2017). X-ray fluorescence maps show for the first-time discrete iron-rich, titanium-rich and manganese/silicon-rich particles present in blast furnace slag grains, and these particles remain intact when the slag is used as a precursor for alkali-activated slag (AAS) binders. These particles appear to be entrained during slag production, and remain stable under the reducing conditions prevailing during alkali-activation. There is no evidence of chemical interaction between these particles and the AAS binder, which mainly comprises calcium silicate hydrates (Bernal et al. 2011).

Rao et al. (2014) conducted experiments for different grades of concrete i.e., M30 to M70 using blend of crushed stone sand (CSS) and granulated slag sand

(GBS) in the ratio of 50:50 of total fine aggregate in concrete. From this study it is observed that GBS sand and CSS blend could be used as alternative construction material for natural sand in cement concrete applications. Singh and Siddique (2016) designed self-compacting concrete mixes and fine aggregates were replaced with 0, 10, 25, and 40% iron slag. The maximum increase in compressive strength is 20% at all ages (7, 28 and 90 days) with 40% replacement. Properties such as slump flow, V-funnel, U-box, L-box showed lesser workability. SEM and XRD analysis were done to examine the microstructure, which indicated that use of iron slag made the microstructure of SCC denser. Rakesh and Bibhuti (2017) investigated the effect of incorporation of Granulated Blast furnace Slag (GBS) as replacement of natural river sand on the properties of concrete mixes. For this, concrete mixes are prepared with two water/cement ratios (0.45 and 0.5) and three different percentages of GBS (20%, 40%, and 60%). Various properties of concrete mixes such as workability, compressive strength after 7, 28 and 90 days, splitting tensile and flexural strength, and rebound number have been studied to ascertain the influence of incorporation of GBS in concrete. The test results showed an improvement in compressive and tensile strength of concrete with the incorporation of GBS in concrete mixes (Oren et al. 2020; Srinivasarao and Reddy 2020; Huang and Wang 2021).

The most optimum percentage of GBS to be used in normal conditions considering both strength and economy factor is from 40% to 50% and for marine conditions it is from 50% to 60%. The long-term strength development of GBS concrete is almost double of normal concrete in both normal and marine conditions. Therefore, usage of blast furnace slag is one of the promising solutions towards sustainable infrastructure without compromising strength and economy. (Gaurav et al. 2015).

Ali and Sanjayan (2015) say that iron slag is a source of silica and aluminium slag is a source of alumina. These aluminosilicate sources with defined silica/alumina weight ratio are evaluated for possibility of geopolymerization. The alumina and silica are provided from individual sources and geopolymerization is performed by manipulating silica/alumina weight ratio. Ali et al. (2017) analysed alkali-activated FA (geopolymer) samples microstructurally after thermal shock. The prepared samples were heated at 1000ºC, and then quenched in water to room temperature. X-ray

41

diffraction (XRD), and energy dispersive spectroscopy (EDS) were used to analyse the samples. The colour of the interior and exterior section of samples were different, where the former was darker than the latter. XRD results showed that hematite forms in small quantities in both interior and exterior sections. EDS analysis showed the presence of iron-rich points in both sections; however, there were many accumulated iron points in the interior section. It was concluded that, to reduce free energy of the system, dissoluble iron during geopolymerization diffuses through molten channels when geopolymer is being heated and forms accumulated iron regions. Therefore, a study of behaviour of Iron slag-based concrete under thermal shocks needs an attention and a good study area.

The influence of the CaO/SiO_2 ratio, the Al_2O_3 and TiO_2 content of the slag composition on the hydration reaction was analyzed utilizing isothermal heat flow calorimetry, compressive strength development of binder samples, to understand the chemistry of blast furnace slag. The variation of the Al_2O_3 content in the blast furnace slag led to different results. A rise in Al_2O_3 content enhanced the strength if activating with NaOH but resulted in a lower strength if activating with potassium silicate. A decrease in the C/S-ratio yielded to a lower heat evolution, whereas the reaction was delayed if activated with potassium silicate with higher silicate content. The increase of the C/S-ratio will be caused in less condensed slag glass and therefore an enhancement of the reaction degree with a simultaneous decrease of silicate chain length (Ricarda et al. 2015).

2.9   SUMMARY AND GAPS IN LITERATURE

From the detailed literature survey, it is understood that the strength and durability of AAC mixes are affected by many factors such as type of binder, chemical composition of the binder, water-to-binder ratio, percentage of sodium oxide dosage (Na_2O), type of alkali activator, modulus of alkaline activator, water content, type of curing, etc. The AAS and AASF if designed properly obtain higher strength properties and better durability as compared to conventional OPC concrete. AAS and AASF mixes containing greater quantities of GGBS can attain sufficient strength properties even at room temperatures, when subjected to air curing, without any need for heat curing and

other methods. The inclusion of higher amounts of FA in AASFC results in decrease in the strength properties, however the workability increases. The activation energy required for alkali activated mixes containing large proportions of FA is higher and hence replacement of GGBS with FA beyond 50% in AASF systems will require a higher dosage of alkaline activator solution. The combination of sodium hydroxide and liquid sodium silicate if used as alkaline activator provides the best activation for alkali activated binders.

The strength and durability properties of AAC mixes are significantly influenced by the sodium oxide dosage (Na_2O) and activator modulus (M_s) of the alkaline solution. There exists an optimal M_s and sodium oxide dosage (Na_2O) for which the maximum strength properties of alkali activated binders can be obtained. The optimal sodium oxide dosage varies between 3% and 6% of weight of binder for AAS mixes, whereas higher dosages may lead to uneconomic mixtures and with efflorescence problems. The optimal activator modulus (M_s) varies between 0.75 and 1.75 for AAS and AASF mixes. The water to binder ratio, sodium oxide dosage (Na_2O) and activator modulus (M_s) are to be controlled so as to obtain the mixes of required range of strength and workability. Processed Iron slag, an industrial by-product can be looked upon as a potential replacement for traditional aggregates in concrete. Improved or satisfactory performance of Iron slag aggregates have been reported by various researchers when used in conventional OPC concrete, as well as AAC.

Aluminium dross has good impact on setting time enhancement because of slower hydration process. The toxicity and adverse effects of Aluminium dross are within the limits in case of other applications also. Utilization of Aluminium dross as a partial replacement of binder in OPC has given acceptable strength up to 20 % replacement. There is a very limited literature available on utilization of Aluminium dross as binder in AASC and AASF mixes. Aluminium dross as a binder alone might have problems associated with volume changes. Therefore, it holds good with minimum replacement level and with FA or GGBS.

Table 2.6. Summary of literature review related to the present study

Research articles	Factors considered	Important outcomes
Yang et al. 2008; Nath and Sarker 2012; Suman et al. 2017; Raheel et al. 2020	Industrial marginal material – Fly ash	Fly ash, sourced from thermal power plants can be effectively used as an alkali activated binder. Up to 50 % FA can be effectively used as a binder along with GGBS in alkali activated system.
Wang et al. 1994; Zongjin and Sifeng 2007; Rajamane 2013; Suman et al. 2017	Industrial marginal material - GGBS	GGBS, sourced from steel industry can be used as a binder in alkali activated systems. GGBS has 100 % replacement efficiency and has high calcium content leading to better strength.
Gireesh et al. 2016; Upendra et al. 2017; Shriraksha et al. 2017; Mithun et al. 2021	Aluminium dross (New industrial marginal material)	Aluminium dross is sourced from Aluminium refinery industry as secondary dross. Up to 5 % replacement was achieved in few studies, also found to be non-hazardous to the construction workers and end users.
Rakesh and Bibhuti 2017; Oren et al. 2020; Srinivasarao and Reddy 2020; Huang and Wang 2021	Processed Iron Slag (New industrial marginal material)	Processed Iron Slag is sourced from Granulated Blast furnace Slag from Iron and steel industry. PIS aggregates are angular in nature and has micropores. Up to 50 % replacement is possible in OPCC mixes.
Narasimhan et al. 2011; Rashad 2013b; Rajamane 2013; Suman et al. 2017	Alkali Activated Binder system - Parameters	Strength and durability of AAC mixes are affected by many factors such as type of binder, chemical composition of the binder, water-to-binder ratio, percentage of sodium oxide dosage (Na_2O), type of alkali activator, modulus of alkaline activator, water content, type of curing. Sodium oxide dosage of 3 - 6 % and Activator modulus of 0.75 to 1.75 can be considered for determining the optimum mix.

Metha and Gjorv 1974; Chi and Huang 2013; Rajamane 2013; Datta and Ghosh 2014	Durability tests – Acid attack and Sulphate attack	Procedure for determining water absorption and permeable void percentage. Procedure for acid attack and sulphate attack tests by immersing the specimens in sulphuric acid and magnesium sulphate solutions respectively.
Lee and Barr 2004; Silva et al. 2006; Hui et al. 2007; Kumar 2012	Fatigue behaviour of concrete – Weibull distribution modelling	Flexural fatigue behaviour depends on strength developed in the concrete mix. Weibull distribution modelling is preferable for concrete / composite mixtures.

Table 2.6 presents the list of references and important outcomes which paved way for the present study. Based on the outcomes of those works, the formulation of methodology and selection of test parameters were done for the present study.

The use of PIS as fine aggregate in concrete is associated with problems related to water absorption and thereby leading to less workability. Even though PIS acts as inert material, it may have slight influence on pozzolanic behaviour of binders showing positive sign about strength gain. It adds strength to concrete because of additional formation of denser C-S-H gel under alkaline activation. Up to 50 % replacement of iron slag is possible without any adverse effects on the concrete mix. However, till date, only few researches have been done to replace iron slag without processing up to 50 %.

CHAPTER 3

MATERIALS AND METHODOLOGY

3.1 GENERAL

The selection of materials for the production of concrete is one of the important steps in the mix design procedure. This chapter provides a detailed description of the various steps involved in the mix design process for OPCC, AASC and AASFC mixes. The materials used, preliminary mix design, preparation of specimens and procedures adopted for the evaluation of hardened concrete in terms of compressive strength, split tensile strength, flexural strength, modulus of elasticity, water absorption, volume of permeable voids etc., are explained in this chapter in detail.

3.2 INGREDIENT MATERIALS

The constituent materials to be used for the production of concrete mix should satisfy the basic requirements as per the relevant standard codes. Proper understanding of the basic properties of these ingredients plays a vital role in the mix design procedure, strength and durability behaviour performance of the concrete. The basic properties of various materials used for the preparation of OPCC, AASC and AASFC mixes are discussed in the following sections.

3.2.1 Cement

Cement is one of the important constituents of the concrete mix. In the present investigation, Ordinary Portland Cement (OPC) of 53 grade conforming to IS: 12269 - 2013 was used. The properties of the cement are tabulated in Table 3.1.

3.2.2 Ground Granulated Blast-Furnace Slag

Ground Granulated Blast furnace Slag is the most widely investigated and probably the most effective cement replacement material used in concrete. In the present investigation, GGBS produced at M/s JSW Iron and Steel Company, Hospet,

Karnataka, India was procured from a local retailer. The chemical composition and physical properties of GGBS are presented in Table 3.2.

Table 3.1. Properties of OPC used in the present study

Sl. No	Tests	Results	Limits as per IS: 12269-2013 / IS: 269-2015
1	Specific Gravity	3.12	-
2	Standard Consistency, %	30	-
3	Fineness of cement (m^2/kg)	330	Minimum 225
4	Setting time - Initial (minutes)	65	Minimum 30
	- Final (minutes)	375	Maximum 600
5	Compressive Strength (MPa) - 3 Days	29	Minimum 27
	- 7 Days	40	Minimum 37
	- 28 Days	57	Minimum 53

Table 3.2. Chemical and Physical properties of GGBS (Suman et al. 2017)

Constituents	Oxide Content
CaO	34.77 %
Al_2O_3	16.70 %
Fe_2O_3	1.20 %
SiO_2	32.52 %
MgO	9.65 %
Na_2O	0.16 %
K_2O	0.07 %
Insoluble Residue	4.03 %
Loss on Ignition	0.04 %
Blaine's Fineness (m^2/kg)	370
Specific gravity	2.90

3.2.3 Fly Ash

Fly ash, is a by-product obtained from coal burning in Thermal power plants. FA (Class F) was procured from Udupi Thermal Power Plant (UTPS), Padubidri, Karnataka, India was used for the present investigation and the chemical and physical properties of FA are tabulated in Table 3.3.

Table 3.3. Chemical and Physical Properties of FA (Class F) (Suman et al. 2017)

Constituents	Oxide content	Requirements as per IS: 3812 (Part II) -2003
SiO_2	58.87 %	35% min
Al_2O_3	32.17 %	SiO_2+ Al_2O_3+ Fe_2O_3
Fe_2O_3	2.93 %	combined 70% min
CaO	0.79 %	5% max
Na_2O	0.37 %	Total alkalies,
K_2O	1.14 %	5% max
SO_3	0.65	2.75% max
Loss on Ignition	0.03%	12% max
Fineness (m^2/kg)	425	320 min
Specific Gravity	2.20	-

3.2.4 Aluminium dross

Aluminium dross is obtained from an Aluminium dross disposal dealer at Mumbai, Maharashtra. Specific gravity of Aluminium dross is 2.9, Fineness is 380 m^2/kg and more than 70 % of the sample is passing 90 micron sieve. Aluminium dross is tested conforming to the standards of OPC Cement (IS: 12269 – 2013). Based on the preliminary investigations, 5% of Aluminium dross was added to the developed concrete mixes through weigh batching.

3.2.5 Fine Aggregates

In the present investigation, locally available river sand conforming to Zone II of IS: 383-2016 was used as fine aggregate. The river sand was tested according to

IS: 2386 (Part I-IV)-1963. The physical properties and gradation of river sand are tabulated in Table 3.4 and 3.5 respectively.

3.2.6 Processed Iron Slag Aggregates

In the present investigation, Processed Iron Slag was obtained from JSW Iron and Steel Industry, Hospet, Karnataka, India. The PIS is greyish in colour, having an angular shape with porous texture surface and glassy appearance. Maximum size of 4.75 mm aggregate was considered for the present study. The chemical composition of PIS constitutes oxides of iron, calcium and silicon as the major composition along with oxides of magnesium, aluminium and other metals in small quantities. Physical properties and gradation of PIS aggregates are tabulated in Table 3.4 and 3.5 respectively. The chemical composition of PIS aggregates is tabulated in Table 3.6.

3.2.7 Coarse Aggregates

Crushed granite aggregates of maximum aggregate size of 20 mm conforming to IS: 383-2016 was used for the present investigation. The physical properties and gradation analysis of natural coarse aggregates are done as per IS: 2386 (Part I - IV) - 1963 and the results are tabulated in Table 3.4 and 3.5 respectively. The aggregates used were in saturated surface dry condition.

Table 3.4. Physical characteristics of aggregates

Sl. No	Test	PIS	River sand	Crushed granite	Method of Test
1	Specific Gravity	2.97	2.62	2.67	IS 2386 (P-III) - 1963
2	Bulk Density: Loose (kg/m^3)	1466	1475	1495	
	Compact (kg/m^3)	1535	1548	1593	
3	Aggregate Crushing Value (%)	-	-	24	
4	Los Angeles Abrasion value (%)	-	-	20	IS 2386 (P-IV) - 1963
4	Aggregate Impact value (%)	-	-	21	
5	Water Absorption (%)	1.97	0.90	0.50	

Table 3.5. Gradation of aggregates used for the study

Fine aggregates				Coarse aggregates		
Sieve No (mm)	IS:383-2016 requirement	% Passing of River Sand (%)	% Passing of PIS aggregates (%)	Sieve No (mm)	Requirement as per IS:383-2016	% Passing of Crushed granite (%)
10	100	100	100	20	95-100	97
4.75	90–100	98	92	10	25-55	38
2.36	75–100	94	82	4.75	0-10	6
1.18	55–90	80	70			
0.6	35–59	39	52			
0.3	8–30	15	24			
0.15	0–10	2	6			

Table 3.6. Chemical composition of PIS

Constituent	Oxide Content (% by weight)
CaO	41.52
Free CaO	5.33
Al_2O_3	4.12
Fe_2O_3	22.54
SiO_2	15.04
MgO	6.17
Na_2O	0.14
K_2O	0.05
SO_3	0.08
Insoluble Residue	9.97
Loss on Ignition	0.25

Chemical composition of PIS aggregates used in the present study is given in Table 3.6. It can be observed that the calcium oxide content is higher in PIS aggregates which may lead to additional reactions when used in alkali activated concrete mixes. Secondary reactions in alkaline medium may enhance strength even though PIS

aggregates are utilized as fine aggregates which has to be inert in nature. But the composition also has free calcium oxide content leading to deposition of calcite on the aggregate particles and hinder the aggregate-paste bonding in concrete mixes developed. Free calcium oxide or free lime along with free magnesia content present in PIS aggregates forms deposition of calcite layer on aggregates if not processed properly before using in the concrete. Therefore, PIS aggregates must be allowed to undergo the weathering process before using as an aggregate for construction purposes because of its expansive nature due to the presence of free lime and free magnesia. The presence of free lime content more than 1% cause adverse effects on the properties of slag aggregates. Free CaO present in the slag react with atmospheric CO_2 to form calcium carbonate ($CaCO_3$); which gets deposited on the surface of aggregates in the form of white powder (FHWA 2012). The FHWA (2012) specifies a maximum free lime content of 7% and 4% in PIS aggregates when used in unbound applications and hot mix bituminous pavements respectively. Maximum free lime content in slag aggregates for use in cement bound layers is not specified. However, it is advisable to subject the slag to weathering until the free lime content is brought to a level, beyond which the volume expansion becomes minimal. Hence, in the present investigation, free lime content in the slag lower than 1% was considered as the "acceptable limit" and the PIS were weathered for a period of more than 2 months. The PIS aggregates were exposed to open air conditions and water was poured regularly up to 60 days in order to bring the free lime and free magnesia contents within acceptable limits.

The weathered PIS aggregates were subjected to washing in order to have the surface of aggregates clean and free from impurities. The free lime contents before and after the weathering were identified using Ethylene Glycol Extraction method (Gebhardt 1988). The volume stability was also conducted using modified auto-clave technique developed by Edw. C. Levy company (Yildirim and Prezzi 2009) and the volume expansion was found to be 0.091% which may be considered negligible. The free lime results determined by ethylene glycol extraction method, by considering average of three trials are 5.33 and 0.16 % for un-weathered and weathered slag samples respectively. The free lime content was reduced by 5.17 % after weathering process. After the free lime content and volume stability were found to be within acceptable

limits, the PIS aggregates were used in AASC and AASFC mixes to test the hardened properties.

3.2.8 Water

Potable tap water available in the institute laboratory was used for casting of all specimens and for the curing of OPC based concrete specimens in the present investigation. The same water was utilized for the preparation of alkaline activator solution.

3.2.9 Super-plasticizer

The super-plasticizer used was commercially available sulfonated naphthalene formaldehyde (SNF) polymer admixture (Conplast SP 430) supplied by FOSROC, Chemicals (India) Pvt. Ltd. Properties of super-plasticizer are tabulated in Table 3.7 (As per the manufacturing company data).

Table 3.7. Properties of Conplast SP 430

Properties	Values
Specific Gravity	1.20
Chloride Content	Nil
Solid content	40%
Operating Temperature	10 to 40°C
Colour	Dark brown liquid

3.2.10 Alkaline Activators

The mixture of sodium hydroxide (NaOH) and liquid sodium silicate (Na_2SiO_3) have proved to deliver the best performance in alkali activated binders (Rashad 2013b). Hence, in the present investigation, a combination of sodium hydroxide and liquid sodium silicate is used as the alkaline activator.

Commercial or industrial grade sodium hydroxide flakes (97% purity) and liquid sodium silicate were procured from local retailers. The liquid sodium silicate was

tested as per IS: 14212-1995 for the physical properties and the results are tabulated in Table 3.8. The physical properties of sodium hydroxide are presented in Table 3.9. The alkaline activator solution was prepared by dissolving the sodium hydroxide flakes in sodium silicate solution in proper proportion in order to achieve the desired activator modulus (Ms = SiO_2/Na_2O) and sodium oxide (Na_2O) dosage. The solution was stirred properly and water was added in order to bring the solution to contain total a water content equivalent to water/binder (w/b) of 0.20 of total binder content. The solution was stored in tight plastic container one day prior to mixing. The solution was brought to the required total water content (water/binder ratio) by mixing extra water during the time of casting of specimen.

Table 3.8. Properties of Sodium Silicate solution

Constituents	Values
Na_2O% (by weight)	14.7
SiO_2% (by weight)	32.8
Water% (by weight)	52.5
% of solids (by weight)	47.5
Ms (SiO_2/Na_2O)	2.23
Specific gravity	1.57

Table 3.9. Properties of Sodium Hydroxide (97% purity)

Constituents	Values
Molar mass	39.9971 g/mol
Appearance	White solid
Specific Gravity	2.1
Solubility in water	114g / 100 ml (25°C)

3.3 OPTIMIZATION OF MIX DESIGN FOR ALKALI ACTIVATED BINDER MIXES

The activator modulus (Ms) and sodium oxide (Na_2O) dosage have significant influence on the strength properties of the alkali activated binders. For each type of binder, there

54

exists an optimal activator modulus for which the mix attains highest strength activated at constant sodium oxide dosage. Hence, it is necessary to identify the optimal activator modulus based on the strength requirement. Preliminary studies were carried out to determine the strength of AASC and AASFC mixes at different activator modulus and sodium oxide dosages. Based on the results, the optimal activator modulus for different mixes were identified and later these mixes further optimized to identify the optimal sodium oxide dosages based on strength requirement. According to the Indian standard code IRC: 58 - 2015, pavement quality concrete (PQC) should have a minimum compressive strength of M40 and a slump value in the range 25+/-15 mm.

Preliminary mix design was carried out for AASC and AASFC mixes in order to identify an optimal sodium oxide dosage and activator modulus to achieve the desired strength grade of M40 with workability (slump cone value) of 25+/-15 mm. The AASC and AASFC mixes were prepared using binder content of 425 kg/m^3 with water to binder ratio (w/b) of 0.40. In case of AASC, 100% GGBS was used as the binder; while in case of AASFC, GGBS: FA in the ratios 75:25, 50:50 and 25:75 were used as binders. The mixes were activated at sodium oxide (Na$_2$O) dosages of 4% and 5% (by weight of binder content) and the activator modulus was varied between 0.75 to 1.75. The activator modulus for which the mix attained the maximum compressive strength was considered for further optimization for determining the optimal content of sodium oxide dosage as per the desired strength. Cube specimens of size 100 mm were prepared and tested for compressive strength after 28 days of air curing. The results are presented in Figs.3.1 to 3.4. The workability was determined using the slump cone test as it would help to carry out water content correction based on the required slump and strength of the mixes tested for compressive strength after 28 days of air curing. The results are presented in Figs.3.1 to 3.4. The workability was determined using the slump cone test as it would help to carry out water content correction based on the required slump and strength of the mixes. The compressive strength results for AASC (100:0) and AASFC (75:25, 50:50 and 25:75) mixes at 4% and 5% sodium oxide dosages and for different activator modulus are depicted in Figs. 3.1 to 3.4 respectively. Also, the values of compressive strength are tabulated in Table 3.10.

Table 3.10. Compressive strength values of AASC and AASFC mixes with varying Ms

Mix Proportions	Compressive Strength in MPa									
	4 % Na$_2$O with Ms of					5 % Na$_2$O with Ms of				
	0.75	1.00	1.25	1.50	1.75	0.75	1.00	1.25	1.50	1.75
AASC (100:0)	43	48	53	49	44	50	56	62	54	49
AASFC (75:25)	41	45	50	45	42	47	52	57	50	46
AASFC (50:50)	37	41	47	40	39	44	47	53	46	42
AASFC (25:75)	33	37	42	36	32	40	44	48	43	41
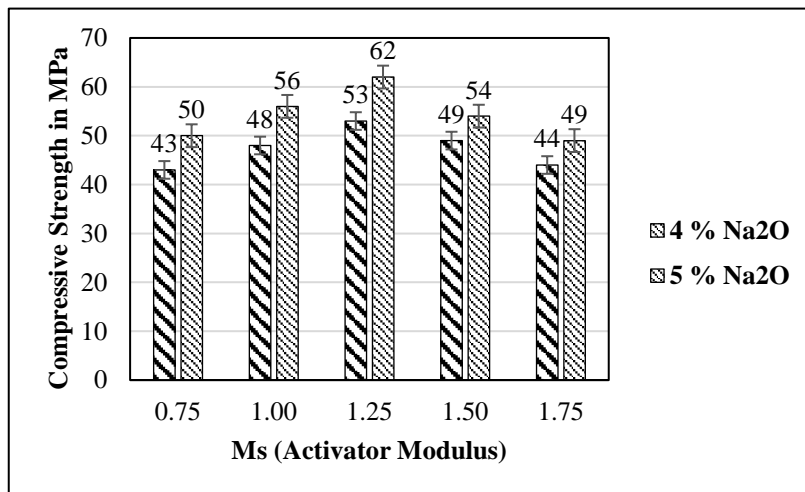
Figure 3.1 Compressive strength of AASC (100:0) with varying Ms
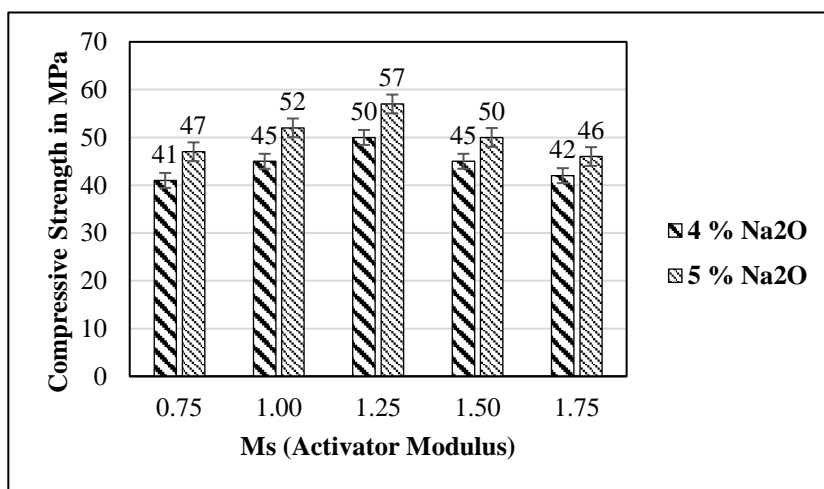
Figure 3.2 Compressive strength of AASFC (75:25) with varying Ms

56
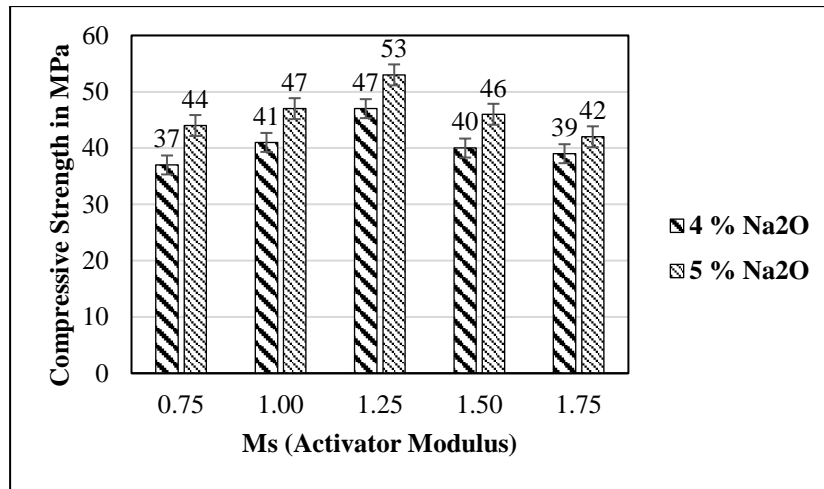
Figure 3.3 Compressive strength of AASFC (50:50) with varying Ms
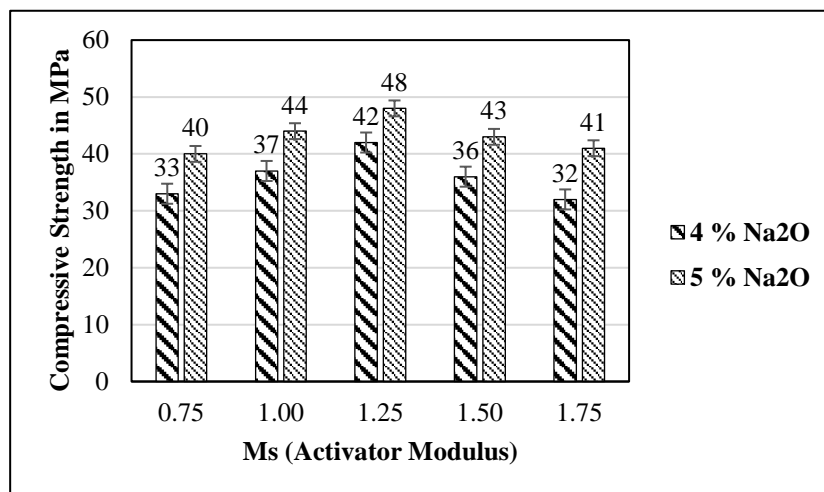
Figure 3.4 Compressive strength of AASFC (25:75) with varying Ms

From the results, it can be noticed that the activator modulus of the solution has significant influence on the compressive strength of AASC and AASFC mixes. All the mixes follow a similar and definite trend line. The compressive strength increases with the increase of activator modulus until an optimal point is reached and later decreases with further increase of activator modulus. The increase in activator modulus implies the increase in the concentration of the anions of sodium silicate in the activator solution which helps the dissolution process of the binder materials contributing higher strength to the mix (Shi and Li 1989). It can be noticed that the mixes 100:0, 75:25 and 50:50 mixes attain the highest compressive strength at an optimal activator modulus of 1.25

at both 4% and 5% sodium oxide dosages; however, for mix 25:75, the optimal activator modulus is 1.50. The strength of AASC mixes (100:0) is higher than AASFC mixes (75:25, 50:50 and 25:75) at all dosages. AASC mix at an activator modulus of 1.25 exhibits the highest strength at 5% Na_2O dosage.

The compressive strengths of the mixes reduced with the incorporation of FA for a constant Na_2O dosage. This may be attributed to the lower reactivity to FA as compared to GGBS. However, the reduction in the strength is not significant at lower level of replacement (i.e., for mix 75:25). Replacement of GGBS beyond 50% (by weight of binder content) with FA resulted in crucial reduction in the compressive strength in AASFC mixes at a constant Na_2O dosage. This indicates that the inclusion of more than 50% (by weight of binder content) FA in the alkali activated binder system affects the kinetics of reaction at early times of curing. This is likely to be due to the alkalinity supplied by the activator, under the formulation conditions assessed, not being sufficient to promote the extensive reaction of the FA at early age. The slow reactivity of the starting material when cured at room temperature for AASFC containing higher content of FA (> 50% by weight of binder content) at 4% Na_2O dosage show the lower compressive strength (Idawati et al. 2013). However, AASFC (25:75) still achieved a compressive strength up to 30 MPa at an activator modulus of 1.5 and at 4% sodium oxide dosage. At room temperature, the lower reactivity of FA leads to slower strength development along ultimate strength in AASFC mixes, containing high amounts of FA in the binder (Nath and Sarker 2012). However, at higher sodium oxide dosages i.e., 5% the AASFC mixes (25:75) developed adequate strength after 28 days of curing. It was noticed that, at constant water/binder ratio of 0.40, the mixes containing FA displayed higher workability. Table 3.11 presents the sodium oxide dosages and activator modulus adopted for AASC and AASFC mixes. In Table 3.11, **A** represents AASC (100:0), **B** represents AASFC (75:25), **C** represents AASFC (50:50) and **D** represents AASFC (25:75).

From the preliminary investigations, it was observed that the mixes AASC (100:0) and AASFC (75:25) satisfied both strength and workability at sodium oxide dosage of 4% and activator modulus of 1.25. However, the mixes AASFC (50:50) and AASFC (25:75) achieved greater slump than the required slump, but did not satisfy the

compressive strength requirements at the optimal activator modulus. Therefore, revision of sodium oxide dosages for AASFC (50:50) and AASFC (25:75) was done with simultaneous reduction in the water/ binder ratio for the optimal activator modulus. Based on trials, sodium oxide dosage of 4.5% with 0.38 w/b and 5.5% with 0.38 w/b ratios was adopted for AASFC (50:50) and AASFC (25:75) respectively. The revised dosages and water binder ratios were selected such that the compressive strength and workability of all mixes fall in the similar range i.e., M40 grade strength and slump value of 25+/-15 mm.

Table 3.11. Sodium oxide dosages and activator modulus for AASC and AASFC

Mix ID	Sodium oxide dosage (%)	Water/binder	Activator modulus (Ms)
A	4.0	0.4	1.25
B	4.0	0.4	1.25
C	4.5	0.38	1.25
D	5.5	0.38	1.50

3.4   CONCRETE MIX DESIGN

The mix design for OPC concrete is based on the procedure suggested by IS: 10262- 2019. The total binder content is restricted to 425 kg/m^3, with water/binder ratio of 0.40 and coarse aggregate : fine aggregate ratio of 0.64 : 0.36. The mixes were designed to achieve a slump value of 25+/-15 mm. A super plasticizer dosage of 0.4 % (by weight of binder content) was added to the mix to arrive at the designated slump.

Aluminium dross was added to the OPCC mixes at 5, 10, 15 and 20 % of the binder, to determine the optimum replacement level. The strength achieved at 5 % aluminium dross was comparable with control concrete mix, whereas the decrement of strength was observed with further increase in aluminium dross content. But, the swelling or expansion of concrete on the surface of cube moulds was observed after initial setting of concrete. The expansion went up to 10 mm which is not acceptable in case of Pavement Quality Concrete (PQC). As the entire surface of pavement slab may

suffer from expansion and thereby undulations resulting in failure of the pavement, Aluminium dross was not used in further stages of development of concrete.

The AASC mixes are proportioned to contain same binder content (425 kg/m^3) and water/binder ratio (0.4) as that of OPCC mix. The AASFC were prepared using similar binder content by mixing GGBS: FA in the ratios 75:25, 50:50 and 25:75 with calculated water /binder ratios as tabulated in Table 3.11. Additionally, Aluminium dross was added at 5% of the total binder content, i.e., 5% of 425 kg/m^3. Even though the swelling effect was lesser in AASC and AASFC mixes when compared to OPCC mixes, the expansion of around 5 mm was witnessed due to aluminium dross replacement. Further, the usage of aluminium dross in AASC and AASFC was dropped, even though it had an advantage of increased setting time in AASC mixes. Total water content in the activator solution for AAB mixes constituted the sum of water readily available in liquid sodium silicate solution plus the extra water added, to arrive at the required water/binder ratio. The alkali activator solutions were proportioned separately for each type of mix to provide desired dosage of Na$_2$O (by weight of binder), with an optimal activator modulus (Ms) and total water/binder ratio as provided in Table 3.11 (as determined from preliminary investigations). No super-plasticizers were added for AAB mixes. Further AASC and AASFC mixes were prepared with PIS fine aggregates by replacing the natural river sand by 25, 50, 75 and 100% (by volume) keeping the volume of total fine aggregates constant. The aggregates used were in saturated surface dry condition. The details of mix proportions for OPCC, AASC and AASFC are listed in Table 3.12.

In Table 3.12, OPCC - represents Portland cement based control mix; 4-A-0 represents AASC mix with river sand at 4% Na$_2$O dosage. 'P-A-Q' AASC mixes with 'Q' (% by volume) of natural aggregates replaced with PIS aggregates at 'P' (% by wt of binder) Na$_2$O dosage. Similarly, B, C and D represent AASFC mixes of 75:25, 50:50 and 25: 75 of FA respectively. CA represents coarse aggregate content in Table 3.12.

3.5 MIXING, PLACING, COMPACTING AND CURING OF CONCRETE MIXES

The mixing, placing and compaction of AASC and AASFC were done in a similar way as that of conventional concrete. The solids constituents of the mix i.e., the aggregates and the binder were dry mixed in the concrete mixer of 100 kg capacity for about two minutes. Later the activator solution is added to the dry mix and wet mixing continued for another two minutes. After proper mixing, the fresh concrete was poured into moulds for preparation of specimen in 3 layers with proper compaction. The wet mix was thoroughly compacted on a vibrator and kept in humid and cool place at ambient room temperature and relative humidity (80-90%) for about 24 hours. After 24 hours, the specimens were demoulded. After demoulding the OPCC specimens were cured in water tank at room temperature while the AASC specimen were subjected to air curing (general laboratory conditions) at relative humidity of 80-90% and room temperature of $(27\pm3°C)$. In order to evaluate the strength and other characteristics, the various specimens were cast. The details of the specimens used for various tests are given in Table 3.13. Sample mix design procedure for OPCC mix and AAS mixes are presented in *Appendices I and II* respectively for better understanding.

3.6 TESTING OF CONCRETE MIXES

After proper mixing of the ingredients in the mixer, the specimens of different dimensions (as given in Table 3.13) were prepared in order to test the hardened and durability properties. All the tests were conducted as per relevant standard codes at different ages.

3.6.1 Workability of Fresh Concrete

In the present investigation, the workability i.e., the ease of compaction was determined using the slump cone test in conformation to IS:1199-1959. The test was conducted immediately after the mixing of ingredients.

Table 3.12. Details of mix designations and mix proportions of concrete mixes

Mix ID	GGBS (kg/m³)	FA (kg/m³)	Sand (kg/m³)	PIS (kg/m³)	CA (kg/m³)	Liquid Na_2SiO_3 (kg/m³)	NaOH Flakes (kg/m³)	Water added (kg/m³)	Total Water (kg/m³)	SP (kg/m³)
OPCC	-	-	655	0	1186	-	-	169		1.7
4-A-0	425	0	643	0	1165	64.8	9.6	136		
4-A-25	425	0	482	181	1165	64.8	9.6	136	170.0	
4-A-50	425	0	322	362	1165	64.8	9.6	136		
4-A-75	425	0	161	543	1165	64.8	9.6	136		
4-A-100	425	0	0	724	1165	64.8	9.6	136		
4-B-0	319	106	643	0	1165	64.8	9.6	136		
4-B-25	319	106	482	181	1165	64.8	9.6	136		
4-B-50	319	106	322	362	1165	64.8	9.6	136	170.0	
4-B-75	319	106	161	543	1165	64.8	9.6	136		
4-B-100	319	106	0	724	1165	64.8	9.6	136		
4.5-C-0	212.5	212.5	641	0	1149	72.9	10.5	123		
4.5-C-25	212.5	212.5	478	179	1149	72.9	10.5	123		
4.5-C-50	212.5	212.5	314	358	1149	72.9	10.5	123	161.5	
4.5-C-75	212.5	212.5	154	540	1149	72.9	10.5	123		
4.5-C-100	212.5	212.5	0	708	1149	72.9	10.5	123		
5.5-D-0	106	319	622	0	1121	106.9	9.9	101		
5.5-D-25	106	319	459	158	1121	106.9	9.9	101		
5.5-D-50	106	319	302	335	1121	106.9	9.9	101	157.3	
5.5-D-75	106	319	132	516	1121	106.9	9.9	101		
5.5-D-100	106	319	0	681	1121	106.9	9.9	101		

Table 3.13. Specimen details for various tests

No.	Types of test	Specimen type	Specimen dimension (mm)	Relevant Standards
1	Compressive strength	Cube	100	IS 516-1959
2	Flexural strength	Beam (L*B*D)	500*100*100	IS 516-1959
3	Split tensile strength	Cylinder	100(dia)*200(height)	IS 5816-1999
4	Modulus of Elasticity	Cylinder	150(dia)*300(height)	IS 516-1959
5	Water absorption and Volume of Permeable Voids	Cube	100	ASTM C642-13
6	Acid Attack	Cube	100	-
7	Sulphate attack	Cube	100	-
8	Flexural fatigue testing	Beam (L*B*D)	500*100*100	-

(L*B*D = Length x Breadth x Depth)

3.6.2 Mechanical and Durability Properties of Hardened Concrete

The concrete specimens were tested at different ages to determine the hardened mechanical and long-term durability properties. The OPCC specimens were tested in wet condition at all ages, while all the AAC specimens were immersed in water for 2 hours before testing. An average of three samples was considered for each mix using calibrated machines. The mechanical properties such as compressive strength, static flexural strength, split tensile strength and modulus of elasticity were determined as per relevant Indian standards. The tests for water absorption and Volume of Permeable Voids (VPV) were performed as per the procedure suggested by ASTM C642-13. The test procedures for sulphuric acid attack and magnesium sulphate attack were adopted from the literature.

3.6.3 Acid Attack

Sulphuric acid resistance tests conducted on 100 mm concrete test specimens immersed in containers filled with 1% sulphuric acid solution (pH = 1). The pH levels of the sulphuric acid solutions were examined by means of a portable digital pH meter (standard error ± 0.05). Concentrated sulphuric acid was often added in regular intervals to maintain the pH level. Acid solution was replaced with fresh 1% solution after every month. The compressive strength was measured up to 365 days at regular intervals.

3.6.4 Sulphate Attack

Sulphate resistance tests on concrete samples were carried out on 100 mm cubes using the test method suggested by Metha and Gjorv (1974). Concrete specimens after 28 days of curing, were immersed in solution, containing 5 to 10% Magnesium Sulphate ($MgSO_4$) by maintaining a constant pH in the range 6.5 to 7.5. The pH was checked every 15 days using portable digital pH meter (standard error $\pm$ 0.05). The pH is balanced to the required level (6.5 to 7.5) by adding calculated amount of concentrated nitric acid (HNO_3) to the magnesium sulphate solution, whenever solution becomes alkaline after immersion of cubes. The solutions in containers were replaced every month up to one year. The compressive strength was measured at regular intervals up

to 365 days / one year. The specimens kept for acid resistance and sulphate resistance tests are shown in Fig. 3.5.

Figure 3.5 Specimens kept for Acid and Sulphate Resistance Tests

3.6.5   Flexural Fatigue Testing

The flexural fatigue tests on OPCC and AAC samples were carried out on beam specimens of dimensions 500 x 100 x 100 mm on MTS servo-controlled hydraulic repeated load testing machine having a capacity of 5 tonnes. The fatigue tests were conducted on OPCC and AASC/AASFC samples containing 0, 50 and 100% PIS aggregates. Five specimens were tested for each mix at each stress ratio. The static flexural strength of the mixes was recorded at 90 days before the fatigue test was conducted. The beam specimens were loaded at the same span (i.e., 400 mm) as it was loaded in case of static flexural tests. The specimens were subjected to loading using constant amplitude half sinusoidal wave form at a frequency of 3 Hz without any rest period. The test setup was calibrated applying initial loading and the frequency of loading was maintained constant throughout the test for all specimens. The minimum load is maintained as zero while the maximum load was adjusted based on the required stress ratio (percentage or fraction of flexural load taken by beam specimens corresponding to the flexural strength of M40 grade concrete).

Fatigue testing is a very time consuming and expensive process and a large number of samples have to be tested. The test was terminated when the specimen fails to take up the load and breaks. In the experimental investigation, it was found that the

specimen reached the maximum number of repetitions (nearly one lakh) at stress ratio 65%. Hence, in this study, the stress ratios were limited to 70, 75, 80 and 85%, denoted as 0.70, 0.75, 0.80 and 0.85 respectively. As the uncertainty involved in this test is very high, the maximum stress ratio was restricted to 85%. The fatigue tests were conducted at different stress ratios, i.e., 70, 75, 80 and 85 % to obtain a relationship between different stress ratios (FL) and the number of cycles to failure (N). The test was conducted at the end of 90 days of curing of beam specimens in order to eliminate the errors occurring due to the strength development of concrete mixes after 28 days of curing. The Fatigue life (N) i.e., the number of cycles up to failure of the sample was recorded for each specimen.

The equipment used in the present study for fatigue analysis was manufactured by M/s Spranktronics, Bengaluru, Karnataka. Fig 3.6 shows the accelerated fatigue testing equipment used in this study and it has the following main components:

1. Loading Frame and loading system
2. Load sensing devices
3. Deflection recording system (LVDTs)
4. Servo Amplifier system
5. Control unit to monitor load and repetitions
6. Computer system

Loading frame and loading system: It consists of a double acting hydraulic cylinder with suitable mounting flanges. It is associated with a power pack unit consisting of pump coupled with motor (1 HP, 3-phase, 1440 rpm), valves and filters, heat exchanger (cooling system), servo valve, pressure gauge, etc.

Load sensing devices: These are used to sense the applied load to the specimen during testing. The load cell used for testing was of capacity 50 kN (5000 kg).

Deflection recorder: LVDTs are used to sense the deflections with the help of suitable signal conditioners and display panels.

Frequency and waveform of loading: The loading is generally with half sinusoidal waveform (zero -maximum load-zero). The application frequency can vary between 1 - 5 Hz with or without rest period.

Servo amplifier system: It is used to link the function generator and the servo valve.

Control unit: It is used to monitor the load and the repetitions. It is connected to the PC with an ADD ON Card to acquire or log the data.

Figure 3.6 Accelerated fatigue testing equipment

3.7 SUMMARY

In this chapter, investigations are discussed which were carried out to characterize the constituent materials. Preliminary investigations were carried out to arrive at the optimized mix design. The mix design for OPCC was carried out as per standard available guidelines. The optimal sodium oxide dosage, activator modulus and water content for different binder types was identified as per the strength (M40) and workability (slump cone value of 25+/-15 mm) requirements and the mix design for AASC and AASFC mixes was optimized. The AASC and AASFC were prepared using binder content of 425 kg/m^3 with water to binder ratio (w/b) of 0.40. In case of AASC, 100% GGBS was used as the binder; while in case of AASFC, GGBS: FA in the ratios 75:25, 50:50 and 25:75 were used as binders. Additionally, aluminium dross was added at 5% of the total binder content and discarded due to expansion issues. The mixes were activated at sodium oxide (Na$_2$O) dosages of 4% and 5% (by weight of binder content) and the activator modulus was varied between 0.75 to 1.75. The mixes 100:0, 75:25 and 50:50 mixes attained the highest compressive strength at an optimal activator modulus of 1.25 at both 4% and 5% sodium oxide dosages; however, for mix 25:75, the optimal activator modulus is 1.50. The compressive strengths of the AASFC mixes

reduced with the incorporation of FA for a constant Na_2O dosage. This may be attributed to the lower reactivity of FA when compared to GGBS. At constant water/binder ratio of 0.40, the mixes containing FA displayed higher workability. The mixes AASC (100:0) and AASFC (75:25) satisfied both strength and workability at sodium oxide dosage of 4% and activator modulus of 1.25. However, the mixes AASFC (50:50) and AASFC (25:75) achieved greater slump than the required slump but did not satisfy the compressive strength requirements at the optimal activator modulus. Therefore, revision of sodium oxide dosages for AASFC (50:50) and AASFC (25:75) was done with simultaneous reduction in the water/ binder ratio for the optimal activator modulus. Based on trials, sodium oxide dosage of 4.5% with 0.38 w/b and 5.5% with 0.38 w/b ratios were adopted for AASFC (50:50) and AASFC (25:75) respectively. PIS aggregates were incorporated in the optimized AASC and AASFC mixes at different replacement levels i.e., 0, 25, 50, 75 and 100% (by volume). The mixing, placing, curing and size of specimens were explained in detail. The preparation of the concrete specimens, properties investigated, the test methodologies followed for testing specimens were explained in detail.

CHAPTER 4

MECHANICAL PROPERTIES OF CONCRETE MIXES DEVELOPED

4.1   GENERAL

In this chapter, the observations made on the mechanical properties of AASC and AASFC mixes with partial or complete replacement of river sand with PIS aggregates both in fresh and hardened state are discussed. The workability and unit weights are initially discussed and this is followed by a detailed discussion on the strength properties like compressive strength, flexural and split tensile strength and modulus of elasticity. The results obtained from the experiments are analyzed and discussed.

4.2   WORKABILITY

The slump cone test was performed according to the procedure suggested in IS: 1199- 1959. The slump values obtained for different concrete mixes are tabulated in Table 4.1. The OPCC, AASC and AASFC mixes attained the target slump values for which they were designed. During the preliminary investigation, it was observed that the slump increased with the inclusion of higher FA content in AASFC mixes. The addition of aluminium dross showed increased setting time which becomes useful in hot weather conditions. It was noticed that the workability increased drastically after inclusion of more than 50% FA in the AASFC mix. The inclusion of FA required less water to achieve desirable workability due to the particle size and morphology of this precursor (Wang et al. 2003), thus facilitating a lower water/binder (w/b) ratio with equivalent workability. Hence the water/binder (w/b) ratios for AASFC (50:50, 25:75) were reduced in order to achieve a slump in the range 25+/-15 mm. Incorporation of PIS in the AASC and AASFC mixes resulted slight decrease in slump value. This is due to the fact that PIS aggregates are porous and angular in shape, which cause a slight decrease in workability. Concrete prepared with PIS aggregates require slightly higher water/binder ratio to achieve a designated slump as compared to the traditional aggregates. This can be attributed to the higher water absorption value of PIS

aggregates when compared to conventional river sand / fine aggregate. However, the slump loss was not significant at 25% replacement of PIS in AAC mixes. The variation in density of concrete with and without PIS may not be of much concern for application in pavements which are constructed on subgrade soil. Unlike buildings and other structures in which the dead weight of the structure also plays a major role, Pavement Quality Concrete is not influenced much with variation in density of mix and higher specific gravity of materials used. Also, the variation of density of AASC and AASFC when compared to OPCC may be negligible. Therefore, densities of the concrete mixes developed are not necessarily be considered in the present study.

4.3 COMPRESSIVE STRENGTH OF CONCRETE MIXES

Compressive strength tests were conducted as per IS: 516-1959 at 3, 7, 28, and 90 days of curing and the results are tabulated in Table 4.1. It can be noticed that all the OPCC, AASC and AASFC specimens display progressive strength development up to 90 days of curing. The 28-days compressive strength of all AASC and AASFC samples with partial or complete replacement of river sand with PIS aggregates are in the range of 55±10 MPa. The AASC mix with natural aggregates exhibit higher compressive strength as compared to OPCC samples. The incorporation of PIS in the AASC and AASFC mixes led to slight decrease in the compressive strength. The AASC and AASFC mixes with 100% PIS exhibit slightly lower compressive strength as compared to that with traditional river sand. This may be due to the presence of pore spaces in PIS and higher water absorption capacity of PIS compared to river sand. The AASC and AASFC mixes with higher proportions of PIS displayed a greater variation in strength in the samples tested for the same mix. This may be attributed to the higher heterogeneity of minerals in PIS particles as compared to natural aggregates. However, the strength variation of AASC and AASFC mixes with PIS aggregates was within normal range of variability. The AASC and AASFC mixes display reduction in the strength with increasing PIS content. No significant difference in strength is observed in AASC and AASFC mixes with PIS content up to 25% (by volume). Similar trend is observed in both AASC and AASFC mixes irrespective of the binder type.

70

Table 4.1. Compressive strength and slump values of various concrete mixes

Mix ID	Compressive strength (MPa)				Slump (mm)
	3 days	7 days	28 days	90 days	
OPCC	23	40	57	63	40
4-A-0	40	48	60	67	30
4-A-25	38	47	56	66	30
4-A-50	38	45	53	62	25
4-A-75	35	43	52	57	15
4-A-100	33	40	50	54	15
4-B-0	36	44	56	62	50
4-B-25	35	43	54	60	45
4-B-50	33	41	53	58	40
4-B-75	32	39	51	54	35
4-B-100	30	38	48	52	30
4.5-C-0	33	43	54	62	55
4.5-C-25	33	41	51	59	55
4.5-C-50	32	40	50	57	50
4.5-C-75	30	38	50	53	40
4.5-C-100	27	37	49	50	35
5.5-D-0	34	45	53	61	60
5.5-D-25	31	42	50	57	55
5.5-D-50	30	41	49	55	45
5.5-D-75	29	37	49	52	40
5.5-D-100	26	35	48	50	40

The AASC and AASFC mixes exhibit high early strength as compared to OPCC i.e., the 3-days and 7-days strength of AASC and AASFC mixes are higher than OPCC. The high early strength of AASC and AASFC mixes may be attributed to the physical and structural characteristics of binders formed. The hydration process in case of AASC and AASFC mixes depends upon the dissolution and precipitation of GGBS which in the presence of high alkaline activator is quite faster than the hydration process occurring in Portland cement (Roy and Silsbee et al. 1992; Wang and Scrivener 1995).

However, rate of strength development slowed down after 7-days and at the end of 90 days the OPCC, AASC and AASFC mixes showed similar strengths. AASC with river sand achieved the highest strength at the end of 90 days when compared to that with PIS. The AASFC specimens (i.e., 5.5-D-0) mix with FA up to 75% (by weight of binder) exhibit comparable mechanical strengths as that of AASC (4-A-0). The lower water/binder ratios and higher sodium oxide dosage used at higher FA content were able to counteract the decrease in strength which would otherwise have been induced by the incorporation of FA. This indicates that the water/binder ratio and sodium oxide dosage can be controlled to achieve the desired strength in alkali-activated concretes formulated with high FA content. All concrete mixes attained sufficient strength at 28 days of curing necessary for application in low and high-volume pavements. The high early strength of AASC and AASFC mixes is of great benefit for PQC as it would allow the early opening of the constructed pavements to the traffic movement. The AASC and AASFC mixes with partial or complete replacement of river sand with PIS aggregates developed acceptable strengths required for application in PQC as per IRC: 58-2015.

From the results, it can be observed that almost 60% of the 28 days strength is achieved at 3 days curing period and 80% of it is achieved after 7 days curing. The traffic can be allowed on the new pavement after 7 days of curing which is an added advantage of AASC and AASFC mixes over OPCC mix. When compared to the 90 days strength values, around 10% increase in strength is observed with respect to 28 days strength. However, all the mixes have achieved the required strength at 28 days curing period itself and few of the mixes have achieved higher strengths.

4.4   FLEXURAL STRENGTH OF CONCRETE MIXES

The flexural strengths for all concrete specimens were determined according to IS: 516-1959. Table 4.2 presents the flexural strength values of concrete mixes developed. Also, Figs. 4.1 to 4.4 depict the variations in flexural strengths of AASC (100:0), AASFC (75:25), AASFC (50:50) and AASFC (25:75) respectively at 28 and 90 days of curing.

Table 4.2. Flexural strength values of various concrete mixes

Mix ID	Flexural Strength in Mpa	
	28 days	90 days
OPCC	6.0	6.4
4-A-0	6.9	7.5
4-A-25	6.6	7.3
4-A-50	6.2	6.8
4-A-75	6.1	6.3
4-A-100	5.9	6.0
4-B-0	6.4	6.8
4-B-25	6.3	6.7
4-B-50	6.1	6.3
4-B-75	5.8	6.2
4-B-100	5.6	5.9
4.5-C-0	6.5	6.9
4.5-C-25	6.5	6.7
4.5-C-50	6.3	6.5
4.5-C-75	5.8	6.1
4.5-C-100	5.5	5.9
5.5-D-0	6.3	6.4
5.5-D-25	6,1	6,3
5.5-D-50	5.8	6.0
5.5-D-75	5.6	5.8
5.5-D-100	5.5	5.6

From the results, it can be observed that the flexural strength decreases with the increase in PIS content in AASC and AASFC mixes. The flexural strength of AASC/AASFC with 100% PIS aggregates is lower than AASC/AASFC with river sand at all ages. AASC and AASFC mixes with 100% river sand display higher flexural strength than OPCC concrete at all ages, which may due to the development of a distinct microstructure in AAC mixes as compared to OPC concrete (Bernal et al. 2012). The

AASFC mix 5.5-D-0, exhibit lower flexural strength as compared to other AASFC mixes (4-B-0, 4.5-C-0) of similar strength grade. It was observed that the inclusion of higher FA in the binder reduced the flexural strength as compared to other AASFC mixes with lower FA content of similar compressive strength grade, which may be due to the differences in the binder chemistry between AASC and AASFC mixes (Provis 2013). The flexural strength reduction behaviour in AASC and AAFSC with increasing contents of PIS aggregates is similar to that observed in reduction behaviour of compressive strength.
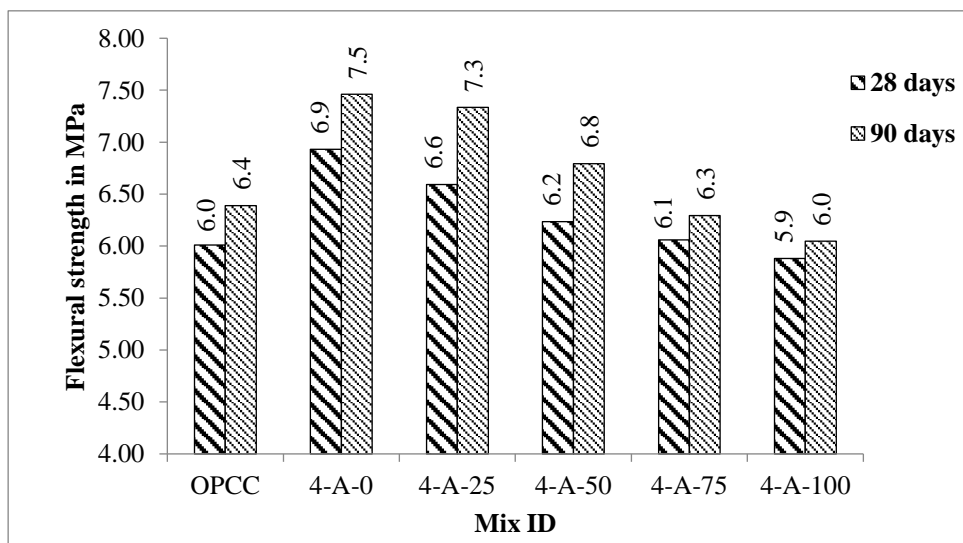
Figure 4.1 Flexural strength test results of AASC (100:0)
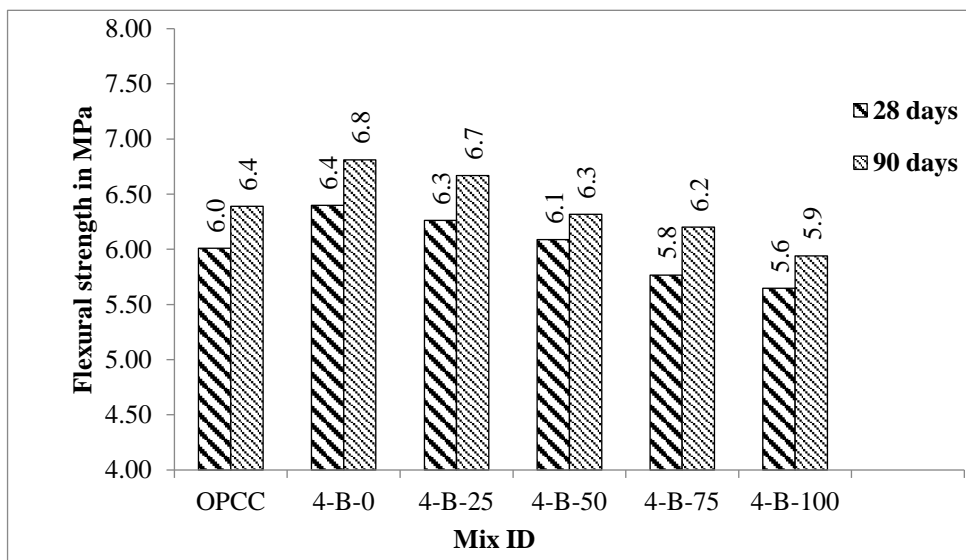
Figure 4.2 Flexural strength test results of AASFC (75:25)

74
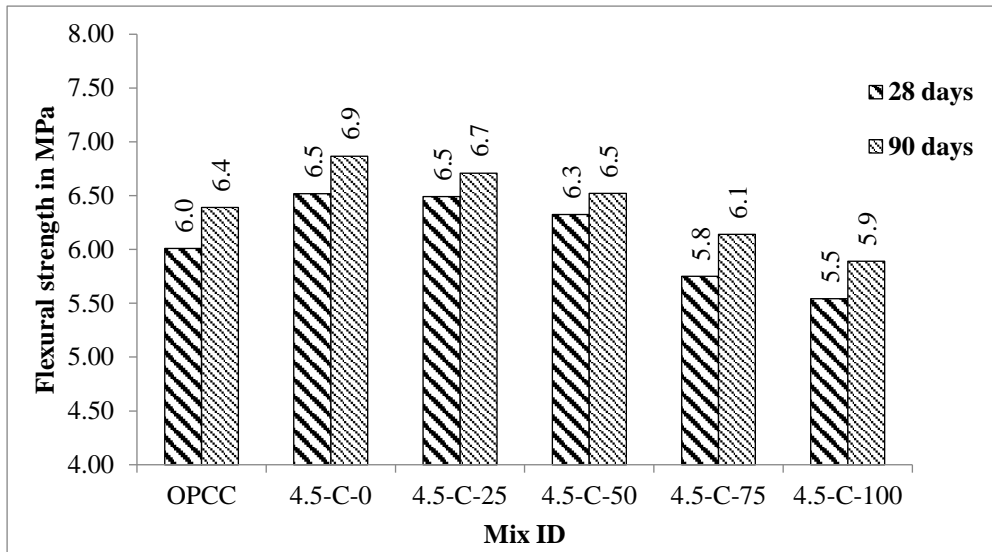
Figure 4.3 Flexural strength test results of AASFC (50:50)
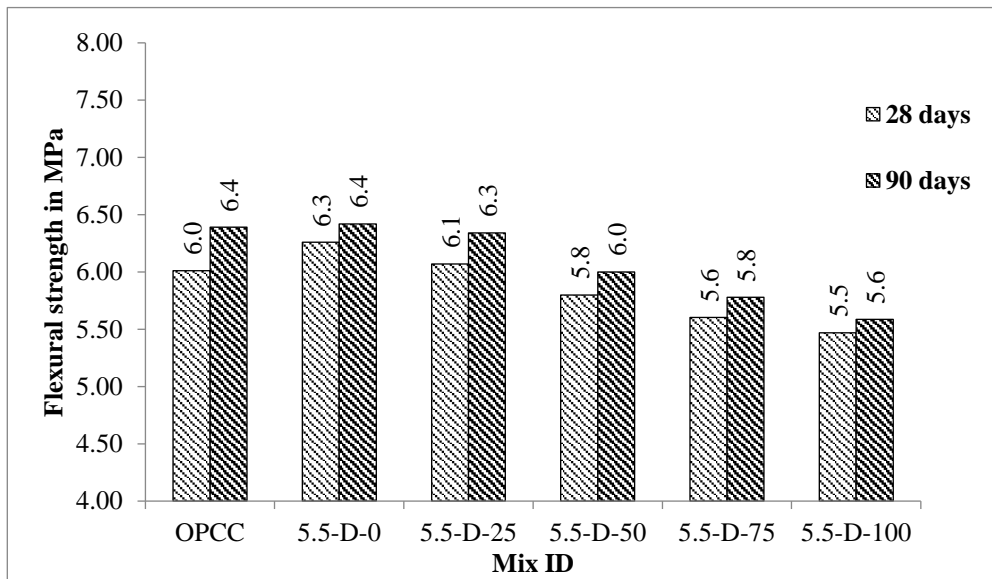
Figure 4.4 Flexural strength test results of AASFC (25:75)

The flexural strength of concrete is one of the important parameters which influence the design of concrete pavements. Since the alkali-activated binders achieved quite higher flexural strength as compared to conventional cement concrete, it may be beneficial in reducing the pavement thickness to some extent. Although, there was a reduction in the flexural strength of AASC and AASFC mixes with incorporation of PIS aggregates, all AASC/AASFC mixes (including 100% PIS aggregates) achieved

75

the minimum strength requirements of 4.5 MPa as suggested by the IRC for rigid pavement design (IRC:58-2015).

Table 4.3. Correlation between compressive and flexural strength values

Mix ID	Compressive strength test result at 28 days curing (f) (MPa)	Corresponding Characteristic strength (f_{ck}) based on the equation $f_{ck} = f - 1.65(S)$ (MPa)	Flexural strength value as per the equation $F = 0.7 \times \sqrt{f_{ck}}$ from IS: 456 (MPa)	Flexural strength from experimental results (F) (MPa)
OPCC	57	48.75	4.89	6.0
4-A-0	60	51.75	5.04	6.9
4-A-25	56	47.75	4.84	6.6
4-A-50	53	44.75	4.68	6.2
4-A-75	52	43.75	4.63	6.1
4-A-100	50	41.75	4.52	5.9
4-B-0	56	47.75	4.84	6.4
4-B-25	54	45.75	4.73	6.3
4-B-50	53	44.75	4.68	6.1
4-B-75	51	42.75	4.58	5.8
4-B-100	48	39.75	4.41	5.6
4.5-C-0	54	45.75	4.73	6.5
4.5-C-25	51	42.75	4.58	6.5
4.5-C-50	50	41.75	4.52	6.3
4.5-C-75	50	41.75	4.52	5.8
4.5-C-100	49	40.75	4.47	5.5
5.5-D-0	53	44.75	4.68	6.3
5.5-D-25	50	41.75	4.52	6.1
5.5-D-50	49	40.75	4.47	5.8
5.5-D-75	49	40.75	4.47	5.6
5.5-D-100	48	39.75	4.41	5.5

The results of flexural strength test show that there is an increment of around 5% from 28 days to 90 days of curing. However, all the mix combinations achieved the required strength of 4.5 MPa for rigid pavement design at 28 days curing period only. As per IS: 456 – 2000, the equation for flexural strength is 0.7 x √fck, where fck is the characteristic strength of concrete for M40 grade (40 MPa). Flexural strength value as per the equation is 4.5 MPa. Similarly, for M30 grade of concrete for low volume roads, flexural strength value is 3.9 MPa. IRC: 58 – 2015 also suggests a minimum of 4.5 MPa flexural strength for rigid pavement design. In the present study, all the mixes have achieved the required strength at 28 days curing itself so that it may not be necessary to go for higher curing periods even when FA is used in the mixture.

Based on the equation 0.7 x √fck, 4.5 MPa of flexural strength is required for pavement design. The characteristic compressive strength values are determined based on the results of compressive strength test. Corresponding flexural strength values are obtained based on the equation 0.7 x √fck, which are presented in Table 4.3. From the corresponding characteristic strengths of concrete calculated from the obatined equations, it was found that the characteristic strengths of developed AASC and AASFC are greater than the requirement of M40 grade strength. This shows the efficiency of AASC and AASFC mixes to be used as PQC.

4.5   SPLIT TENSILE STRENGTH OF CONCRETE MIXES

Figs. 4.5 to 4.8 present the 28-day split tensile strength values of AASC (100:0), AASFC (75:25), AASFC (50:50) and AASFC (25:75) in comparison with OPCC. The spilt tensile strength test was conducted as per IS: 5816-1999. The split tensile strength of AASC and AASFC mixes with river sand is higher than OPCC. The split tensile strength of AASC and AASFC mixes is found to decrease with replacement of natural river sand by PIS aggregates. At lower levels of replacement up to 25% (by volume) PIS; no appreciable change in split tensile strength is noticed, however split tensile strength of AASC/AASFC at 100% PIS aggregates is found to be lower than AASC/AASFC with natural river sand.
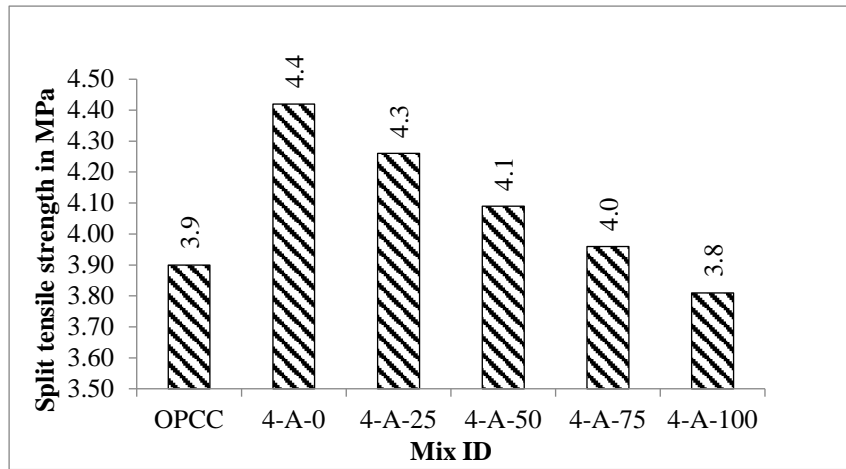
Figure 4.5 Split tensile strength value at 28 days for AASC (100:0)
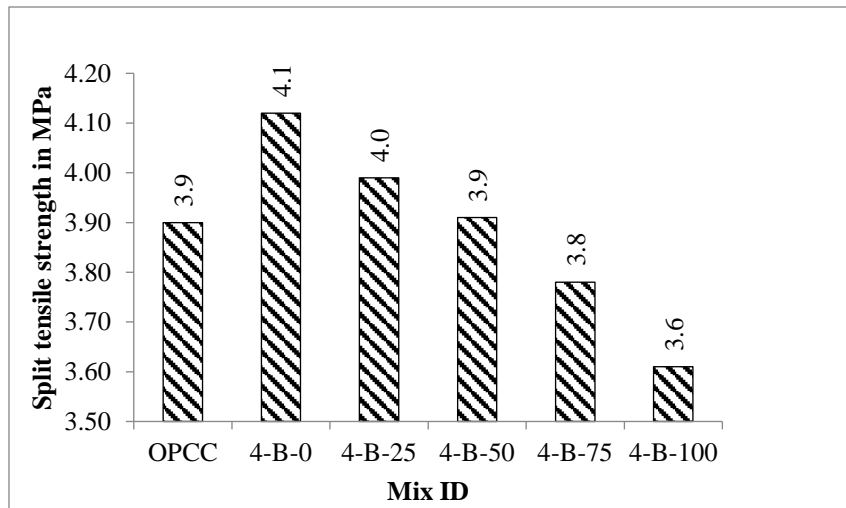
Figure 4.6 Split tensile strength value at 28 days for AASFC (75:25)
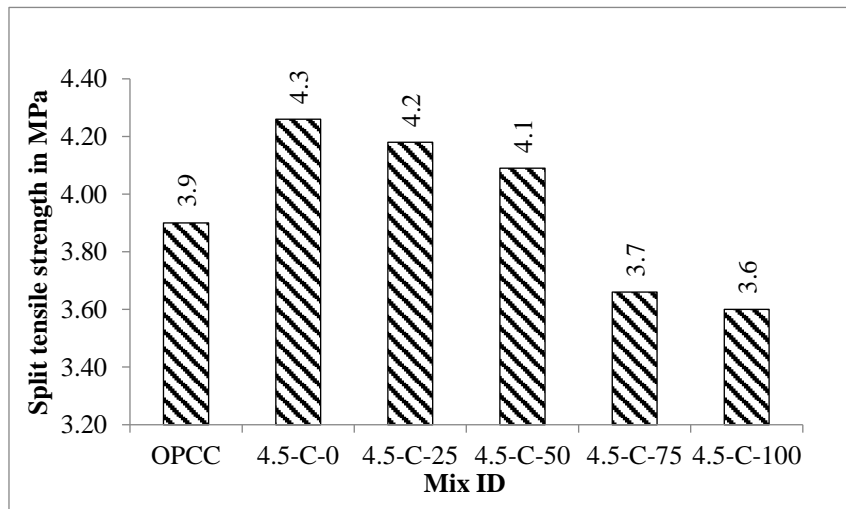
Figure 4.7 Split tensile strength value at 28 days for AASFC (50:50)
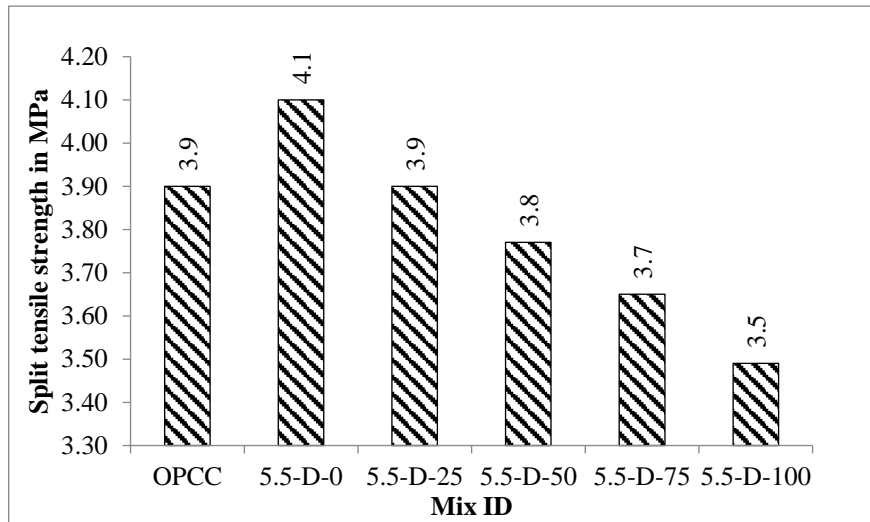
Figure 4.8 Split tensile strength value at 28 days for AASFC (25:75)

4.6 MODULUS OF ELASTICITY OF CONCRETE MIXES

The test for modulus of elasticity / Young's modulus was conducted as per IS: 516 - 1959. Fig. 4.9 presents the static modulus of elasticity values of AASC (100:0), AASFC (75:25), AASFC (50:50) and AASFC (25:75) in comparison with OPCC after 28 days of curing. It can be observed that the static modulus of elasticity of OPCC mixes is higher than that of AASC and AASFC mixes. The modulus of elasticity of AASFC mixes exhibit lower values with replacement of GGBS with FA. The results obtained are in similar trend as that in previous works (Rajamane 2013). The relationship between 28-day compressive strength and other mechanical such as flexural, tensile, elastic modulus differ as a function of binder chemistry. This has been demonstrated for alkali activated materials with regard to flexural strength and elastic modulus (Sofi et al. 2007a; Diaz-Loya et al. 2011; Bernal et al. 2012), which show different dependence on the 28-day compressive strength than the well-known (and standardized) relationships that hold good for normal-strength OPC concretes. AASC and AASFC, both being subsets of the general class of alkali activated materials, show very different strength development rates under the same curing conditions up to 28 days of age and also micro structural differences that would be expected to lead to differences in flexural and elastic properties (Provis 2013). The modulus of elasticity of AASC and AASFC mixes decrease with the replacement of river sand with PIS

aggregates. However, at lower levels of replacement, the variation in modulus of elasticity is marginal. The type and properties of aggregates and binder chemistry affect the modulus of elasticity of concretes. The nature of the constituent material and nature of interfacial transition zone between the paste and the aggregates affect the elastic modulus of the concrete (Alexander and Milne 1995).

The modulus of elasticity for AASFC mix 5.5-D-100 (with 100% PIS aggregates) is lower than the minimum requirement of modulus of elasticity (3.2×10^4 MPa) for M40 grade PQC (IRC:58:2015). Higher sodium oxide dosage (>5.5%) may lead to increased strength with corresponding higher modulus of elasticity in the mix 5.5-D-100. However, higher sodium oxide dosage implies higher cost which may not be desirable. Also, higher sodium oxide dosage requires higher amount of sodium hydroxide and sodium silicate. As the production of sodium hydroxide and sodium silicate also involves emission of carbon dioxide as in case of OPCC, it may not be desirable to adopt higher amounts. Hence, considering the modulus of elasticity, the river sand in AASFC (25:75) mixes may be replaced up to 75% (by volume) with PIS aggregates to control the cost and to maintain a balance in carbon emissions.

As per IS: 456 – 2000, the equation for modulus of elasticity is 5000 x $\sqrt{f_{ck}}$, where f_{ck} is the characteristic strength of concrete (40 MPa). Modulus of elasticity value as per the equation is 3.2×10^4 MPa. Similarly, for M30 grade of concrete for low volume roads, Young's modulus value is 2.8×10^4 MPa. The mixes 4-A-100, 4-B-100 and 4.5-C-100 with full replacement of PIS have achieved the required Young's modulus value corresponding to M40 grade of concrete. Also, other mixes with 25, 50 and 75 % of PIS aggregates are satisfying all the requirements of M40 grade of concrete. The mix 5.5-D-100 with 75% of FA achieved required Young's modulus value for M30 grade of concrete and it can be considered for low volume roads.

Based on the equation 5000 x $\sqrt{f_{ck}}$, 3.2×10^4 MPa of modulus of elasticity is required for pavement design. By considering the modulus of elasticity values obtained for all the mixes developed, corresponding equations can be formed. Based on the equations, corresponding characteristic strengths of concrete can be calculated. The

characteristic strengths of developed AASC and AASFC are in the range of M40 grade strength, except for the mix with 75% FA and 100% PIS aggregates (5.5-D-100).
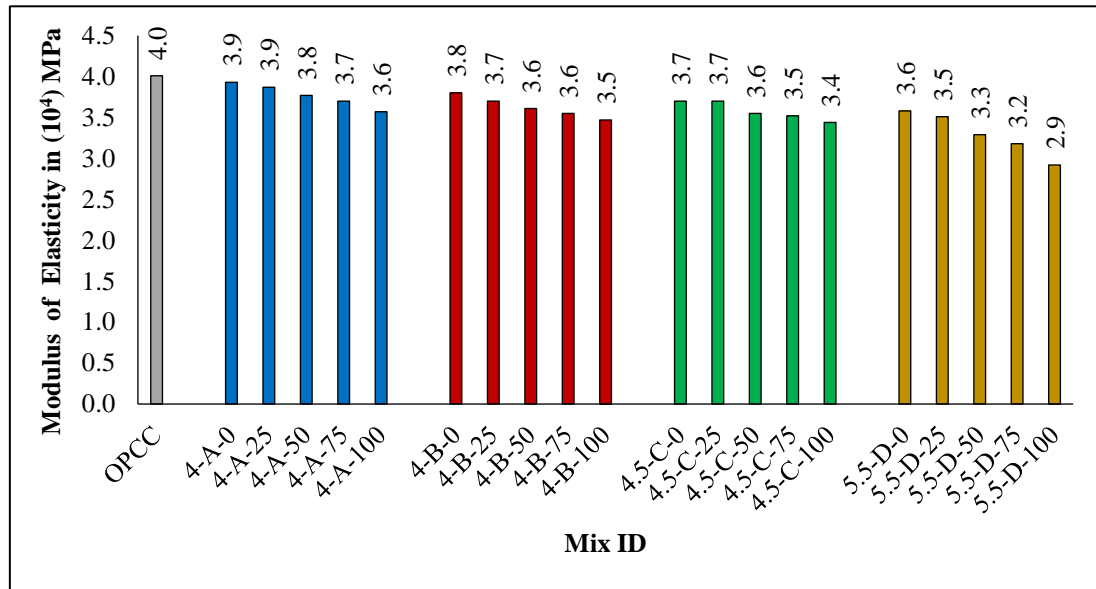
Figure 4.9 Modulus of Elasticity values at 28 days for AASC and AASFC mixes

Even though the strength is directly proportional to the modulus of elasticity value, there may not be a exact correlation between the results that may be due to the heterogeneity of concrete. Also, the modulus of elasticity value is slightly lesser in AASC and AASFC mixes when compared to OPCC mixes.

4.7   SCANNING ELECTRON MICROSCOPE ANALYSIS

SEM analysis proves that the concrete mix is a composite system having different phases of solids, voids, cracks and water molecules with heterogenous magnitude. This heterogenous magnitude has to be studied at different levels. The concrete mix includes the matrix of cement and aggregate particles embedded within the matrix. If the cement paste is considered as single entity, then the mixture is composed of different hydration products, void spaces, water molecules, unreacted cement particles and other filler materials present in the matrix.

Approximately 10-12 gm of AASC and AASFC specimens were collected after carrying out the compressive strength test for the cube specimen. The collected pieces of the concrete sample after compressive strength test were analysed for microstructure

analysis for mixes 4-A-100, 4-B-100, 4.5-C-100, 5.5-D-75 and 5.5-D-100, which are satisfying the strength requirements of M40 and M30 grade of PQC. Fig. 4.10 distinctly shows that the activation of slag particles has initiated more effectively at the higher alkalinity of the activator solution, i.e., at 4.5 and 5.5 % of Na_2O dosage.

It can be observed from the SEM images that the mixes at different stages of hydration having GGBS shows small traces of gradually developing C-A-S-H products in stratified layers with a minimal number of un-hydrated particles. But few minor voids can be observed in the mixes that may be due to the porosity or slag particles. The final dense microstructures are developed in almost all the mixes due to the complete activation of most slag particles in the presence of hydroxyl ions available from the activator solution. The fully developed denser microstructures, preferably without accompanying micro-cracks/voids, are responsible for higher strengths of AASC mixes prepared at 4 % Na_2O dosage. The negligible amount of un-reacted slag and fly ash particles in the mixes (5.5-D-75 and 5.5-D-100) is visible with the dark spots. The complete reaction of slag particles is visible in the mixes 4-A-100 and 4-B-100.

The increased Na_2O dosage with silicate from activator solution and the silica available in source material condenses the microstructure of the AASC mix. From the SEM images, it is apparent that in a given sample, reacted slag particles are more in quantity as the Na_2O dosage increases and modulus value decreases from 4% to 5.5% and 1.50 to 1.25, respectively. The excess hydroxyl ion concentration due to increased Na_2O dosage and soluble silica concentration from alkaline liquid enhances the polymerization reaction, a similar observation made by Nath and Sarker (2014). The increased NaOH concentration leads to adequate solubilization and accelerates the formation of C-A-S-H / N-A-S-H gel in AASC / AASFC mixes. This is the reason for increase in strength in the mixes with higher Na_2O dosage even though the mixes had FA and higher PIS aggregates in their matrix. Few larger particles become physically embedded in the glassy matrix, even though they may not undergo complete polymerization and forms dense microstructure in the mixes having higher PIS aggregate replacement.
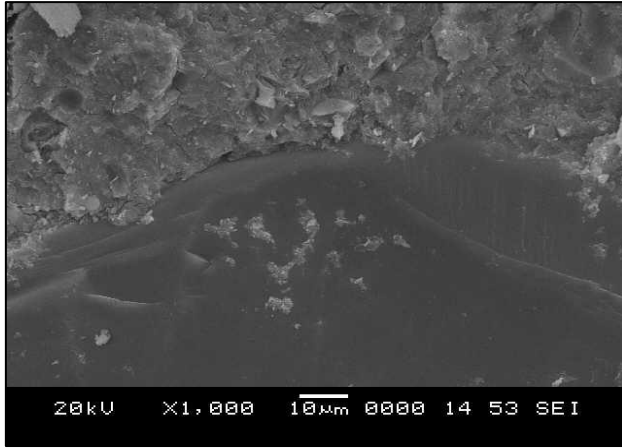
(a)
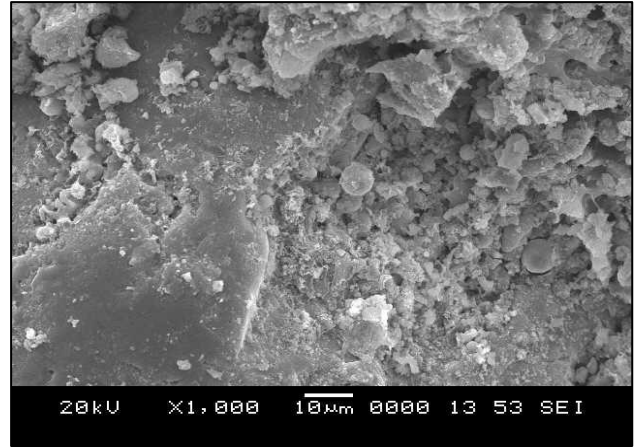
(b)
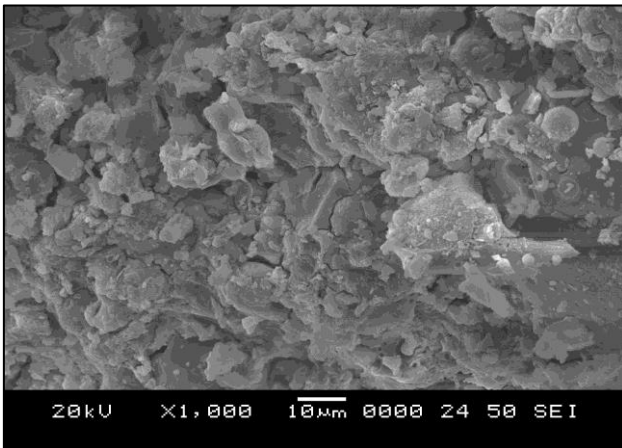
(c)
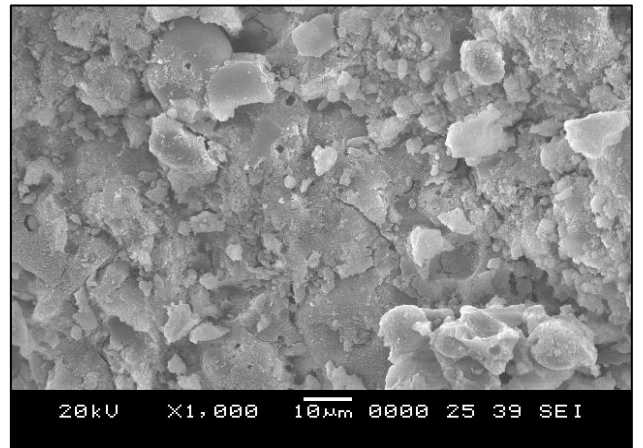
(d)

(e)

Figure 4.10 SEM images of mixes (a). 4-A-100, (b). 4-B-100, (c). 4.5-C-100, (d). 5.5-D-75 and (e). 5.5-D-100.

83

4.8   SUMMARY

The mechanical properties of AASC and AASFC mixes with partial or complete replacement of river sand with PIS aggregates were discussed in this chapter. It was observed that AASC and AASFC mixes attained sufficient mechanical properties required for application in pavement quality concrete. The incorporation of PIS aggregates in AASC and AASFC mixes slightly affected the workability and unit weight of the concrete mixes. The AASC and AASFC mixes with PIS aggregates showed reduced workability; along with increase in the unit weight of the concrete mixes as compared to those concrete mixes with river sand. All the AASC and AASFC mixes with partial or complete replacement of river sand with PIS aggregates attained compressive strengths in range 55±10 MPa and flexural strengths greater than 5.5 MPa after 28 days of curing. The incorporation of PIS fine aggregates slightly lowered the mechanical properties in both AASC and AASFC mixes which is mainly due to the higher water absorption of PIS aggregates. The AASC and AASFC mixes displayed high early strength which is advantageous for PQC as it would allow the early opening of the constructed pavements to the traffic movement. The inclusion of higher contents of FA in the AASFC slightly resulted in decrease of tensile properties and modulus of elasticity properties for similar compressive strength grade as compared to AASC. AASC and AASFC mixes with partial or complete replacement of river sand with PIS fine aggregates displayed satisfactory results for its use in highway application.

CHAPTER 5

DURABILITY PROPERTIES OF CONCRETE MIXES DEVELOPED

5.1 GENERAL

Concrete and cement based materials find its applications in diverse environments such as buildings, drainage structures, water supply units, industrial infrastructure etc. Although concrete provide good mechanical strength, the concrete needs to be durable since it is exposed to various aggressive environments. The aggressive environments are usually aqueous in nature, which may either be natural occurring such as sea waters, soft waters or may be man-made such as industrial, waste water or polluted environments. Under such environments, concrete undergoes degradation through the processes of ion exchange and chemical reactions, thus leading to changes in the matrix microstructure and ultimately reduction in the strength of the material. The durability of concrete is rapidly affected by acidic environments, especially sulphuric acid. The sulphuric acid may arise from various ways like acidic soils, industrial effluents, sewage wastes, etc. Concrete is known to undergo degradation in sulphate environments which may arise from sulphate rich soils, industrial effluents, etc. (Shi et al. 2006). In the present chapter, the durability properties of AASC and AASFC mixes with 0%, 50% and 100% (by volume) PIS as fine aggregates are evaluated and compared with OPCC. Durability properties such as water absorption, Volume of Permeable Voids (VPV), resistance to the sulphuric acid environment and resistance to magnesium sulphate environment are studied in detail.

5.2 WATER ABSORPTION AND VOLUME OF PERMEABLE VOIDS

The water absorption and VPV were evaluated according to ASTM C 642-13. A set of three cubes of 100 mm size was tested for each mix. The water absorption and VPV of different mixes at 28-days of curing are presented in Table 5.1.

Table 5.1. Water absorption and VPV of concrete mixes

Mix ID	Water Absorption (%)	VPV (%)
OPCC	3.7	9.4
4-A-0	3.3	8.1
4-A-50	3.7	9.2
4-A-100	4.2	10.5
4-B-0	3.6	9.1
4-B-50	3.9	10.3
4-B-100	4.4	11.6
4.5-C-0	3.9	9.8
4.5-C-50	4.2	11.1
4.5-C-100	4.7	12.3
5.5-D-0	4.4	11.1
5.5-D-50	4.8	12.7
5.5-D-100	5.1	13.6

AASC and AASFC (75:25) mixes with river sand having same binder content and water-binder ratio as OPCC, show reduced water absorption and VPV values as compared to OPCC at 28 days of curing. This may be due to the presence of very refined closed pore structure in the AASC samples (Shi 1996) which restrict the water from penetrating into the structure. The water absorption and VPV values increased with FA replacements in the AASFC mixes. The inclusion of FA in AASFC show significantly higher VPV. The higher VPV with higher contents of FA is attributed to the nature of the gel type forming in the binder (Idawati et al. 2013). Binding type gels such as C-A-S-H dominate the microstructure of AASFC with GGBS inclusion up to 50 % of wt. of binder, which are denser than the geopolymer (alkali aluminosilicate) type gels dominating the microstructure of binders mostly composed of activated FA (Bernal et al. 2011). A study conducted by Provis et al. (2012) for activated GGBS/FA blends, via X-ray microtomography, reported that each binding gel promotes a different pore structure and hence different porosities. The presence of more bound water, induced by the presence of Ca in C-A-S-H type products, provides greater pore-filling capacity to this type of gel, than geopolymer type gels. Furthermore, GGBS has a much

finer particle size which can fill the pore and result in lower water absorption and VPV in AASC (Idawati et al. 2013). The water absorption and subsequent total VPV increase with the replacement of PIS aggregates is witnessed in both AASC and AASFC mixes. This may be attributed to the higher water absorption of PIS aggregates as compared to river sand. The presence of pores in PIS may have resulted in the increase in VPV in the mixes.

5.3   ACID ATTACK TEST

The Fig. 5.1 presents the percentage loss in compressive strength with time for AASC (100:0), AASFC (75:25), AASFC (50:50) and AASFC (25:75) mixes in comparison with OPCC. The results are also tabulated in Table 5.2. From the results, it can be observed that all the concrete mixes show progressive strength loss with time after immersion in sulphuric acid solution. The AASFC mixes with high amount of FA (> 50%, say mixes C and D) exhibited better resistance as compared to OPCC, AASC (100:0) and AASFC (75:25). All AAC mixes with river sand exhibited better resistance to sulphuric acid as compared to OPCC which may be attributed to the properties and structure of binders. The main reaction products formed in OPC are portlandite $(Ca(OH)_2)$ and calcium silicate hydrate (C-S-H) which are vulnerable to chemical degradation (Adam 2009), while AAS pastes consist mainly of C–S–H with a Ca/Si ratio of around 1, without any formation of $Ca(OH)_2$ (Wang and Scrivener 1994). The absence of portlandite $(Ca(OH)_2)$ and the low lime content in AASC and AASFC mixes is an advantage which leads to slower degradation and better resistance as compared to OPCC when subjected to acid environment. However, binder structures formed in AASC and AASFC mixes also undergo degradation, in the form of decalcification of C-S-H and formation of gypsum which is reflected by the formation of expansive cracks on the specimen. The combined effect of decalcification of C-S-H which is the main binding phase and the volume instability caused due to formation of gypsum lead to decrease in the compressive strength in AASC and AASFC mixes. The replacement of GGBS with FA slightly improved the acid resistance of the AAC mixes i.e., AASFC mixes. It may be noticed that the mix 4-A-0 [AASC (100:0) with 100% natural aggregates] display loss in strength of around 37% as compared to 24% in case of mix

87

5.5-D-0 [AASFC (25:75) with 100% river sand] after exposure to 365 days of sulphuric

Loss in Compressive Strength (%)
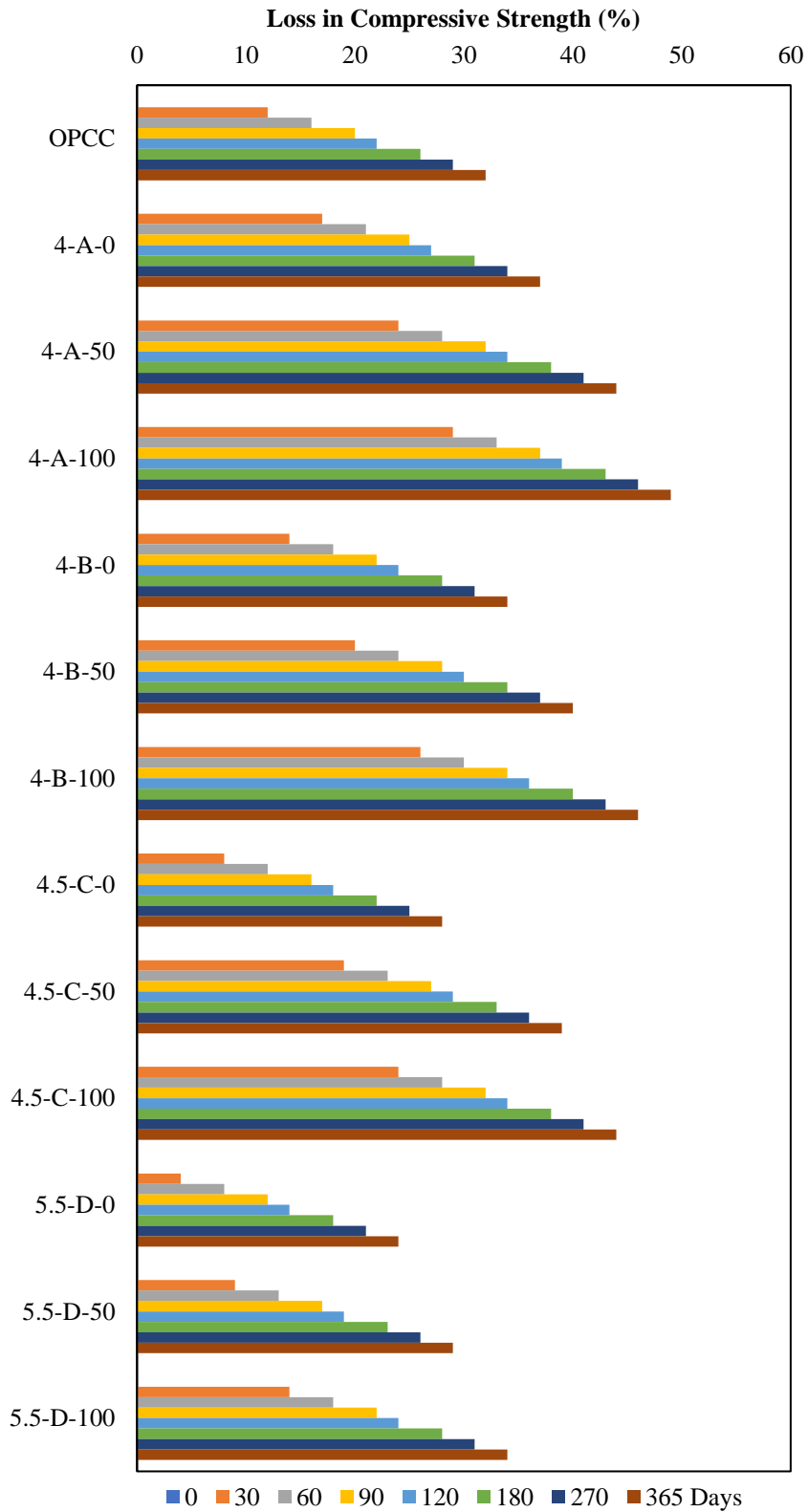
Figure 5.1 Strength loss in AASC and AASFC mixes in acid solution

acid solution. This may be attributed to further decrease in calcium content in the binder with addition in the FA content which tends to make the binder resistant to acid attack.

Table 5.2. Loss in compressive strength of AASC and AASFC mixes in acid solution

Mix ID	Loss in compressive strength (%)							
	0 days	30 days	60 days	90 days	120 days	180 days	270 days	365 days
OPCC	0	11	17	20	22	26	29	32
4-A-0	0	16	21	26	28	31	34	38
4-A-50	0	24	28	31	33	38	41	44
4-A-100	0	29	33	38	40	45	47	49
4-B-0	0	13	18	20	22	28	31	34
4-B-50	0	20	24	28	31	36	39	41
4-B-100	0	29	32	36	38	40	43	46
4.5-C-0	0	9	12	18	20	25	28	30
4.5-C-50	0	20	23	27	30	34	36	39
4.5-C-100	0	23	26	30	32	3	40	43
5.5-D-0	0	5	8	12	15	19	21	23
5.5-D-50	0	10	13	18	20	22	27	29
5.5-D-100	0	12	16	20	22	26	28	31

The acid resistance of AAC mixes decreased with the replacement of river sand with PIS. It may be noticed that the 4-A-0 displayed a strength loss of 37% as compared to 4-A-50 and 4-A-100 which undergo a strength loss of 44% and 49% respectively after being immersed in sulphuric acid solution for 365 days. Similar decreases in compressive strength with inclusion of PIS aggregates is observed in mixes B, C and D. The strength loss with PIS aggregates may be attributed to the deterioration of PIS due to leaching out of calcium present in the aggregates. Apart from displaying deterioration, the PIS aggregates replaced concrete suffered softening/corrosion under the action of sulphuric acid. The mix 5.5-D-100 displayed slightly lower loss in strength and slower rate of strength loss with age as compared to 4-A-100 which may be

attributed to better stability of the binder due to high FA content. The acid resistance of 4-A-100 was found to be lower than OPCC at the end of 365 days of immersion, while the mix 5.5-D-100 performed better at the early days of immersion which may be due to the contribution of the high FA content binder as compared to GGBS binder, however at the end of 365 days, the strength loss of OPCC and D-100 was almost similar.

5.4 SULPHATE ATTACK TEST

The Fig. 5.2 presents the percentage loss in compressive strength with time for AASC (100:0), AASFC (75:25), AASFC (50:50) and AASFC (25:75) mixes in comparison with OPCC after immersion in magnesium sulphate solution up to 365 days. Table 5.3 also presents the results of sulphate resistance test.

Table 5.3. Loss in compressive strength of AASC and AASFC mixes in sulphate solution

Mix ID	Loss in compressive strength (%)							
	0 days	30 days	60 days	90 days	120 days	180 days	270 days	365 days
OPCC	0	8	12	16	19	21	23	26
4-A-0	0	7	9	10	12	14	16	19
4-A-50	0	12	14	15	17	19	21	24
4-A-100	0	16	18	19	21	23	25	28
4-B-0	0	4	6	7	9	11	13	16
4-B-50	0	7	9	10	12	14	16	19
4-B-100	0	13	15	16	18	20	22	25
4.5-C-0	0	2	3	5	7	8	10	12
4.5-C-50	0	5	7	8	10	12	14	17
4.5-C-100	0	9	11	12	14	16	18	21
5.5-D-0	0	2	4	6	7	8	9	10
5.5-D-50	0	3	4	5	6	8	10	13
5.5-D-100	0	6	8	9	11	13	15	18
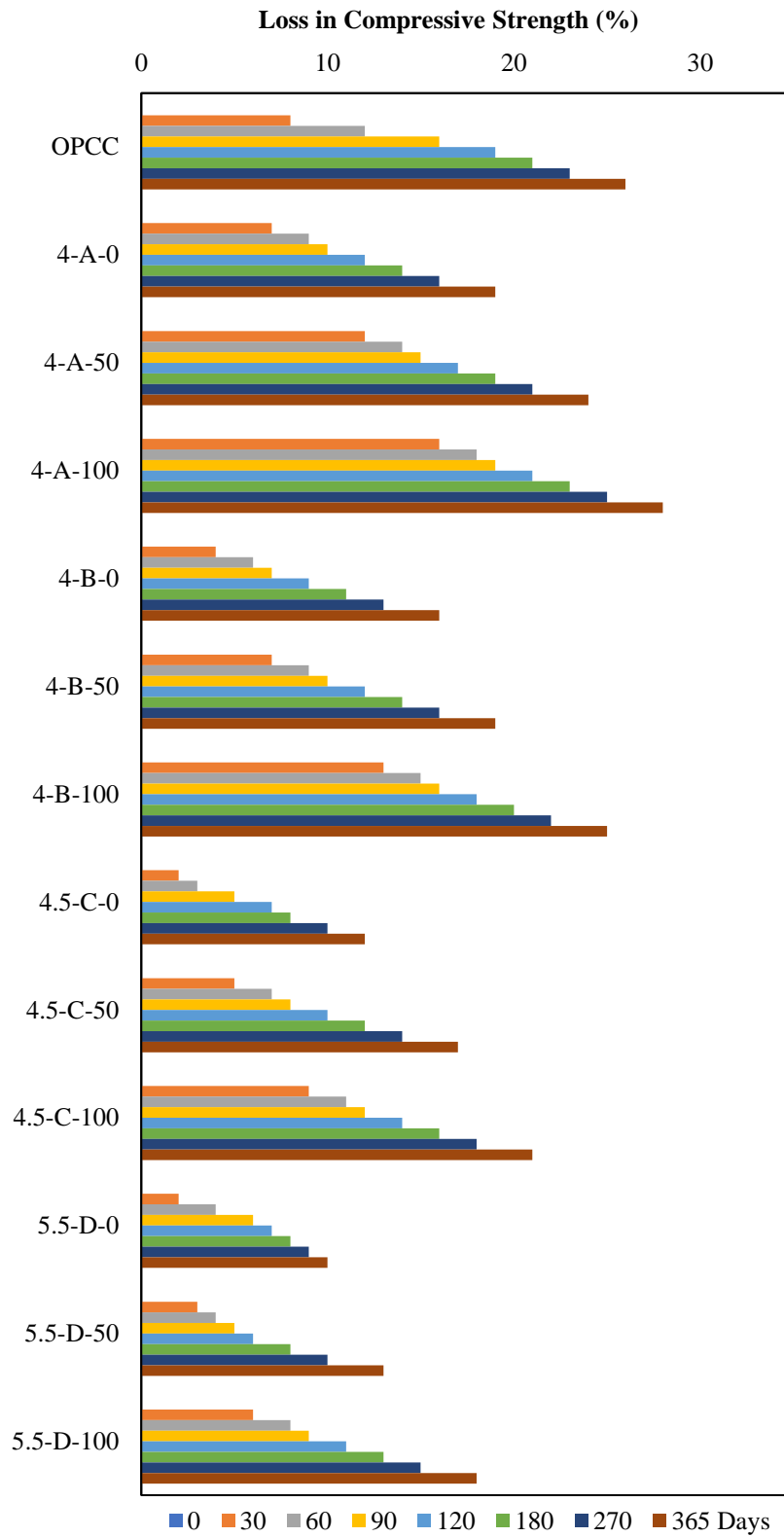
Figure 5.2 Strength loss in AASC and AASFC mixes in sulphate solution

It may be observed from the results that all the concrete mixes display gradual strength loss at the end of 365 days after immersion in magnesium sulphate solution. The OPCC samples exhibit lower resistance to magnesium sulphate environment as compared to AAC mixes with river sand. The OPCC displayed around 26% reduction in strength, while the mix 4-A-0 displayed reduction in strengths up to 19% at the end of 365 days of immersion.

The AASFC mixes with 100% river sand i.e., 4-B-0, 4.5-C-0 and 5.5-D-0 displayed a reduction in strength of 16%, 12% and 10% respectively when tested at the end of 365 days of immersion. The higher reduction in compressive strength in OPCC may be attributed to presence of $Ca(OH)_2$ in OPCC, which undergoes dissolution after reacting with magnesium sulphate, thus leading to decalcification of C-S-H structure and formation of gypsum. Since, the pH of the surrounding environment is maintained in the range 6.5-7.5 (neutral), the consumption of $Ca(OH)_2$ occurs, to increase the pH of the solution (Metha and Gjorv 1974).

With the consumption of $Ca(OH)_2$, the C-S-H structure becomes unstable and releases Ca^{2+} ions along with further liberation of $Ca(OH)_2$ into the surrounding solution to increase the pH. As the reaction progresses, reduction in the Ca/Si ratio occurs in the C-S-H of OPCC and at advanced stages of attack the Mg^{2+} ion can replace Ca^{2+} in the C-S-H to form magnesium silicate hydrate (M-S-H), which is reported to be non-cementitious (Bonen 1992). The combined effect of dissolution of $Ca(OH)_2$ and decalcification of C-S-H along with formation of gypsum lead to strength reduction in OPCC. The binders in AASC and AASFC mixes with lower Ca/Si ratio and absence of portlandite undergo lower degradation and display better resistance to sulphate environment as compared to OPCC as discussed in earlier section (Lu 1992; Blaakmeer 1994). The reduction in the strength of AASC and AASFC mixes may be due to direct attack on the C-S-H by $MgSO_4$ which can also cause the formation of M-S-H and secondary gypsum (Bonen and Cohen 1992). The Mg^{2+} ions present in the solution leads to the decalcification of Ca-rich gel structures in the AASC and AASFC binders, leading to degradation of the binder system and precipitation of gypsum. The products resulting from the attack of magnesium sulphate on the binder system are expansive and poorly cohesive, which causes dimensional instability in binder system and thus reduces the mechanical performance (Idawati et al. 2013). It is reported that alkali-

92

activated GGBS–FA cements have very good resistance to acidic, sulphate and seawater attacks (Lu 1992; Blaakmeer 1994) which can be explained by the low Ca/Si ratio of C–S–H in the alkali-activated GGBS–FA cements. Slightly better performance of AASFC (25:75) with high FA contents can be explained by further reduction in calcium in the binder with increased content of FA.

The incorporation of PIS in the AAC resulted in the higher reduction in the strength after immersion in magnesium sulphate solution. It may be noticed that 4-A-0 displayed a strength loss of 19% as compared to 4-A-50 and 4-A-100 which undergo a strength loss of 24% and 28% respectively after being immersed in magnesium sulphate solution for 365 days. The higher strength loss due to PIS aggregates may be probably due to expansion due to the fact that magnesium sulphate solution forms gypsum thereby weakening the aggregates and the paste. Similar trend was noticed in AASFC mixes with PIS aggregates.

5.5   SUMMARY

The durability properties of AASC and AASFC with partial or complete replacement of river sand with PIS were discussed in this chapter. AASC and AASFC mixes with PIS aggregates displayed higher water absorption and VPV which may be attributed to higher water absorption of PIS aggregates as compared to natural aggregates. The acid resistance of AAC mixes decreased with the replacement of natural aggregates with PIS. Mix 4-A-0 displayed a strength loss of 37% as compared to 4-A-50 and 4-A-100 which undergo a strength loss of 44% and 49% respectively after being immersed in sulphuric acid solution for 365 days. Similar decreases in compressive strength with inclusion of PIS aggregates was observed in mixes B, C and D. The higher reduction of strength with PIS aggregates may be due to the deterioration of PIS aggregates. The incorporation of PIS in AAC resulted in higher reduction in compressive strength after immersion in magnesium sulphate solution. 4-A-0 displayed a strength loss of 19% as compared to 4-A-50 and 4-A-100 which undergo a strength loss of 24% and 28% respectively after being immersed in magnesium sulphate solution for 365 days. The inclusion of PIS aggregates slightly reduced the durability performance of AASC and AASFC mixes.

CHAPTER 6

FATIGUE PERFORMANCE OF CONCRETE MIXES DEVELOPED

6.1 GENERAL

Concrete pavements may undergo failure in different types under the action of vehicular loads during their service life; one such type of failure may be due to fatigue. The fatigue strength of concrete structures subjected to repetitive loads such as pavements, and bridges. It is one important parameter to be considered in the design of such structures. Fatigue is often described by a parameter "Fatigue life" which essentially represents the number of cycles the material can withstand under a given pattern of repetitive loading, before failure. The failure due to fatigue occurs as a result of development of internal cracks and progressive growth of cracks under the action of cyclic loadings, which leads to failure of the pavements at loads smaller than the modulus of rupture of the concrete (Lee and Barr 2004). Fatigue testing is a very time consuming and a large number of samples have to be tested. In the present study, the flexural fatigue performance of AASC and AASFC mixes incorporating 0%, 50% and 100% (by volume) of PIS aggregate were investigated. The specimens were subjected to different stress ratios (0.70, 0.75, 0.80 and 0.85) and the number of cycles for failure of the specimen was determined. Stress ratios were considered based on trials and also IRC: 58 - 2002 suggests expected number of repetitions for different set of stress ratios. A probabilistic analysis of fatigue test data was carried out to ascertain the fatigue life of the material.

6.2 S-N CURVE

Most of the researchers adopted the relationship between stress ratio (ratio of maximum applied stress to the modulus of rupture) and the number of repetitions 'N' causing failure, to predict the fatigue life of a material. The relationship established is known as Wohler equation and is shown by S-N Curve or Wohler curve (Oh, 1986). The use of S-N curves or Wohler curve is the most basic method of representing the fatigue

behaviour of concrete specimen. S-N curve is an important parameter in the analysis of fatigue data in which 'S' denotes the stress amplitude and 'N' denotes the number of cycles to complete failure. This S-N curve enables one to predict the mean fatigue life of concrete under given stress level or amplitude of cyclic stress (Roylance 2001).

6.3 PROBABILISTIC ANALYSIS OF FATIGUE DATA

As the fatigue test data of concrete shows considerable scatter and is random in nature, a probabilistic approach can be introduced for analyzing the fatigue data and evaluating probability of unfavourable performance (Oh 1986). The fatigue life may be assumed to be normally distributed and thus a log-normal distribution is extensively used (Mohammadi and Kaushik 2005). Later experimental studies on the basis of physical valid assumptions have shown that the distribution of fatigue life of concrete under given stress ratio follows the Weibull distribution and is most commonly employed in assessing reliability of composite structures (Sakin and Ay 2008). A Weibull distribution is characterized by three parameters:

1) Shape parameter (α) which describes the shape of the distribution;
2) Characteristic life or scale parameter (μ); and
3) Location parameter (n_0).

The hazard function (Mohammadi and Kaushik 2005) can be obtained from,

$$h_N(n) = \alpha \left(\frac{n-n_0}{\mu-n_0}\right)^{\alpha-1} ; n \geq n_0 \tag{6.1}$$

The hazard function or failure rate function of Weibull distribution increases with time or with an increase in the number of cycles for $\alpha \geq 1$ only, which is compatible with the expected fatigue behaviour of engineering material (Singh and Kaushik 2000). When location parameter is set to zero ($n_0=0$), it is reduced to two parameter Weibull distribution.

There are several methods of estimating external parameters namely: 1) Graphical method; 2) Method of maximum likelihood; and 3) Method of moments. Graphical method is considered in the present investigation.

6.3.1 Graphical method

The survival function of Weibull distribution can be expressed as follows:

$$\text{LN (n)} = \exp\left[-\left(\frac{n}{\mu}\right)^{\alpha}\right] \qquad (6.2)$$

Where, 'n' represents specific value of random variable, 'α' represents shape parameter or Weibull slope at stress ratio 'S' and μ is characteristic life at stress ratio 'S'. Taking twice the logarithm of both sides of Eq. 6.2.

$$\left[\ln\left[\ln\left(\frac{1}{L_N(n)}\right)\right]\right] = \alpha \ln(n) - \alpha \ln(\mu) \qquad (6.3)$$

Eq. 6.3 may be written in the following form:

$$Y = \alpha X - B \qquad (6.4)$$

Where, $\quad Y = \left[\ln\left[\ln\left(\frac{1}{L_N(n)}\right)\right]\right],$

$X = \ln(n)$

$B = \alpha \ln(\mu).$

The distribution parameters 'α' and 'μ' can be obtained from the straight line if fatigue life data follows Weibull distribution, which is possible if the relationship between X and Y in Eq.6.4 is linear. Hence, linear regression analysis for fatigue life data needs to be performed to get the relation for each stress ratio 'S' as in Eq. 6.4.

In order to obtain a graphic form of Eq.6.4, the fatigue life data at a given stress ratio are arranged in ascending order of cycles to failure. The empirical survivorship function $L_N(n)$ for each fatigue life data ranked in the order of number of cycles to failure at a given stress ratio is calculated using mean rank.

The empirical survivorship function L_N (n) for each fatigue life data at a given stress ratio is calculated using the following Eq.6.5 (Mohammadi and Kaushik, 2005).

$$\text{LN (n)} = 1 - \frac{i}{k+1} \qquad (6.5)$$

Where, 'i' represent failure order number and 'k' represents sample size under consideration at a particular stress ratio.

By plotting a graph between $\left[\ln\left[\ln\left(\frac{1}{L_N(n)}\right)\right]\right]$ and ln(n), the parameters 'α' and 'μ' of Weibull distribution can be directly obtained; where slope of line provides shape factor 'α' while the characteristic life 'μ' can be calculated from the equation,

B= α ln(μ). The graph between [ln[ln $\left(\frac{1}{L_N(n)}\right)$] and ln (n) is plotted for all the stress ratios and for all concrete mixes and the Weibull distribution parameters are calculated.

6.4   FATIGUE LIFE OF CONCRETE MIXES

The fatigue life (N) i.e., the number of cycles up to failure for OPCC, AASC and AASFC mixes with/without PIS aggregates are tabulated in Table 6.1 - 6.4. From Table 6.1, it can be noticed that the AASC/AASFC mixes with river sand display higher resistance to fatigue failure as compared to OPCC irrespective of the applied stress ratio. This may be due to the highly dense interfacial transition zone between

Table 6.1. Fatigue life of OPCC and AASC (100:0) mixes

Mix ID	Specimen No.	Stress ratio			
		0.85	0.80	0.75	0.70
OPCC	1	76	498	8978	28475
	2	118	788	24758	39763
	3	140	901	30866	59247
	4	220	1578	48145	79868
	5	317	1986	57835	97587
4-A-0	1	91	578	12014	30254
	2	111	876	30758	47369
	3	163	970	32677	63471
	4	326	1842	46339	98565
	5	364	2124	61214	99723
4-A-50	1	69	602	8325	12614
	2	132	645	16768	24786
	3	157	889	37896	69753
	4	204	1309	40707	75649
	5	350	1698	49175	92475
4-A-100	1	76	236	6012	23485
	2	126	764	26981	42141
	3	189	1104	34859	54756
	4	223	1176	43111	67348
	5	291	1478	54014	85412

the paste and the aggregate occurring in alkali activated binders as compared to that occurring in conventional OPCC (Bernal et al. 2012).

98

Table 6.2. Fatigue life of AASFC (75:25) mixes

Mix ID	Specimen No.	Stress ratio			
		0.85	0.80	0.75	0.70
4-B-0	1	80	521	6412	33689
	2	121	723	16994	39475
	3	142	1022	33258	50782
	4	244	1766	55241	83695
	5	340	2018	59146	97561
4-B-50	1	84	395	7697	20258
	2	112	488	20475	30475
	3	159	978	31789	46987
	4	173	1481	32547	79863
	5	321	1576	63545	82456
4-B-100	1	55	212	8475	14587
	2	69	612	30217	33477
	3	207	1006	35961	41223
	4	254	1075	41578	59336
	5	346	1374	44696	89621

Table 6.3. Fatigue life of AASFC (50:50) mixes

Mix ID	Specimen No.	Stress ratio			
		0.85	0.80	0.75	0.70
4.5-C-0	1	64	601	7658	24758
	2	170	741	26335	43694
	3	188	893	32558	79866
	4	245	1691	49689	94758
	5	377	2344	64124	99826
4.5-C-50	1	73	512	11245	20174
	2	98	683	15785	49687
	3	155	752	37863	56869
	4	201	1254	42012	67586
	5	349	1855	55974	94786
4.5-C-100	1	61	411	4755	17258
	2	110	824	18142	24758
	3	186	903	29874	46878
	4	140	1102	45332	72586
	5	287	1653	52369	85747

Table 6.4. Fatigue life of AASFC (25:75) mixes

Mix ID	Specimen No.	Stress ratio			
		0.85	0.80	0.75	0.70
5.5-D-0	1	54	758	11058	12087
	2	144	873	36985	45712
	3	293	1424	46123	68211
	4	310	1896	56778	90117
	5	422	2175	67963	98899
5.5-D-50	1	61	312	4785	32401
	2	83	1025	16896	39888
	3	187	1259	28796	61201
	4	332	1674	50485	71356
	5	391	1910	54278	87633
5.5-D-100	1	79	357	2253	19324
	2	96	501	19312	45398
	3	212	1050	37801	50147
	4	241	1388	44777	61476
	5	306	1469	47213	81204

Table 6.5. Relationship between fatigue cycle (N) and stress ratio (SR)

Mix ID	Equations for No of Repetitions	R^2
OPCC	$\ln(N)=0.953-SR/0.02$	0.903
4-A-0	$\ln(N)=0.957-SR/0.02$	0.904
4-A-50	$\ln(N)=0.954-SR/0.02$	0.879
4-A-100	$\ln(N)=0.948-SR/0.02$	0.882
4-B-0	$\ln(N) = 0.954-SR/0.02$	0.899
4-B-50	$\ln(N) = 0.952-SR/0.02$	0.888
4-B-100	$\ln(N) = 0.944-SR/0.02$	0.855
4.5-C-0	$\ln(N)=0.955-SR/0.02$	0.894
4.5-C-50	$\ln(N)=0.951-SR/0.02$	0.898
4.5-C-100	$\ln(N)=0.950-SR/0.02$	0.880
5.5-D-0	$\ln(N)=0.956-SR/0.02$	0.856
5.5-D-50	$\ln(N)=0.953-SR/0.02$	0.885
5.5-D-100	$\ln(N)=0.949-SR/0.02$	0.867

The fatigue life of AASC mixes decreased with the inclusion of PIS aggregates. Similar trend was observed in other AASFC mixes incorporating PIS aggregates. The fatigue behaviour with higher contents of FA in AASFC mixes could not be clearly

understood. It was observed that specimens exhibit lower fatigue life when subjected to higher stress ratios, while at lower stress ratios, specimens exhibited higher fatigue lives. The failures of the specimens were visually examined and were found to have failed within the middle one third spans.
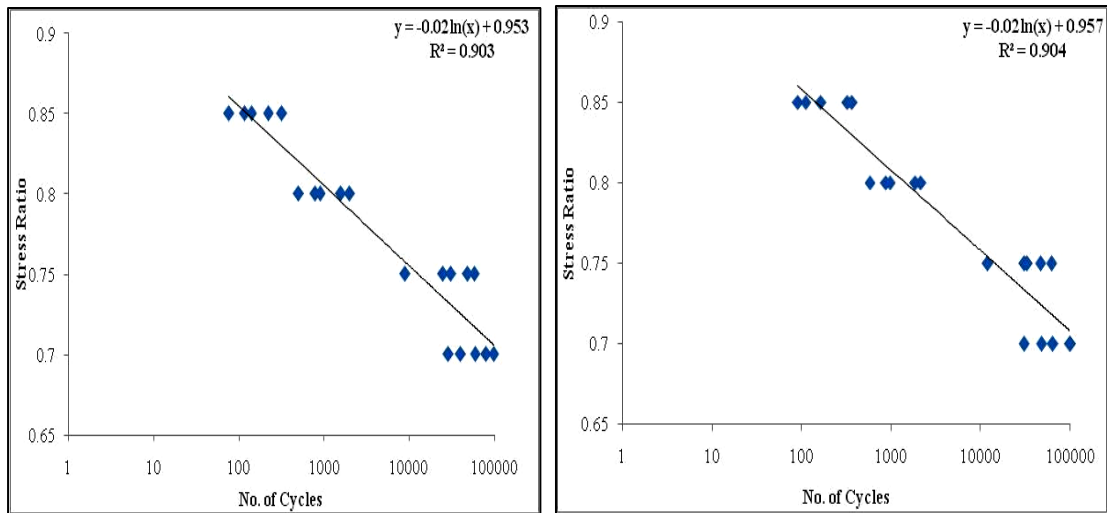
(a) OPCC

(b) 4-A-0
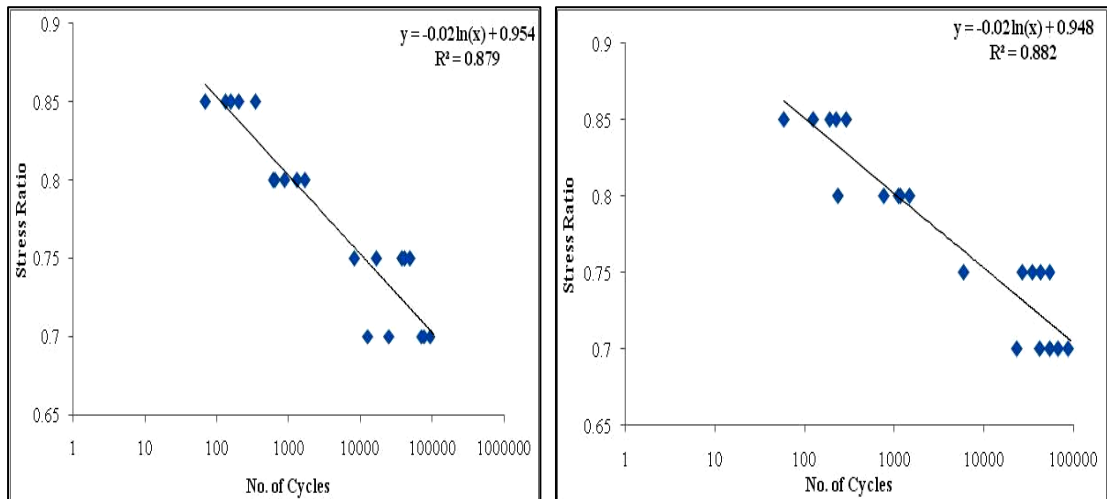
(c) 4-A-50

(d) 4-A-100

Figure 6.1 S-N curves for AASC mixes with/without PIS aggregates

The S-N curves obtained by plotting stress ratio (SR) v/s number of cycles (N) up to failure for OPCC and AASC (100:0) with partial or complete replacement of river sand with PIS aggregates are presented in Fig.6.1. Similarly, S-N curves for AASFC (75:25), AASFC (50:50) and AASFC (25:75) with different replacement levels

101

of PIS aggregates have to be plotted to obtain the equations. The equations obtained from the S-N curves can be utilized for estimation of fatigue cycle at any stress ratio. The equations generated in the similar way for different concrete mixes are tabulated in Table 6.5. The statistical correlation coefficient values from the Table 6.5 for different concrete mixes and different stress ratios were found to be in the range 0.85 to 0.91 indicating statistical significance.

6.5 PROBABILISTIC ANALYSIS OF FATIGUE RESULTS

The experimental fatigue data of concrete generally exhibit scatter and variability even when tested under controlled due to heterogeneity of materials and other reasons. Hence, in order to obtain satisfactory information on fatigue resistance and prediction of fatigue life of structures, it is desirable to make use of probabilistic approach in the fatigue design of structures (Ramakrishnan et al. 1996). The fatigue data of concrete mixes were statistically analyzed at each stress ratio to obtain fatigue equation with survival probability. Due to its relative ease in use, well developed statistics and sound experimental verification, the two parameter Weibull distribution is the most widely accepted method for analyzing fatigue data of concrete structures (Oh 1991; Kumar et al. 2012). The Weibull distribution takes into account two major parameters; 'α' which defines the shape of the distribution and 'μ' which defines the characteristic life. The parameters α and μ can be estimated using different methods, however in this investigation, the graphical method is used due to its relative ease in use.

6.6 ESTIMATION OF WEIBULL DISTRIBUTION PARAMETERS USING GRAPHICAL METHOD

The graph between $[\ln[\ln\left(\frac{1}{L_N(\mathrm{n})}\right)]$ and $\ln(\mathrm{n})$ is plotted for all the stress ratios and for all concrete mixes and the Weibull distribution parameters were determined. Fig. 6.2 presents the sample plot for mix 4-A-100 at stress level of 0.70. The Weibull distribution parameters for OPCC and AASC/AASFC mixes at different stress ratios are tabulated in Table 6.6 to 6.9. From Table 6.6 to 6.9, it may be observed that correlation coefficients of mixes at different stress ratios are in the range 0.87 to 0.97, thus indicating that the fatigue life data for OPCC and AASC/AASFC mixes

with/without PIS aggregates follow Weibull distribution. The Weibull distribution parameters may be utilized for predicting the fatigue life cycles considering desired probability of failure.
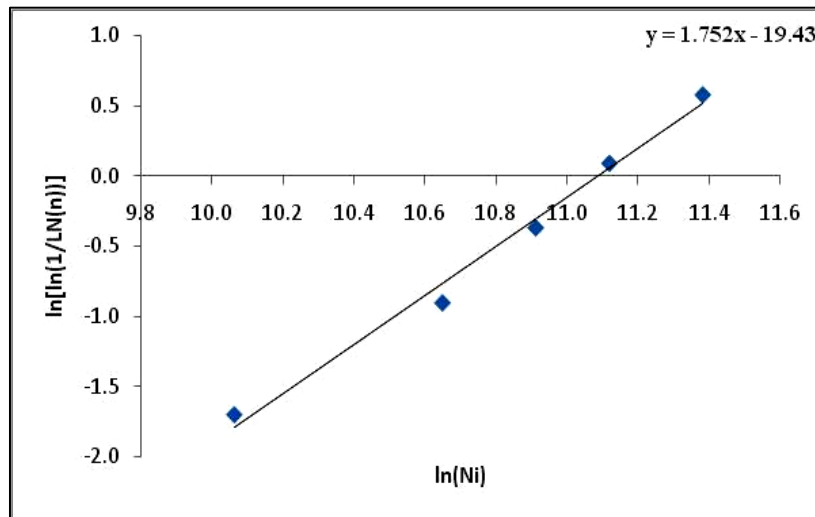
Figure 6.2 Graphical analysis of fatigue data for 4-A-100 at stress ratio 0.70

Table 6.6. Weibull parameters for AASC (100:0) mixes at different stress ratios

Mix ID	OPCC			4-A-0		
SR	α	μ	R^2	α	μ	R^2
0.85	1.578	207	0.972	1.408	247	0.929
0.80	1.568	1366	0.963	1.584	1515	0.937
0.75	1.185	42184	0.955	1.339	46482	0.936
0.70	1.752	71790	0.988	1.761	79488	0.997
Mix ID	4-A-50			4-A-100		
SR	α	μ	R^2	α	μ	R^2
0.85	1.468	217	0.971	1.404	215	0.969
0.80	1.888	1208	0.910	1.136	1216	0.875
0.75	1.143	38222	0.930	0.951	42721	0.869
0.70	0.992	68810	0.923	1.752	65524	0.988

Table 6.7. Weibull parameters for AASFC (75:25) mixes at different stress ratios

Mix ID	OPCC			4-B-0		
SR	α	μ	R²	α	μ	R²
0.85	1.578	207	0.972	1.382	224	0.947
0.80	1.586	1374	0.976	1.508	1443	0.961
0.75	1.185	42184	0.955	0.936	42491	0.960
0.70	1.992	70946	0.950	1.777	73444	0.922
Mix ID	4-B-50			4-B-100		
SR	α	μ	R²	α	μ	R²
0.85	1.689	201	0.928	1.035	230	0.917
0.80	1.347	1197	0.9547	1.138	1080	0.912
0.75	1.11	38506	0.952	1.165	41217	0.808
0.70	1.424	62715	0.959	1.29	57598	0.983

Table 6.8. Weibull parameters for AASFC (50:50) mixes at different stress ratios

Mix ID	OPCC			4.5-C-0		
SR	α	μ	R²	α	μ	R²
0.85	1.578	207	0.972	1.322	244	0.989
0.80	1.586	1374	0.976	1.462	1498	0.900
0.75	1.185	42184	0.955	1.002	48943	0.918
0.70	1.992	70946	0.950	1.416	84272	0.947
Mix ID	4.5-C-50			4.5-C-100		
SR	α	μ	R²	α	μ	R²
0.85	1.419	209	0.961	1.41	239	0.983
0.80	1.646	1193	0.913	1.704	1164	0.964
0.75	1.246	39891	0.937	0.886	38467	0.937
0.70	1.452	73010	0.935	1.301	58915	0.971

Table 6.9. Weibull parameters for AASFC (25:75) mixes at different stress ratios

Mix ID	OPCC			5.5-D-0		
SR	α	μ	R^2	α	μ	R^2
0.85	1.578	207	0.972	1.045	318	0.912
0.80	1.568	1366	0.963	1.851	1674	0.942
0.75	1.185	42184	0.955	1.165	55185	0.883
0.70	1.752	71790	0.988	0.977	80813	0.898
Mix ID	5.5-D-50			5.5-D-100		
SR	α	μ	R^2	α	μ	R^2
0.85	1.087	258	0.964	1.296	224	0.896
0.80	1.161	1564	0.893	2.254	1293	0.934
0.75	0.867	38985	0.948	0.717	39900	0.850
0.70	2.119	68043	0.97	1.581	62545	0.928

6.7 GOODNESS-OF-FIT TEST FOR FATIGUE RESULTS

From the analysis, it is established that the fatigue life at various stress ratios of OPCC, AASC and AASFC with/without PIS aggregates can be described using Weibull distribution. However, it would be convincing to carry out a goodness-of-fit test in order to confirm that it is a valid distribution model for statistical description of fatigue life of OPCC and AASC/AASFC. Hence the Kolmogorov-Smirnov test was carried out for this purpose (Mohammadi and Kaushik 2005).

The Kolmogorov–Smirnov test can be performed by using Eq.6.6.

$$D = \max_{i=1}^{k} [|F^+(X_i) - F_N(X_i)|] \qquad (6.6)$$

Where, $F^+(X_i) = i/k$ = observed cumulative histogram.

i = order number of the data point.

k = total number of data points in the sample under consideration at a given stress ratio.

F (Xi) = hypothesized cumulative distribution function given by Eq.6.7.

$$F_N(n) = 1 - \exp\left[-\left(\frac{n-n_0}{\mu-n_0}\right)^\alpha\right]; n \geq n_0 \qquad (6.7)$$

Where, n is the specific value of a random variable N; α=shape parameter or Weibull slope at stress ratio S; μ=scale parameter or characteristic life at given stress ratio S; and n_0=location parameter or minimum life at stress ratio S.

Table 6.10 shows the results calculated by Kolmogorov–Smirnov test of fatigue life for 4-A-100 at stress ratio S = 0.70.

Table 6.10. Kolmogorov–Smirnov test of fatigue life for 4-A-100 at S=0.70

i	X_i	$F^+(X_i) = i/k$	$F(X_i)$	$\|F^+(X_i) - F(X_i)\|$
1	23485	0.2	0.1527	0.0473
2	42141	0.4	0.3696	0.0304
3	54756	0.6	0.5181	0.0819
4	67348	0.8	0.6498	0.1502
5	87548	1	0.8101	0.1899

From Table 6.10, it can be observed that the maximum difference is 0.1899 (for i=5) for this case. The critical value D_c for n=5 and 5% significance level was found to be 0.563 from Kolmogorov–Smirnov Table. Since $D_t < D_c$ (0.1899< 0.563), the present two parameter Weibull distribution model for fatigue life at stress ratio S=0.70 is acceptable at the 5% significance level. The goodness-of-fit test is performed for the fatigue life data for OPCC and AASC/AASFC at different stress ratios and the model was found to be acceptable at 5% level of significance in all the cases.

6.8 SURVIVAL PROBABILITY AND S–N RELATIONSHIP

The fatigue life for different probability of failure (Chandrashekar 2013) can be expressed as follows:

$$n = exp\left[\frac{\ln\left\{\ln\left(\frac{1}{1-P_f}\right)\right\} + \alpha \ln(\mu)}{\alpha}\right] \qquad (6.8)$$

Where, P_f is the probability of failure.

(a) OPCC   (b) 4-A-0

(c) 4-A-50   (d) 4-A-100
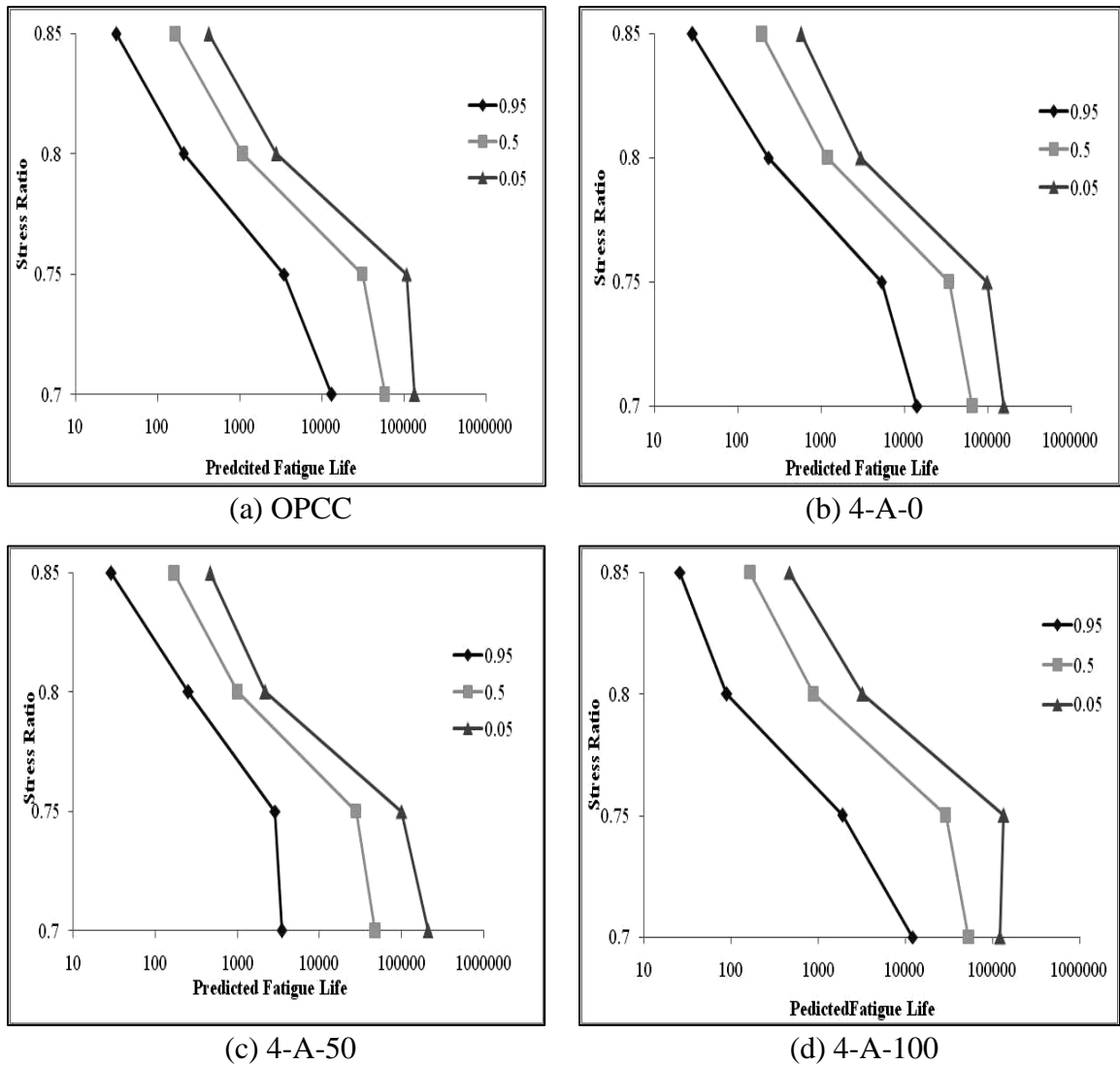
Figure 6.3 Predicted fatigue lives corresponding to different survival probabilities

Since the fatigue life data of concrete mixes follow Weibull distribution, it can be used for the calculation of fatigue lives corresponding to different survival probabilities. The Eq.6.8 gives the fatigue life (n) for different failure probabilities. Using the values of Weibull distribution parameters ('α' and 'μ') obtained earlier for the fatigue life data of concrete mixes, the Eq.6.8 can be used to calculate the fatigue lives corresponding to different failure probabilities (P_f). Fig.6.3 presents the predicted flexural fatigue life of OPCC and AASC mixes with/without PIS aggregates calculated at different survival probabilities (0.05, 0.5 and 0.95) using Eq.6.8. From Fig. 6.3, it can be noticed that for a particular stress ratio, the number of expected cycles which a concrete mix can sustain decreases with the increasing probability of failure. The

107

expected number of cycles is greater at lower probability of failure i.e., at 0.95 (failure probability=5%).

6.9   SUMMARY

The present chapter summarizes the results of the fatigue experiments carried out on concrete mixes. The flexural fatigue performance of AASC and AASFC mixes incorporating 0%, 50% and 100% (by volume) of PIS aggregate was investigated. The specimens were subjected to different stress ratios (0.70, 0.75, 0.80 and 0.85) and the number of cycles for failure of the specimen was determined. The fatigue data was represented using S-N curves. A probabilistic analysis of the obtained fatigue test data was carried out to ascertain the fatigue life of the material using two parameter Weibull distribution. Graphical method was adopted to determine the Weibull parameters. The test for goodness-of-fit was carried out to verify the statistical significance of the obtained data. The outcome of the Weibull distribution was analyzed to predict the fatigue life of concrete mixes with desired probability of failure. The AASC/AASFC mixes with river sand display higher resistance to fatigue failure as compared to OPCC irrespective of the applied stress ratio. This may be due to the highly dense interfacial transition zone between the paste and the aggregate occurring in alkali activated binders as compared to that occurring in conventional cement. The fatigue life of AASC mixes decreased with the inclusion of PIS aggregates in AASC and AASFC (75:25) mixes. Similar trend was observed in other AASFC mixes incorporating PIS aggregates. The fatigue behaviour with higher contents of FA in AASFC mixes could not be clearly understood. The fatigue data of concrete mixes were found to follow two parameter Weibull distribution with a statistical significance greater than 0.85. Probabilistic analysis of fatigue data was carried out and it was found that the Weibull distribution parameters can be used to predict the fatigue life of concrete mixes with the desired survival probability. The goodness-of-fit test was performed for the fatigue life data for OPCC and AASC/AASFC at different stress ratios and the model was found to be acceptable at 5% level of significance in all the cases.

CHAPTER 7

COST COMPARISON AND RECOMMENDATIONS

7.1 GENERAL

Economy is one of the main criteria in any infrastructure projects. Especially, roads are important in any country's infrastructure development. Large quantity of raw materials is needed for road construction since the length of the roads will spread across the country in networks. In India, more importance is given for road infrastructure projects. Government aims at reducing the cost of construction by utilizing alternate sources of materials. Also, the environmental concerns associated with OPC production and depleting aggregate sources need a vital attention. The present study was taken up to address the concerns by utilizing marginal materials from iron and steel industries across India.

7.2 COST OF MARGINAL MATERIALS

In the present study, GGBS and FA were taken as alternative binders to be used in Alkali Activated System, by avoiding the usage of OPC. PIS was used as fine aggregate replacement. GGBS is a by-product of iron and steel industry which was available for free in the initial days. FA is generated in thermal power plants as a waste material. Both GGBS and FA are available in market now from the retailers at cheaper cost covering the transportation and handling expenditures. Wholesale price of GGBS and FA as per the local market is Rs. 2200 per metric tonnes and Rs. 300 per metric tonnes respectively. The alkaline activators – NaOH and Na_2SiO_3 are priced at Rs. 27 / kg and Rs. 13 / kg respectively with local retailers. PIS was procured free of cost from JSW Steel Ltd., Hospet, Karnataka. Transportation from source, i.e., Hospet, Karnataka to the place of study, i.e.,, Mangalore, Karnataka was charged at Rs. 20,000 per truck load having around 23 metric tonnes of material. Therefore, the transportation cost for 1 tonne of PIS stands at Rs. 870. As the demand grows for the material, the retailers may procure the slag material and sell at wholesale price to the end users. Also, the

utilization of PIS in the proximity of 5 to 10 kilometers from the source or industry becomes highly economical as the transportation cost may be only around Rs. 2000 or even free from the industry side. Utilization of industrial marginal materials always have better advantage in the nearby proximity to those industries.

For low and high volume roads, M30 and M40 grade of concrete is specified as per the guidelines. As per the recent Schedule of Rates at Mangalore, Karnataka (2018-19), the cost of M30 mix of concrete stands at around Rs. 6000 / m^3 and for M40 mix it is around Rs. 6400 / m^3. Schedule of rates also specifies the rate of river sand and crushed granite coarse aggregates of 20 mm size as Rs. 1700 / m^3 and Rs. 1525 / m^3. Approximate cost of mixing water stands at Rs. 0.05 /litre and that of Super-plasticizer is Rs. 131 / litre. Based on the density of water and Super-plasticizer, the cost is Rs. 0.05 / kg and Rs. 111 / kg respectively.

7.3   RECOMMENDED MIXES

Based on the results of mechanical properties, durability and flexural fatigue behaviour of all the mixes developed, few of the mixes can be recommended for low and high volume road construction. As per the outcomes of the study, few mixes have not performed well in terms of workability, modulus of elasticity values, durability performance. Overall outcome of the present study suggests four mixes for high volume roads and one mix for low volume roads. Recommended mixes are tabulated in Table 7.1 and 7.2.

Table 7.1. Mixes for high volume roads

Mix Designation	Na$_2$O Dosage (%)	Water/Binder Ratio	Activator Modulus	Compressive Strength (MPa)			Flexural Strength (MPa)	Modulus of Elasticity (MPa)	Slump (mm)
				3 Days	7 Days	28 Days			
4-A-100 GGBS:FA=100:0 100% Slag	4	0.40	1.25	33	40	50	5.9	3.6 x 10^4	15
4-B-100 GGBS:FA=75:25 100% Slag	4	0.40	1.25	30	36	49	5.6	3.5 x 10^4	30
4.5-C-100 GGBS:FA=50:50 100% Slag	4.5	0.38	1.25	27	39	51	5.5	3.4 x 10^4	35
5.5-D-75 GGBS:FA=25:75 75% Slag	5.5	0.38	1.50	29	37	49	5.6	3.2 x 10^4	40

Table 7.2. Mixes for low volume roads

Mix Designation	Na$_2$O Dosage (%)	Water/Binder Ratio	Activator Modulus	Compressive Strength (MPa)			Flexural Strength (MPa)	Modulus of Elasticity (MPa)	Slump (mm)
				3 Days	7 Days	28 Days			
5.5-D-100 GGBS:FA=25:75 100% Slag	5.5	0.38	1.50	26	35	50	5.5	2.9 x 10^4	40

The AASC and AASFC mixes recommended are achieving around 60 % of the strength in 3 days and 80 % of the strength in 7 days which is an advantage in road construction to open for traffic at the earliest.

7.4   COST COMPARISON

AASC and AASFC mixes recommended in the above tables can be considered for road construction in the place of present study, i.e., Mangalore, Karnataka. The cost per cubic meters of each of the materials is tabulated in Table 7.3 for the benefit of end users.

Table 7.3. Cost of materials with respect to the recommended mixes

Sl. No.	Mix ID	Total Cost (Rs/m³)
1	OPCC	5900
2	4-A-100	4170
3	4-B-100	3970
4	4.5-C-100	3860
5	5.5-D-75	4220
6	5.5-D-100	4020

Total cost of materials for construction of one cubic meter of pavement is presented in the above table in comparison with control concrete mix based on OPC. It can be observed that the AASC and AASFC mixes are economical with lesser cost when compared to conventional OPC based concrete mix. OPCC costs around Rs. 5900 / m³ for high volume road construction corresponding to M40 grade of concrete. There can be slight reduction in cost for M30 grade of concrete for low volume roads. 4-A-100, 4-B-100, 4.5-C-100 and 5.5-D-75 are recommended for high volume road construction and costs around Rs. 4170 / m³, Rs. 3970 / m³, Rs. 3860 / m³ and Rs. 4220 / m³ respectively. These mixes cost around 30% lesser than that of OPCC mixes, proving to be economical. With respect to low volume roads, 5.5-D-100 is recommended and costs around Rs. 4020 / m³. This mix is also approximately 30 % cheaper when compared to OPCC based mixes for low volume pavements.

CHAPTER 8

CONCLUSIONS AND FUTURE SCOPE

8.1   CONCLUSIONS

The development and understanding of AASC and AASFC mixes with industrial waste materials as aggregates are of significant interest because these new materials can be made cost-effective to Ordinary Portland cement (OPC) and exhibiting acceptable mechanical and durability properties. The present thesis presents information on investigations carried out on the suitability of GGBS, FA, PIS to produce concrete. Characteristics of AASC and AASFC mixes with partial or complete replacement of river sand with PIS were found to be satisfactory for highway applications.

The following conclusions are drawn based on the experimental results on the engineering and durability properties of AASC and AASFC mixes with PIS as fine aggregate.

- The strength of the AASC and AASFC mixes depend on the sodium oxide dosage of the alkaline activator. Higher the sodium oxide dosage, higher is the strength achieved.

- The replacement of natural aggregates with PIS as fine aggregate in alkali activated concrete mixes (AASC/AASFC) results in a slight reduction of the workability, but satisfies the requirement of 25+/-15 mm for highways.

- The AASC and AASFC mixes exhibited high early and ultimate strength as compared to OPCC. AASC/AASFC mixes with PIS aggregate exhibited lower compressive, tensile strength and modulus of elasticity as compared to AASC/AASFC mixes with 100% natural aggregate. However, the requirement of M40 for highways is satisfied by all the mixes.

- All AASC and AASFC mixes with partial or complete replacement of river sand with PIS attained 28-day compressive strength in the range of 55±10 MPa and flexural strengths greater than 5.5 MPa after 28 days of curing.

- The inclusion of higher content of FA (beyond 25%) in the AASFC mixes slightly resulted in decrease in tensile properties and modulus of elasticity for similar compressive strength grade as compared to AASC mix.

- AASC/AASFC mixes with PIS exhibited high VPV and water absorption values as compared to natural fine aggregates, due to the porous nature and higher water absorption of PIS aggregates respectively.

- The AASC/AASFC mixes with PIS displayed lower fatigue life as compared to AASC mix with 100% natural aggregates. The two parameter Weibull distribution can be approximately used for modelling the fatigue life of OPCC, AASC and AASFC mixes.

- The goodness-of-fit test is performed for the fatigue life data of OPCC and AASC/AASFC mixes at different stress ratios and the model was found to be acceptable at 5% level of significance. Prediction of fatigue life cycles of OPCC and AASC/AASFC mixes at different survival probabilities can be done by utilizing the Weibull distribution parameters.

- Alkali activated concrete mixes with 100% natural aggregates exhibited better resistance to sulphuric acid and magnesium sulphate environments as compared to OPCC, which may be attributed to properties/structure of binders. The acid and sulphate resistance of alkali activated concrete mixes decreased with replacement of natural aggregates with PIS.

- SEM analysis shows the denser microstructure in case of AASC mixes when compared to AASFC mixes. Inclusion of PIS showed higher C-A-S-H or N-A-S-H gel formation and thereby lesser unreacted particles as well as micro-crack development.

- However, at 100% Processed Granulated Blast furnace replacement, the AASFC mixes with 75% FA also produces required strength, workability and durability.
  All the recommended mixes (Chapter 7) attain almost 60% of the strength after air curing for 3 days and 80% after 7 days which is an added advantage to open the pavement for traffic at the earliest.

- The waste material from aluminium resmelting process, i.e., aluminium dross can be effectively used as a partial replacement for binder in AASC AND AASFC mixes.

5% addition with respect to the total binder content is recommended with no negative influence on strength gain and durability of concrete. From the Test results it is evident that the effective utilization of aluminium dross is not possible due to its adverse effect on Concrete. The changes in chemical composition by adding some additives might be the further research work that can be carried out.

The results of tests conducted on various strength and durability considerations have revealed that, the use of PIS based AASC/AASFC concrete mixes have been generally at par or marginally lower than the conventional OPC-based concrete mixes. It can be concluded that the AASC and the AASFC mixes with PIS as coarse aggregate can have several advantages over OPCC such as,

a) Usage of industrial marginal materials (PIS, GGBS, FA, Aluminium dross).
b) Consumption of river sand can be reduced, which in-turn reduces environmental and ecological problems associated with mining.
c) Reduction in PIS stock piles would solve environmental problems.
d) Due to air curing, water can be saved.
e) High early strength development can be effectively used for early strip-off of formwork, thus helping faster construction and early use of pavements.

8.2   LIMITATIONS

Although, PIS aggregates provide satisfactory strength and durability performance in AASC and AASFC mixes, special attention needs to be paid for proper weathering of the aggregates. Immediate implementation of PIS aggregates in concrete pavements without study of long-term properties is not advisable. When PIS used in AASC and AASFC concrete mixes, it is important to optimize the mix design appropriately in order to guarantee the desired level of durability. The mixes containing PIS aggregates may be aimed at higher compressive strength and lower water penetration as main characteristics. The PIS must be tested to determine the free lime or magnesia content along with tests for volume expansion. The PIS aggregate must be carefully selected and used in concrete pavements only if the aggregate has minimal volume expansion and low free lime or free magnesia contents.

117

8.3   SCOPE FOR FURTHER STUDY

The present investigation can be extended to:

- Extensive study on the micro-structural behaviour of AAC mixes with PIS as fine aggregates can be carried out.

- Evaluation on the temperature differential of AAC slabs.

- Performance evaluation of concrete mixes when PIS is subjected to different weathering process such as air aging, hot water aging and steam aging.

- Processing / weathering of aluminium dross with advanced processing techniques for avoiding swelling issues.

APPENDIX - I

MIX DESIGN METHOD FOR CONTROL CONCRETE

For the concrete mix, OPC 53 grade cement was used. Sand conforming to Zone - II was used. Locally available crushed stone granite aggregates of 20 mm down size were used. For the design IS code method was followed (IS: 10262 – 2019; IS: 456-2000).

Input parameters

Derived characteristics strength of concrete f_{ck}	=	40 MPa
Grade of cement	=	53
Specific gravity of cement	=	3.12
Specific gravity of sand	=	2.62
Specific gravity of coarse aggregate	=	2.67
Maximum size of aggregate	=	20 mm
Slump in mm	=	25+/-15 mm

Estimation of ingredients for M_{40} grade concrete:

(1) Target mean strength of concrete (TMS)

TMS = f_{ck} + 1.65 * S.D = 40 + 1.65 * 5= 48.25 N / mm^2

(2) Selection of water cement ratio

For Extreme exposure condition the water cement ratio = 0.40

(From Table 5, IS: 456 - 2000)

(3) Selection of Water content

From Table 2 of IS: 10262 – 2019, Max water content for 20 mm aggregate = 186 litre

(for 25 to 50mm slump range)

Estimated water content for 75 mm slump range   = 186 litre

Based on trials super plasticizer with 0.4% water content is reduced to 170 litre

Water content (w) = 170 kg/ m^3

(4) Calculation for cement content

Water-cement ratio = 0.4

Cement content = 170/0.4 = 425 kg/m^3

(5) Proportion of volume of coarse aggregate and fine aggregate content

Coarse aggregate content as percent of aggregate by absolute volume = 62% (From Table 4, IS 10262 - 2019)

For change in water cement ratio following adjustment is required

Volume adjustment required for coarse aggregates

For decrease in water cement ratio by 0.1 (0.5-0.4), Water content coarse aggregate in total aggregates = +.02. (From section 4.4, IS 10262 - 2019)

Therefore, required Coarse aggregate content as percentage of total aggregate by absolute volume, = 0.62+0.02 = 0.64.

(6) Mix Calculations

(a) Volume of concrete = $1m^3$

(b) Volume of cement = (Mass of cement/specific gravity of cement)*1/1000

   = (425/3.120)/1000

   = $0.136 \ m^3$

(c) Volume of super plasticizer (0.5% by mass of cement)

= (Mass of chemical admixture/specific gravity of chemical admixture)*1/1000

= (1.7/1.18)

= $0.00144 \ m^3$

Water to add = 170 – water present in super plasticizer

   = 170 – (1.7*0.5) = 169 litres

(d) Volume of water = (Mass of water/sp gravity of water)*1/1000

   = 169/1000 = $0.169 \ m^3$

(e) Volume of all in aggregate = [a-(b + c+ d)]

   = 1-(0.136+0.0014+0.169)

   = $0.694 \ m^3$

(f) Mass of coarse aggregate

= e * volume of coarse aggregate * specific gravity of coarse aggregate* 1000

= 0.694*0.64*2.67*1000

=1185.9 kg/m^3

(g) Mass of fine aggregate

= e * volume of fine aggregate * specific gravity of fine aggregate* 1000

= 0.694*0.36*2.62*1000

= 654.5 kg/m^3

(7) Mix proportions (considering aggregates in SSD condition)

Ingredients of mix	Cement (kg/m^3)	Fine aggregate (kg/m^3)	Coarse aggregate (kg/m^3)	Water (kg/m^3)	Super Plastisizer (kg/m^3)
	425	655	1186	169	1.7

APPENDIX - II

SAMPLE MIX DESIGN FOR ALKALI ACTIVATED SLAG CONCRETE

For AASC mix 100% GGBS by weight is replaced by weight of OPC and alkali solution is used instead of only water.

Input parameters:

Derived characteristics strength of concrete f_{ck}	=	40 MPa
Specific gravity of GGBS,	=	2.9
Specific gravity of sand	=	2.62
Specific gravity of coarse aggregate	=	2.67
Specific gravity of alkali solution (4% Na_2O, Ms 1.25)	=	1.22
Maximum size of aggregate	=	20 mm
Slump in mm	=	25+/-15 mm

Estimation of ingredients for AASC:

(1) Target mean strength of concrete (TMS)

TMS = f_{ck} + 1.65 * S = 40 + 1.65 * 5= 48.25 N / mm^2

(2) Na_2O Dosage Required: 4%

   Ms Required : 1.25

(3) Calculations for alkali solution

   Sodium silicate solution having Na_2O = 14.7%, SiO_2 = 32.8%, water = 52.5% by weight

   Hence, 1 kg of sodium silicate contains 0.147 kg of Na_2O, 0.328 kg of SiO_2 and 0.525 kg of water.

   Ms of sodium silicate = SiO_2/Na_2O = 32.8/14.7 = 2.23

   NaOH flakes having Na_2O fraction = 62/80 = 0.775

   1 kg of NaOH contains 0.775 kg of Na_2O

   Na_2O required by weight for 425 kg of GGBS at 4% = 425*0.04 = 17 kg

   SiO_2 required by weight for 425 kg of GGBS at 1.25 Ms = SiO_2/Na_2O = 1.25

   Then SiO_2 required = 1.25*Na_2O

$$= 1.25*17 = 21.25 \text{ kg}$$

Amount of Sodium silicate solution required for 21.25 kg for SiO_2

$$= SiO_2 \text{ required/ } SiO_2 \text{ present in sodium silicate solution}$$

$$= 21.25/0.328 = 64.78 \text{ kg}$$

Na_2O present in 64.78 kg sodium silicate solution = 64.7*0.148 = 9.58 kg

Then Na_2O required from NaOH = 17 – 9.58 = 7.41 kg

NaOH flakes required = 7.41/0.775 = 9.60 kg

Extra water required to make w/b ratio of 0.4 = 170 – water present in sodium silicate

$$= 170 – (64.7*0.525)$$

$$= 136 \text{ kg}$$

Alkali solution = 64.78+9.60+136 = 210.4 kg

(4) Mix Calculations

(a) Volume of concrete = 1m^3

(b) Volume of GGBS = (Mass of GGBS/specific gravity of GGBS)*1/1000

$$= (425/2.9)/1000$$

$$= 0.146 \text{ m}^3$$

(c) Volume of Alkali Solution

= (Mass of Alkali Solution/specific gravity of Alkali Solution)*1/1000

= (210.4/1.22)/1000

= 0.172 m^3

(d) Volume of all in aggregate = [a-(b+c)]

$$= 1-(0.146+0.172)$$

$$= 0.682 \text{ m}^3$$

(e) Mass of coarse aggregate

= d * volume of coarse aggregate * specific gravity of coarse aggregate* 1000

= 0.682*0.64*2.67*1000

=1165.4 kg/m^3

(f) Mass of fine aggregate (sand)

= d * volume of fine aggregate * specific gravity of fine aggregate* 1000

= 0.682*0.36*2.62*1000

= 643.3 kg/m^3

(g) <u>Mass of PIS aggregates (75% natural aggregates + 25% PIS)</u>

Mass of fine aggregates * volume of fine aggregates * 0.75* specific gravity of fine aggregates aggregate* 1000

Mass of natural fine aggregates = 0.682*0.36*0.75*2.62*1000 = 482.45 kg/m^3

Mass of PIS = 0.682*0.36*0.25*2.95*1000 = 181.07 kg/m^3

Total mass of fine aggregate = 663.5 kg/m^3

(8) Mix proportions (all quantities in kg/m^3) (For 4-A-0)

Ingredients of mix	GGBS	Sand	Coarse aggregate	Water	Sodium Silicate	NaOH
	425	643	1165	136	64.78	9.6

APPENDIX III

COST COMPARISON

The Table below gives the weight of materials for 1 m^3 of concrete as per the mixes designed. Cost of materials for unit quantity are considered as per the Schedule of Rates.

Sl. No.	Mix	Materials	Quantity of Materials per cubic meters (kg/m^3)	Unit cost of Material (Rs/kg)	Cost (Rs/m^3)	Total Cost (Rs/m^3)
1	OPCC	OPC	425	5.875	2496.88	5900
		Sand	655	2.575	1686.63	
		CA	1186	1.275	1512.15	
		Water	169	0.05	8.45	
		SP	1.7	111	188.7	
2	4-A-100	GGBS	425	2.2	935	4170
		FA	0	0.3	0	
		Sand	0	2.575	0	
		Slag	724	0.875	633.5	
		CA	1165	1.275	1485.375	
		NaOH	9.6	27	259.2	
		Na$_2$SiO$_3$	64.8	13	842.4	
		Water	136	0.05	6.8	
3	4-B-100	GGBS	319	2.2	701.8	3970
		FA	106	0.3	31.8	
		Sand	0	2.575	0	
		Slag	724	0.875	633.5	
		CA	1165	1.275	1485.375	
		NaOH	9.6	27	259.2	
		Na$_2$SiO$_3$	64.8	13	842.4	
		Water	136	0.05	6.8	

Sl. No.	Mix	Materials	Quantity of Materials per cubic meters (kg/m^3)	Unit cost of Material (Rs/kg)	Cost (Rs/m^3)	Total Cost (Rs/m^3)
4	4.5-C-100	GGBS	212.5	2.2	467.5	3860
		FA	212.5	0.3	63.75	
		Sand	0	2.575	0	
		Slag	708	0.875	619.5	
		CA	1149	1.275	1464.975	
		NaOH	10.5	27	283.5	
		Na$_2$SiO$_3$	72.9	13	947.7	
		Water	123	0.05	6.15	
5	5.5-D-75	GGBS	106	2.2	233.2	4220
		FA	319	0.3	95.7	
		Sand	132	2.575	339.9	
		Slag	516	0.875	451.5	
		CA	1121	1.275	1429.275	
		NaOH	9.9	27	267.3	
		Na$_2$SiO$_3$	106.9	13	1389.7	
		Water	123	0.05	6.15	
6	5.5-D-100	GGBS	106	2.2	233.2	4020
		FA	319	0.3	95.7	
		Sand	0	2.575	0	
		Slag	681	0.875	595.875	
		CA	1121	1.275	1429.275	
		NaOH	9.9	27	267.3	
		Na$_2$SiO$_3$	106.9	13	1389.7	
		Water	123	0.05	6.15	

REFERENCES

Adam, A.A. (2009). "Strength and durability properties of alkali activated slag and fly ash-based geopolymer concrete." Doctoral Dissertation, School of Civil, Environmental and Chemical Engineering, RMIT University Melbourne, Australia.

Ahmad, Z.N.S., Zakaria, M.Z.H., Baini, R., Rahman, M.R., Mohammed, S.N. and Hamdan, S. (2016). "Influence of Alkali Treatment on the Surface Area of Aluminium Dross." *Advances in Material Science and Engineering*, Hindawi Publishing Corporation.

Alexander, M.G., and Milne, T.I. (1995). "Influence of cement blend and aggregate type on stress– strain behavior and elastic modulus of concrete." *ACI Material Journal*, 92 (3), 227–234.

Alexander, M., Bertron, A. and Belie, N.D. (2013). "Performance of cement-based materials in aggressive aqueous environments." State-of-the-Art Reports, 10, RILEM.

Ali, N. and Sanjayan, J.G. (2015). "Synthesis of geopolymer from industrial wastes." *Journal of Cleaner Production*, 99, 297-304.

Ali, N., Ali, B., Melissa, D., Chathumini, M. Peita, Z., Samuel, Z. and Sanjayan, J.G. (2017). "The behaviour of iron in geopolymer under thermal shock." *Construction and Building Materials*, 150, 248-251.

Altan, E. and Erdogan, S.T. (2012). "Alkali activation of a slag at ambient and elevated temperatures." *Cement and Concrete Composites*, 34, 131–139.

Anshuman, T., Sarbjeet, S. and Ravindra, N. (2016). "Feasibility assessment for partial replacement of fine aggregate to attain cleaner production perspective in concrete: A review." *Journal of Cleaner Production*, 135, 490-507.

Arimanwa, J., Onwuka, D., Arimanwa, M. and Onwuka, U. (2011). "Prediction of the compressive strength of aluminum waste-cement concrete using Scheffe's theory." *Journal of Materials in Civil Engineering*, 24(2),177–183.

Arunabh, M. and Kamalesh, K.S. (2018). "Recovery of valuable products from hazardous aluminium dross: A review." *Resources, Conservation and Recycling*, 130, 95-108.

ASTM C642-13. (2013). "Standard test method for density, absorption, and voids in hardened concrete." *American Society for Testing of Materials*, USA.

Aydın, S. and Baradan, B. (2012). "Mechanical and microstructural properties of heat cured alkali-activated slag mortars." *Materials and Design*, 35, 374–383.

Bajpai, R., Soni, V., Shrivastava, A. and Ghosh, D. (2021). "Experimental investigation on paver blocks of fly ash-based geopolymer concrete containing silica fume." *Road Materials and Pavement Design.*

Bakharev, T. (2005). "Geopolymeric Materials Prepared Using Class F Fly Ash and Elevated Temperature Curing." *Cement and Concrete Research*, 35(6), 1224-1232.

Bakharev, T., Sanjayan, J. G. and Cheng, Y. B. (1999). "Alkali Activation of Australian Slag Cements." *Cement and Concrete Research*, 2 (1), 113- 120.

Bakharev, T., Sanjayan, J.G. and Cheng, Y. B. (2000). "Effect of Admixtures on Properties of Alkali-activated Slag Concrete." *Cement and Concrete Research*, 30(9), 1367- 1374.

Bakharev, T., Sanjayan, J.G. and Cheng, Y. B. (2002). "Sulfate attack on alkali-activated slag concrete." *Cement and Concrete Research*, 32(2), 211–216.

Bakharev, T., Sanjayan, J.G., and Chen, Y.B. (2003). "Resistance of alkali activated slag concrete to acid attack." *Cement and Concrete Research*, 33(10), 1607–1611.

Balaguru, P., Kurtz, S. and Rudolph, J. (1997). "Geopolymer for Repair and Rehabilitation of Reinforced Concrete Beams." *The Geopolymer Institute*, www.geopolymer.org.

Bernal, S. A., Mejra de Gutierrez, R. and Provis, J. L. (2012). "Engineering and Durability Properties of Concretes Based on Alkali-activated Granulated Blast Furnace Slag/Metakaolin Blends." *Construction and Building Materials*, 33, 99–108.

Bernal,S.A., Gutiérrez, R.D., Alba, L. P., Provis, J.L., Rodriguez, E.D. and Delvasto, S. (2011). "Effect of Binder Content on the Performance of Alkali-activated Slag Concretes." *Cement and Concrete Research*, 41(1), 1–8.

Bhattacharya. (2005). "Scope of concrete roads in India." *Keynote address at National Workshop on Sustainability of Road Infrastructure-Scope of concrete roads*, jointly organized by CMA India and ICI Kolkata, India.

Bilim, C., Karahan, O., Cengiz, D.A. and Serhan, L. (2015). "Effects of Chemical Admixtures and Curing Conditions on some Properties of Alkali-Activated Cementless Slag Mixtures." *KSCE Journal of Civil Engineering*, 19(3), 733-741.

Blaakmeer, J. (1994). "An alkali activated slag Fly Ash binder for acid resistant Concrete." *1st International Conference on Alkaline Cements and Concretes* (edited by Krivenko), 1, Kiev, Ukraine, 347–360.

Bonen, D. (1992). "Composition and appearance of magnesium silicate hydrate and its relation to deterioration of cement based materials." *Journal of American Ceramic Society*, 75(10), 2904–2906.

Bonen, D. and Cohen, M.D. (1992). "Magnesium sulphate attack on Portland cement paste – I. Microstructural analysis." *Cement and Concrete Research,* 22, 169–180.

Cengiz, D., Atis,C.B., Zlem, O., Elik, C. and Okan,K. (2009). "Influence of Activator on the Strength and Drying Shrinkage of Alkali-activated Slag Mortar." *Construction and Building Materials*, 23(1), 548–555.

Chandrashekhar, A., Ravi Shankar, A.U. and Girish, M.G. (2010). "Fatigue Behaviour of Steel Fiber Reinforced Concrete with Fly Ash." *Highway Research Journal*, 9-20.

Chen, W., Brouwers, H.J.H. (2007). "The hydration of slag. Part 1: Reaction models for alkali-activated slag." *Journal of Material Science*, 42, 428–443.

Chi, M. (2012). "Effects of Dosage of Alkali-activated Solution and Curing Conditions on the Properties and Durability of Alkali-activated Slag Concrete." *Construction and Building Materials*, 35, 240–245.

Chi, M. and Huang, R. (2013). "Binding Mechanism and Properties of Alkali-activated FA/Slag Mortars." *Construction and Building Materials*, 40, 291–298.

Collins, M.P., Mitchell, D. and MacGregor, J.G. (1993). "Structural Design Considerations for High Strength Concrete." *ACI Concrete International*, 15(5), 27-34.

Collins, F.G. and Sanjayan, J.G. (1999). "Workability and Mechanical Properties of Alkali Activated Slag Concrete." *Cement and Concrete Research,* 29(3), 455–458.

Davidovits, J.J. (1994). "Properties of Geopolymer Cements." *First International Conference on Alkaline Cements and Concretes*, Kiev, Ukraine, SRIBM, Kiev State Technical University, 131-149.

Davidovits, J.J. (1991). "Geopolymers: Inorganic. Polymeric New Materials." *Journal of Thermal Analysis*, 37, 1633-1656.

Davidovits, J.J. (1979). "Synthesis of New High Temperature Geo-polymers for Reinforced plastics Composites." *SPE PACTEC 79 Society of Plastic Engineers, Brookfield Centre*, 151–154.

Davidovits, J.J. (2005). "Geopolymer chemistry and Sustainable Development. The Poly (sialate) Terminology: A very useful and simple model for the promotion and understanding of green-chemistry." *Proceedings of the World Congress Geopolymer, Davidovits, J. (Ed.), Saint Quentin, France*, 9-15.

Diaz-Loya, E. I., Allouche, E. N. and Vaidya, S. (2011). "Mechanical Properties of Fly-ash-based Geopolymer Concrete." *ACI Material Journal*, 108, 300–306.

Douglas, E. and Brandstetr, J.A. (1990). "Preliminary study on the alkali activation of ground granulated blast-furnace slag." *Cement Concrete Research,* 20, 746–756.

Datta, D. and Ghosh, S. (2014). "Effect of curing profile on fly ash geopolymer with slag as supplementary." *International Journal of Engineering Sciences and Research Technology*, 3(12), 143-148.

Duxson, P., Fernandez-Jimenez, A., Provis, J. L., Lukey, G. C., Palomo, A. and Deventer, J. S. J. V. (2007). "Geopolymer Technology: the current state of the art." *Journal of Materials Science, 42*(9), 2917-2933.

Elinwa, A.U. and Mbadike, E. (2011). "The use of aluminum waste for concrete production." *J. Asian Architecture Building Engineering*, 10(1), 217–220.

Ewais, E., Khalil, N., Amin, M., Ahmed, Y. and Barakat, M. (2009). "Utilization of aluminum sludge and aluminum slag (dross) for the manufacture of calcium aluminate cement." *Ceram. Int*., 35(8), 3381–3388.

Fernández-Jiménez, A. and Palomo, A. (2003). "Characterisation of FA: Potential Reactivity as Alkaline Cements." *Fuel*, 82(18), 2259-2265.

Fernandez-Jimenez, A. and Palomo, A. (2005). "Composition and Microstructure of Alkali Activated Fly Ash Binder: Effect of the activator." *Cement and Concrete Research*,35 (10), 1984-1992

Fernandez-Jimenez, A., Palomo, J. G. and Puertas, F. (1999). "Alkali-activated slag mortars: Mechanical strength behavior." *Cement and Concrete Research*, 29(8), 1313-1321.

Fernandez-Jiménez, F.A., Palomo, A. and Criado, M. (2005). "Microstructure development of alkali-activated fly ash cement: a descriptive model." *Cement and Concrete Research,* 35(6), 1204–1209.

Fernando, S., Gunasekara, C., David, W. L., Nasvi, M.C.M., Setunge, S. and Dissanayake, R. (2022). "Engineering properties of waste-based alkali activated concrete brick containing low calcium fly ash and rice husk ash: A comparison with traditional Portland cement concrete brick." *Journal of Building Engineering,* 46, 103810.

FHWA, (2012). "User guidelines for byproducts and secondary use materials in pavement construction*."* Publication Number: FHWA-RD-97-148.

Gambhir, M.L. (2004). "Concrete technology, theory and practice." T*ata McGraw-hill (Education) Private limited,* fourth edition.

Garcia, E., Campos, V.K., Gorokhovsky, A. and Fernandez, J.A. (2006). "Cementitious Composites of Pulverized Fuel Ash and Blast Furnace Slag Activated by Sodium Silicate: effect of Na_2O Concentration and Modulus." *Advanced Applied Ceramics*, 105(4), 201–208.

Gaurav, S., Souvik, D., Abdulaziz, A.A., Showmen, S. and Somnath, K. (2015). "Study of Granulated Blast Furnace Slag as Fine Aggregates in Concrete for Sustainable

Infrastructure." *World Conference on Technology, Innovation and Entrepreneurship, Procedia - Social and Behavioral Sciences,* 195, 2272 – 2279.

Gebhardt, R.F. (1988). "Rapid methods for chemical analysis of hydraulic cement." STP985 *American Society for Testing Materials.*

Girish, M., Sujay, R.N., Sreedhara, B.M., Manu, D.S., Parameshwar, H. and Jayakesh, K. (2016). "Investigation of concrete produced using recycled aluminium dross for hot weather concreting conditions." *Resource Efficient Technologies,* 2, 68-80.

Glukhovsky, V. D. (1959). "Soil Silicates." *Kiev, Ukraine: Gastroi Publishers*.

Glukhovsky, V.D. (1994). "Alkaline Cements and Concretes." *First International Conference, Kiev*, Ukraine,1-8.

Gourley, J. T. (2003). "Geopolymers; Opportunities for Environmentally Friendly Construction Materials." *Materials Conference: Adaptive Materials for a Modern Society, Sydney, Institute of Materials Engineering Australia.*

Gray, W.H., McLaughlin, J.F. and Antrim, J.C. (1961). "Fatigue Properties of Lightweight Aggregate Concrete." *ACI Journal Proceedings,* 58(8), 149-162.

Guerrrieri, M. and Sanjayan, J. (2009). "Behaviour of Combined FA/Slag Based Geopolymers when Exposed to High Temperatures." *Fire and Materials*, 34 (4), 163-175.

Hafa M.B., Saout, G.L., Winnefeld, F. and Lothenbach, B. (2011). "Influence of activator type on hydration kinetics, hydrate assemblage and micro structural development of alkali-activated blast-furnace slags." *Cement and Concrete Research,* 41, 301–310.

Hansen, S. and Sadeghian, P. (2020). "Recycled gypsum powder from waste drywalls combined with fly ash for partial cement replacement in concrete." *Journal of Cleaner Production*, 274, 122785.

Huang, W. and Wang, H. (2021). "Geopolymer pervious concrete modified with granulated blast furnace slag: Microscale characterization and mechanical strength." *Journal of Cleaner Production,* 328, 129469.

Hui, Mao-hua, Z. and Jin-ping, O. (2007). "Flexural fatigue performance of concrete containing nano particles for pavements." *International Journal of Fatigue,* 29(7), 1292-1301.

IBEF (India Brand Equity Foundation). (2022). "Road Infrastructure in India." https://www.ibef.org/industry/roads-india.aspx, Last accessed on 15/03/2022.

IBEF (India Brand Equity Foundation). (2022). "Cement Industry in India." https://www.ibef.org/industry/cement-india.aspx, Last accessed on 15/03/2022.

Idawati, I., Susan, A.B., John, L.P., Rackel, S. N., David, G.B., Adam, R. K., Sinin, H. and van Deventer, J.S.J. (2013). "Influence of Fly Ash on the water and chloride permeability of alkali-activated slag mortars and concretes." *Construction and Building Materials*, 48, 1187–1201.

Idawati, I., Susan, A.B., John, L.P., Rackel, S.N., Hamdan, S., and van Deventer, J.S.J. (2014), "Modification of phase evolution in alkali activated blast furnace slag by the incorporation of Fly Ash." *Cement and Concrete Composites,* 45, 125-135.

IRC: 58-2002. (2002). "Guidelines for the design of plain jointed rigid pavements for highways." Second Revision, *Indian Road Congress*, New Delhi, India.

IRC: 58-2015. (2015). "Guidelines for the design of plain jointed rigid pavements for highways." Third Revision, *Indian Road Congress*, New Delhi, India.

IRC: SP:62-2004. (2004). "Guidelines for the design and construction of cement concrete pavements for rural roads." *Indian Road Congress,* New Delhi, India.

IS: 1199-1959. (1959). "Method for sampling and analysis of concrete." *Bureau of Indian Standards*, New Delhi, India.

IS: 12269–2013. (2013). "Specifications for 53 grade Ordinary Portland Cement." *Bureau of Indian Standards,* New Delhi, India.

IS: 14212-1995. (1995). "Sodium and potassium silicates- Methods of test." *Bureau of Indian Standards,* New Delhi, India.

IS: 2386 (Parts I-IV) -1963. (1963). "Methods of test for aggregates for concrete." *Bureau of Indian Standards*, New Delhi, India.

IS: 269-2015. (2015). "Ordinary Portland Cement – Specification (Sixth Revision)." *Bureau of Indian Standards*, New Delhi, India.

IS: 3812-Part II-2003. (2003). "Specification for pulverized fuel ash, part 2: for use as admixture in cement mortar and concrete." *Bureau of Indian Standards,* New Delhi, India.

IS: 383-2016. (2016). "Indian standard specification for coarse and fine aggregates from natural sources for concrete (Second revision)." *Bureau of Indian Standards*, New Delhi, India.

IS: 456–2000. (2000). "Plain and Reinforced Concrete – Code of Practice." *Bureau of Indian Standards,* New Delhi, India.

IS: 516–1959. (1959). "Methods of tests for strength of concrete." *Bureau of Indian Standards*, New Delhi, India.

IS: 5816-1999. (1999). "Splitting Tensile Strength of Concrete - Method of Test." *Bureau of Indian Standards*, New Delhi, India.

IS: 9103–1999. (1999). "Specification for concrete admixtures." *Bureau of Indian Standards*, New Delhi, India.

IS: 10262-2019. (2019). "Indian standard concrete mix proportioning." *Bureau of Indian Standards*, New Delhi, India.

Jaarsveld, J.G.S.V., Deventer, J.S.J.V. and Lukey, G.C. (2002). "The characterization of source materials in fly ash-based geopolymers." *Materials Letters*, 3975-3985.

Kapoor, K., Singh, S.P. and Singh, B. (2021). "Permeability of self-compacting concrete made with recycled concrete aggregates and Portland cement-fly ash-silica fume binder." *Journal of Sustainable Cement-based Materials*, 04(10), 213-239.

Klaiber, F.W., Thomas, T.L. and Lee, D.Y. (1979). "Fatigue Behavior of Air-Entrained Concrete: Phase II." Report, Ames, Iowa, *Engineering Research Institute, Iowa State University,* Ames, USA.

Kovtun, M., Ziolkowski, M., Shekhovtsova, J. and Kearsley, E. (2016). "Direct electric curing of alkali-activated fly ash concretes: a tool for wider utilization of fly ashes." *Journal of Cleaner Production,* 133, 220-227.

Krivenko, P. D. (1994). "Alkaline cements." *In: Proceedings of 1st International Conference on Alkline Cement and Concrete, Kiev, Ukraine*, SRIBM, Kiev State Technical University, 11-14.

Krizan, D. and Zivanovic, B. (2002). "Effects of Dosage and Modulus of Water Glass on Early Hydration of Alkali-slag Cements." *Cement and Concrete Research*, 32(8), 1181-1188.

Kumar, S.K., Kamalakara, G.K., Kamble, S. and Amaranth, M.S. (2012). "Fatigue analysis of high-performance cement concrete for pavements using probabilistic approach." *International Journal of Emerging Technology and Advanced Engineering,* 2(11), 640-644.

Law, D.W., Adam, A.A., Molyneaux, T.K. and Patnaikuni, I. (2012). "Durability assessment of alkali activated slag (AAS) concrete." *Materials and Structures,* 45, 1425-1437.

Lee, M. K. and Barr, B.I.G. (2004). "An overview of the fatigue behaviour of plain and fiber reinforced concrete." *Cement and Concrete Composites,* 26, 299-305.

Lee, W.K.W. and Deventer, J.S.J.V. (2002). "The effect of ionic contaminants on the early-age properties of alkali-activated Fly Ash-based cements." *Cement and Concrete Research,* 32, 577–584.

Lu, C. (1992). "The research and the reactive products and mineral phase for FKJ cementitious material." *9th International Congress on the Chemistry of Cement*, New Delhi, India, III, 319–324.

Manfredi, O., Wuth, W. and Bohlinger, I. (1997). "Characterizing the Physical and Chemical Properties of Aluminum Dross." *JOM.*

Maochieh, C. (2015). "Effects of modulus ratio and dosage of alkali-activated solution on the properties and micro-structural characteristics of alkali-activated fly ash mortars." *Construction and Building Materials,* 99, 128-136.

Maochieh, C. and Ran, H. (2012). "Effects of dosage and modulus ratio of alkali-activated solution on the properties of slag mortars." *Advanced Science Letters,* 5, 1-6.

Mbadike, E.M. (2014). "Effect of incorporation of aluminium waste in concrete matrix using different mix ratio and water cement ratio." *J. Advanced Biotechnology*, 2(1), 58–74.

Mehta, P. K. and Gjory, O. E. (1974). "A New Test for Sulfate Resistance of Cements." *Journal of Testing and Evaluation, JTEVA*, 2(6), 510-514.

Mehrzad, M.Y., Ahmet, B. and Ramazan, D. (2015). "The effects of silica modulus and aging on compressive strength of pumice-based geopolymer composites." *Construction and Building Materials,* 94, 767-774.

Mindess, S., Young, J.F. and Darwin, D. (2003). "Concrete." Second Edition, *Prentice-Hall,* Upper Saddle River, New Jersey, USA.

Ministry of Power, Government of India. (2021). "Report on Fly ash generation at Coal / Lignite based Thermal Power Stations and its utilization in the country for the year 2020 – 21." https://cea.nic.in/wp-content/uploads/tcd/2021/09/Report_Ash_Yearly_2020_21. pdf, Last accessed on 15/03/2022.

Ministry of Steel, NITI Aayog, Government of India. (2018). "Strategy Paper on Resource Efficiency in Steel Sector through recycling of Scrap and Slag." https://www.niti.gov.in/writereaddata/files/RE_Steel_Scrap_Slag-FinalR4_28092018.pdf, Last accessed on 15/03/2022.

Mithun, B.M. and Narasimhan, M.C. (2015). "Performance of alkali activated slag concrete mixes incorporating copper slag as fine aggregates." *Journal of Cleaner Production*, 1–8.

Mithun, B.M., Marathe, S. and Acharya, G. (2021). "Studies on high-performance concrete containing Aluminium dross." Sustainability Trends and Challenges in Civil Engineering, Lecture Notes in Civil Engineering, *Springer Publishers*, *Singapore*, Vol. 162, 979-989.

Mohammadi, Y. and Kaushik, S.K. (2005). *"Flexural fatigue life distributions of plain and fibrous concrete at various stress ratios." Journal of Materials in Civil Engineering*, ASCE, 17, 650-658.

Morsy, M.S., Rashad, A.M. and Shebl, S.S. (2008). "Effect of elevated temperature on compressive strength of blended cement mortar." *Building Research Journal,* 56 (2–3), 173–185.

MoRTH (Ministry of Road Transport and Highways) – 5th Revision. (2022). "Road Transport – Introduction." https://www.morth.nic.in/road-transport, Last accessed on 15/03/2022.

Naik, T.R. (2008). "Sustainability of concrete" *Construction Practice Period on Structural Design and Construction*, ASCE, 98-103.

Narasimhan, M.C., Nayak,G., Ajith,B.T. and Rao, M.K. (2011). "Development of Alternative Binders to Portland Cement Concrete using FA and Blast Furnace Slag: Some Experiences." *Proceedings of the International UKIERI Concrete Congress*, *New Delhi, India*, 43-60.

Nath, P. and Sarker, P.K. (2012). "Geopolymer Concrete for Ambient Curing Condition." *Australasian Structural Engineering Conference: The past, present and future of Structural Engineering.* Barton, A.C.T.: Engineers Australia, 225-232.

Neville, A.M. (2000). "Properties of Concrete." (Fourth Edition), *Pearson Education,* Longman Group, England.

Oh, B.H. (1986). "Fatigue analysis of plain concrete in flexure." *Journal of Structural Engineering,* ASCE, 112 (2), 273-288.

Oh, B.H. (1991). "Cumulative damage theory of concrete under variable-amplitude fatigue loadings." *ACI Materials Journal,* 88(1), 41-48.

Oren, O.H., Gholampour, A., Gencel, O. and Ozbakkaloglu, T. (2020). "Physical and mechanical properties of foam concretes containing granulated blast furnace slag as fine aggregate." *Construction and Building Materials*, 238, 117774.

Ouda, A.S. and Abdel-Gawwad, H.A. (2015). "The effect of replacing sand by iron slag on physical, mechanical and radiological properties of cement mortar." *HBRC Journal.*

Pacheco-Torgal, F., Castro-Gomes, J., and Jalali, S. (2007). "Tungsten Mine Waste Geopolymeric Binder versus Ordinary Portland Cement Based Concrete. Abrasion and

Acid Resistance." *International Conference Alkali Activated Materials – Research, Production and Utilization*, *Prague*, 693-702.

Palacios, M. and Puertas, Y.F. (2005). "Effect of superplasticizer and shrinkage-reducing admixtures on alkali-activated slag pastes and mortars." *Cement and Concrete Research,* 35, 1358–1367.

Palomo, A., Grutzeck, M.W. and Blanco, M.T. (1999). "Alkali-activated FAes: A cement for the future." *Cement and Concrete Research, 29*(8), 1323-1329.

Petavratzi, E. and Wilson, S. (2007). "A case study: Residues from aluminium dross recycling in cement." WRT177/WR0115, 1–8.

Phull, Y.R. and Rao, J.P. (2007). "Assuring Adequacy of Concrete Pavements: Some Essential Needs." *Indian Highways,* No.3, 9-19.

Prošek, Z., Nežerka, V., Hlůžek, R., Trejbal, J., Tesárek, P. and Karra'a, G. (2019). "Role of lime, fly ash, and slag in cement pastes containing recycled concrete fines." *Construction and Building Materials,* 201, 702-714.

Provis, J. L. (2013). "Alkali-activated Binders and Concretes: The Path to Standardization Geopolymer Binder Systems." *American Society for Testing of Materials*, STP 1566, 185-195.

Provis, J.L., Myers, R.J., White, C.E/, Rose, V. and van Deventer, J.S.J. (2012). "X-ray microtomography shows pore structure and tortuosity in alkali-activated binders." *Cement and Concrete Research*, 42(6), 855–864.

Puertas, F., Martinez-Ramirez, S., Alonso, S. and Vazquez, T. (2000). "Alkali activated FA/Slag Cements: Strength Behaviour and Hydration Products." *Cement and Concrete Research*, 30(10), 1625-1632.

Purdon, A. O. (1940). "The Action of Alkalis on Blast-furnace Slag." *Journal of the Society of Chemical Industry*, 59(12), 191–202.

Raheel, M., Rahman, F. and Ali, Q. (2020). "A stoichiometric approach to find optimum amount of fly ash needed in cement concrete." *SN Appl. Sci. Journal,* 2**,** 1100.

Rajamane, N.P. (2013). "Studies on development of ambient temperature cured FA and GGBS based geopolymer concretes." *Doctoral dissertation*, VTU, Belgaum, India.

Rakesh, K.P. and Bibhuti, B.M. (2017). "Influence of incorporation of granulated blast furnace slag as replacement of fine aggregate on properties of concrete." *Journal of Cleaner Production,* 165, 468-476.

Ramakrishnan, V., Meyer, C., Naaman, A.E., Zhao, G. and Fang, L. (1996). "Cyclic behaviour,fatigue strength, endurance limit and models for fatigue behaviour of FRC." *In:Spon E, Spon FN, editors. High performance fiber reinforced cement composites*, 2, 101–148.

Rangan, B. V. and Hardijto, D. (2005). "Development and Properties of Low Calcium Fly ash based Geopolymer Concrete." *Research report GC-1, Curtin University of Technology, Perth, Australia.*

Rao, G.M. and Rao T.D.G. (2018). "A quantitative method of approach in designing the mix proportions of fly ash and GGBS-based geopolymer concrete." *Australian Journal of Civil Engineering*, 01(16), 53-63.

Rao, M.S. and Bhandare, U. (2014). "Application of Blast Furnace Slag Sand in Cement Concrete–A Case Study." *International Journal of Civil Engineering Research,* 5(4), 453-458.

Rashad, A.M., Zeedan, S.R. and Hassan, A. (2012). "A preliminary study of autoclaved alkali-activated slag blended with quartz powder." *Construction and. Building Materials,* 33, 70 – 77.

Rashad, A. M. (2013a). "Utilizing of Alkali Activation of Fly ash Concrete Blended with Slag." *Iran Journal of Material Science Engineering*, 10(1), 57–64.

Rashad, M.A. (2013b). "A Comprehensive Overview about the Influence of Different Additives on the Properties of Alkali-activated Slag – A guide for Civil Engineer." *Construction and Building Materials*, 47, 29–55.

Ricarda, T., Anja, B. and Dietmar, S. (2015). "Effect of slag chemistry on the hydration of alkali-activated blast-furnace slag." *Materials and Structures*, 48, 629-641.

Rodriguez, E., Bernal, S., Guterrez M.R., and Puertas, Y.F. (2008). "Alternative concrete based on alkali-activated slag." *Materiales De Construcción*, 58 (291), 53–67.

Roy, D.M. and Silsbee, M.R. (1992). "Alkali activated materials - An overview." *Material Resource Society Symposium Proceedings* 1992, 245,153–164.

Roylance, D. (2001). "Fatigue." *http://ocw.mit.edu/courses/materials-science-and-engineering/3-11-mechanics-of-materials-fall-1999/modules/fatigue.pdf.*

Sakin, R. and Ay, I. (2008). "Statistical analysis of bending fatigue life data using Weibull distribution in glass-fiber reinforced polyester composites." *Materials and Design*, 29, 1170-1181.

Sarker, P.K., Grigg, A. and Chang, E.H. (2007a). "Bond Strength of Geopolymer Concrete with Reinforcing Steel." *Proceedings of Recent Developments in Structural Engineering, Mechanics and Computation,* Editor: A. Zingoni, Millpress, Netherlands, 1315-1320.

Sarker, P.K. and deMeillon, T. (2007b). "Residual Strength of Geopolymer Concrete After Exposure to High Temperature." *Proceedings of Recent Developments in Structural Engineering, Mechanics and Computation,* Editor: A. Zingoni, Millpress, Netherlands, 1566-1571.

Satish, C. (1996). "Waste materials used in concrete." *Standard Publishers and Distributers*, Delhi, India.

Satish, R.M. and Neerja, D. (2016). "Mechanical and durability aspects of concrete incorporating secondary aluminium slag." *Resource Efficient Technologies,* 2, 225-232.

Sakulich, A. R., Anderson, E., Schauer,C. and Barsoum, M.W. (2009). "Mechanical and Microstructural Characterization of an Alkali-activated Slag/limestone Fine Aggregate Concrete." *Construction and Building Materials* ,23(8), 2951–2957.

Sharma, B.M., Sitaramanjaneyalu, K. and Kanchan, P.K. (1995). "Effect of vehicle axle loads on pavement performance." *Road Transport Technology-4, University of Michigan,* Transportation Research Institute, Ann Arbor, 263-272.

Shekhovtsova, J., Kearsley, E.P. and Kovtun, M. (2014). "Effect of activator dosage, water-to-binder-solids ratio, temperature and duration of elevated temperature curing on the compressive strength of alkali-activated fly ash cement pastes." *Journal of South African Institute Civil Engineering,* 56, 44-52.

Shi, C. (1996). "Strength, pore structure and permeability of alkali-activated slag mortars." *Cement and Concrete Research*; 26 (12), 1789–1799.

Shi, C. and Li, Y. (1989). "Investigation on some factors affecting the characteristics of alkali-phosphorus slag cement." *Cement and Concrete Research,* 19(4), 527-533.

Shi, C., Krivenko, P.V. and Roy, D. (2006). "Alkali-Activated Cements and Concretes." *Taylor and Francis*, ISBN 0-415-70004-3.

Shrinivasarao, Ch. and Vijaya Bhaskar Reddy, S. (2020). "Study of standard grade concrete consisting of granulated blast furnace slag as a fine aggregate." *Materials Today: Proceedings*, Part 2, Vol. 27, 859-865.

Shriraksha, J., Chandrashekar, A.R., Sujay, R.N., Manu, D.S., Parameshwar, H., Preethi, H.G. and Vinod, K.N. (2017). "Eco-concrete for sustainability: utilizing aluminium dross and iron slag as partial replacement materials." *Clean Technologies and Environmental Policy,* 19, 2291-2304.

Silva, A.C.R., Silva, F.J. and Thaumaturgo, C. (2006). "Fatigue Behavior of Geopolymer Cement Concrete." *41th International Symposium on Macromolecules,* Rio de Janeiro, 2006.

Singh, G. and Siddique, R. (2016). "Strength properties and micro-structural analysis of self-compacting concrete made with iron slag as partial replacement of fine aggregates." *Construction and Building Materials,* 127, 144–152.

Siddiqui, K.S. (2007). "Strength and Durability of Low-Calcium FA-based Geopolymer Concrete." *Final Year Honours Dissertation, The University of Western Australia,* Perth, Australia.

Siddique, R. (2008). "Ground Granulated Blast furnace Slag." *Industrial Waste materials and by-products in concrete, Springer,* Heidelberg, Berlin, 1–39.

Sofi, M., van Deventer, J. S. J., Mendis, P. A. and Lukey, G. C. (2007a). "Engineering Properties of Inorganic Polymer Concretes (IPCs)." *Cement and Concrete Research*, 37, 251–257.

Sofi, M., Deventer J.S.J.V., Mendis, P.A. and Lukey, G.C. (2007b). "Bond Performance of Reinforcing Bars in Inorganic Polymer Concrete (IPC)." *Journal of Materials Science,* 42(9), 3007-3016.

Subash, N. and Kumar, S.A. (2021). "A simplified geopolymer concrete mix design considering five mineral admixtures." *European Journal of Environmental and Civil Engineering.*

Suman, S. and Rajasekaran, C. (2017). "Enhancement of the properties of FA based geopolymer paste by incorporating GGBS." *Construction and Building Materials,* 146, 615-620.

Swanepoel, J.C. and Strydom, C.A. (2002). "Utilization of fly ash in a geopolymeric material." *Applied Geochemistry,* 17(8), 1143-1148.

Tripathy, P.S. and Mukherjee, S.N. (1997). "Perspectives on bulk use of FA." *Allied Publishers Limited*, New Delhi, India.

Tripathi, B., Misra, A. and Chaudhary, S. (2012). "Strength and abrasion characteristics of ISF slag concrete." *Journal of Materials in Civil Engineering,* 25(11), 1611–1618.

Upendra, S., Ansari, M.S., Puttewar, S.P. and Agnihotri, A. (2017). "Studies on Process for Conversion of Waste Aluminium Dross into Value Added Products." *Russian Journal of Non-ferrous Metals*, 57(4), 296–300.

Wallah, S.E. and Rangan, B. V. (2006). "Low-calcium FA-based Geopolymer concrete: Long-term properties." *Research Report GC 2, Curtin University of Technology, Perth, Australia*.

Wang, A., Zhang, C. and Sun, W. (2003). "FA effects: I. The morphological effect of FA." *Cement and Concrete Research*, 33(12), 2023–2029.

Wang, S.D. and Scrivener, K.L. (1995). "Hydration products of alkali-activated slag cement." *Cement and Concrete Research*, 25 (3), 561–571.

Wang, S.D., Pu, X.C., Scrivener, K.L. and Pratt, P.L. (1994). "Factors affecting the Strength of Alkali Activated Slag." *Cement and Concrete Research*, 24(6), 1033-1043.

William, G.V.S. and Ruby, M.G. (2017). "Performance of geopolymer concrete composed of fly ash after exposure to elevated temperatures." *Construction and Building Materials,* 154, 229–235.

Xu, H. and Deventer, J.S.J.V. (2000). "The geopolymerization of alumino-silicate minerals." *International Journal of Mineral Processing,* 59(3), 247-266.

Yang, K., Song, J., Lee, E. and Ashrour, A. F. (2008). "Properties of Cementless Mortars Activated by Sodium Silicate." *Construction and Building Materials*, 22, 1981–1989.

Yildirim, I.Z. and Prezzi, M. (2009). "Use of PIS in subgrade applications." *Final Report,* FHWA/IN/JTRP- 2009-32.

Young-Keon, C., Sung-Won, Y., Sang-Hwa, J., Kwang-Myong, L. and Seung-Jun, K. (2017). "Effect of Na2O content, SiO_2/Na_2O molar ratio and curing conditions on the compressive strength of FA-based geopolymer." *Construction and Building Materials,* 145, 253-260.

Yuksel, I. (2017). "A review of PIS usage in construction industry for sustainable development." *Environment, Development and Sustainability,* 19(2), 369–384.

Zongjin, L. and Sifeng, L. (2007). "Influence of Slag as Additive on Compressive Strength of Fly Ash based Geopolymer." *Journal of Materials in Civil Engineering,* 19(6), 470-474.

LIST OF PUBLICATIONS

Peer Reviewed Publications:

Panditharadhya B J, Vargala Sampath, Raviraj H Mulangi and A U Ravi Shankar (2018). "Mechanical properties of pavement quality concrete with secondary aluminium dross as partial replacement for Ordinary Portland Cement." IOP Series: Materials Science and Engineering, Vol. 431. DOI: https://doi.org/10.1088/1757-899X/431/3/032011

Panditharadhya B J, Raviraj H Mulangi and A U Ravi Shankar (2019). "Impact of alternate fine aggregate from iron and steel industry on workability and mechanical properties of pavement quality concrete." International Journal of Civil Engineering and Technology, Vol. 10, Issue 06, 627-639.
DOI:https://doi.org/10.17605/OSF.IO/2F5DS

Panditharadhya B J, Raviraj H Mulangi, A U Ravi Shankar and Amulya S (2019). "Performance of Concrete mix with Secondary Aluminium Dross as a partial replacement for Portland Pozzolana Cement." Airfield and Highway Pavements 2019 - ASCE Library, 408-416. DOI: https://doi.org/10.1061/9780784482469.041

Panditharadhya B J, Raviraj H Mulangi and A U Ravi Shankar (2021). "Effect of aluminium dross on workability and setting time of cement and concrete." International Journal of Research in Applied Science and Engineering Technology, Vol. 09, Issue 07, 1851-1859. DOI: https://doi.org/10.22214/ijraset.2021.36724

Panditharadhya B J, Raviraj H Mulangi and A U Ravi Shankar (2022). "Effect of Aluminium industry waste as a binder in concrete." International Journal of Engineering and Technology Innovations. *(Under Review).*

Panditharadhya B J, Raviraj H Mulangi and A U Ravi Shankar (2022). "Experimental and analytical evaluations of concrete produced with processed granulated blast furnace slag as fine aggregate." KSCE Journal of Civil Engineering, Springer Publishers *(Under Review).*

International Conferences:

Panditharadhya B J, Raviraj H Mulangi, A U Ravi Shankar and Susheel Kumar (2018). "Mechanical Properties of Pavement Quality Concrete Produced with Reclaimed Asphalt Pavement Aggregates." International Conference on Sustainable Construction and Building Materials (ICSCBM – 2018) held at National Institute of Technology Karnataka, *Surathkal, India* on June 18-22, 2018.

Panditharadhya B J, Raviraj H Mulangi and A U Ravi Shankar (2018). "Mechanical properties of pavement quality concrete with secondary aluminium dross as partial replacement for Ordinary Portland Cement." 14th International Conference on Concrete Engineering and Technology (CONCET) held at University of Malaya, *Kaula Lumpur, Malaysia* on August 8-9, 2018.

Panditharadhya B J, Raviraj H Mulangi and A U Ravi Shankar (2018). "Effect of aluminium dross as a cementitious material." Conference on Next Frontiers in Civil Engineering - Sustainable and Resilient Infrastructure held at IIT Bombay, *Mumbai, India* on 30 Nov-1 Dec, 2018.

Panditharadhya B J, Raviraj H Mulangi and A U Ravi Shankar (2019). "Effect on workability and setting time of concrete with Aluminium Dross as partial replacement for Ordinary Portland Cement." 8th International Engineering Symposium - IES 2019 held at Kumamoto University, *Kumamoto, Japan* on 13-15 March, 2019.

Panditharadhya B J, Raviraj H Mulangi and A U Ravi Shankar (2019). "Strength characteristics of concrete produced with aluminium dross as partial replacement for Portland Pozzolana Cement." 15th World Conference on Transport Research 2019 held at IIT Bombay, *Mumbai, India* on 26–31 May, 2019.

Panditharadhya B J, Raviraj H Mulangi, A U Ravi Shankar and Amulya S (2019). "Performance of Concrete mix with Secondary Aluminium Dross as a partial replacement for Portland Pozzolana Cement." International Airfield and Highway Pavements Conference 2019 held at American Society of Civil Engineers (ASCE), *Chicago, Illinois, USA* on 21–24 July, 2019.

Panditharadhya B J, Raviraj H Mulangi and A U Ravi Shankar (2020). "Durability Studies on Concrete produced with Processed Iron Slag as Fine Aggregate." Second ASCE India Conference on "Challenges of Resilient and Sustainable Infrastructure Development in Emerging Economies" (CRSIDE2020) held at ASCE India Chapter, *Kolkata, India* on 2-4 March, 2020.

Panditharadhya B J, Raviraj H Mulangi and A U Ravi Shankar (2020). "Effect of Processed Granulated Blast furnace Slag as an alternate Fine Aggregate in Pavement Quality Concrete." International Conference on Green Highway Construction – A Sustainable Approach held at National Institute of Technology Karnataka, *Surathkal, India* on 14-15 September, 2020.

BIO-DATA

Name	: **Panditharadhya B J**
Department	: Civil Engineering
Specialisation	: Transportation Engineering
Gender	: Male
Date of Birth	: 30-05-1991
Email ID	: pandith23@gmail.com
Mobile Number	: +91-9844919460
Address	: No. 947/168, 2nd Main, 4th Block,
	Rajajinagar, Bangalore – 560 010,
	Karnataka

Academic Profile:

Degree	Year of Completion	Institution	Board	Percentage/ CGPA
Ph.D. (Civil Engineering)	2022	National Institute of Technology Karnataka, Surathkal	Deemed University	-
M.Tech. (Highway Technology)	2014	Dayananda Sagar College of Engineering, Bengaluru	Visvesvaraya Technological University, Belagavi	82.5
B.E. (Civil Engineering)	2012	East West Institute of Technology, Bengaluru	Visvesvaraya Technological University, Belagavi	77.5
PUC (PCMB)	2008	KLE Society's S Nijalingappa PU College, Bengaluru	Department of Pre-University Education, Karnataka	60.0
SSLC	2006	Rajajinagar Parents' Association High School, Bengaluru	Karnataka Secondary Education Examination Board	91.2